UNIVERSIDADE DE LISBOA
FACULDADE DE CIÊNCIAS
DEPARTAMENTO DE QUÍMICA E BIOQUÍMICA

Role of CFTR and TMEM16 for Regulated Cell Death

Filipa Bica Simões

Mestrado em Bioquímica
Especialização em Bioquímica Médica

Dissertação orientada por:
Prof. Dr. med. Karl Kunzelmann, Prof. Dr. Margarida Amaral

2016

ACKNOWLEDGMENTS/AGRADECIMENTOS

First of all, I would like to express my appreciation to my supervisors – Prof. Karl Kunzelmann and Prof. Margarida Amaral – for giving me the incredible opportunity of pursuing my studies in science while gaining new insight about life abroad. For all the guidance, support, help and knowledge, I truly thank Prof. Karl Kunzelmann. I also want to show my gratitude to Prof. Rainer Schreiber for being available to answer my questions, give new ideas and share his experience.

A special thank goes to Ji, who followed my work very close, always showing an energetic attitude, helping and pushing me to get the best out of my project. I will never forget all the technique and 'small tricks' that she taught me! To Inês, who introduced me the life in Regensburg and always kept a positive mind, making the craziest excuses to party all night long! Thank you for all the support, conversations and bell ringing every morning!! To Roberta, for all the true friendship with lots of love and kicking! Thank you for teaching me when compounds are frozen and for loving my açorda! – You will always be my 'you-know-what'! To Kip, for being my essential companionship in the cell culture room, for always giving me tips about my cells and especially for never give up on trying to make me think positive! – I will always remember that! To Gam, for all the laughter, dinners, parties and lessons in the lab! To Joana, for all the morning coffees, opinions and Sunday afternoons doing experiments! All of you made my days easier and brought really funny and unforgettable moments into my life! I also want to show my appreciation to Brigitte, Tini, Susi, Patricia and Silvia for all the help and good mood in the lab!

Obrigada a toda a minha família pela atitude sempre positiva, por todo o apoio e pela boa disposição, mesmo nos momentos mais difíceis!

Aos meus pais, por me ensinarem a seguir os meus sonhos e a enfrentar os obstáculos na vida, crescendo com eles. À minha mãe, por me fazer sentir que nunca estive ausente, partilhando todos os momentos comigo e não passando uma única manhã sem me desejar um bom dia de trabalho! Ao meu pai, por, apesar da distância, manter sempre a naturalidade, pelos conselhos e por todas as músicas partilhadas! Ao Nuno, por todo o carinho, maluqueiras e parvoíces, conseguindo sempre pôr-me um sorriso na cara. És a prova de que um irmão pode ser um melhor amigo!

Um agradecimento muito especial a todos os meus avós, por me acompanharem sempre e me ensinarem a ser uma pessoa integra – o meu orgulho é eterno! Obrigada aos meus tios e primos, pelo apoio e carinho incondicionais. Ao Miguel por ser meu amigo, companheiro e segundo irmão!

Obrigada a todos os meus amigos pela amizade verdadeira, pelas brincadeiras e por me fazerem sentir que nunca estive longe! Em especial à Ana (Frafrá), por ter partilhado esta grande experiência comigo, por todas as gargalhadas, viagens, cervejas e companhia: sem ti tudo teria sido muito mais complicado!! Muito obrigada, também, por matares os bichos que apareciam no meu quarto! À Ana e ao André, por serem amigos incansáveis, honestos, bons ouvintes e conselheiros: a festa recomeça agora!!

SUMMARY

Regulated or programmed cell death is defined as an intracellular program that plays a complementary role to mitosis in maintaining a stable population of cells. Apoptosis is the main form of regulated cell death, allowing the silent elimination of harmed or aged cells without triggering any inflammatory response.

Anoctamin 6 (ANO6, TMEM16F) is a multifunctional protein from a family of ten members, identified as an endogenous Ca^{2+}-activated Cl^- channel (CaCC). Apart from its function as a CaCC, ANO6 is also described as a volume-regulated and outwardly rectifying Cl^- channel (ORCC), a non-selective cation channel and a Ca^{2+}-dependent phospholipid scramblase. It has an ubiquitous expression, being involved in many physiological processes including apoptosis. Nonetheless, ANO6 role in this process is not entirely understood.

The Cystic Fibrosis Transmembrane conductance Regulator (CFTR) is a cyclic adenosine monophosphate (cAMP)-gated Cl^- channel expressed in the apical membrane of epithelial cells from the intestine, pancreas, airways and sweat glands, where it is responsible to maintain ion and fluid homeostasis. Moreover, it regulates the intracellular redox status, acidification and ceramide content in lipid rafts, three different functions that may explain CFTR involvement in apoptosis. Mutations in the CFTR gene are the cause for Cystic Fibrosis (CF), the most common life-threatening autosomal recessive disease in Caucasians.

Understanding ANO6 and CFTR role in regulated cell death may help to overcome the apoptotic dysfunction found in Cystic Fibrosis. Here it is shown that ANO6 is activated by ROS (Reactive Oxygen Species) during apoptosis, acting as a Ca^{2+}-activated Cl^- channel, non-selective cation channel and phospholipid scramblase in different *in vitro* systems. The channel has a dual contribution for this process, transporting ions to the extracellular space and mediating phosphatidylserine (PS) exposure in the outer membrane leaflet. Furthermore, a CFTR contribution to ROS-mediated apoptosis was found in CFBE cells, a mechanism independent of pore opening and channel stimulation. Co-expression studies of ANO6 and CFTR in HEK293 cells revealed a functional relationship of these proteins during ROS-mediated apoptosis not only in terms of whole-cell current but also regarding phospholipid scrambling.

A possible interaction between ANO6 and CFTR is also proposed to explain why cells overexpressing both proteins have an enhanced spontaneous and ROS-induced apoptosis. Exposure of cells to oxidative stress and consequent ROS production leads to mitochondrial permeabilization, release of Ca^{2+} and pro-apoptotic proteins, responsible for caspase cleavage. These events terminate with ANO6 activation, which may support cell shrinkage and phospholipid scrambling, two apoptotic hallmarks enhanced in the presence of CFTR.

Key-words: Regulated cell death, Apoptosis, Anoctamin 6, CFTR, Cystic Fibrosis

RESUMO

A morte celular programada é um mecanismo homeostático que desempenha um papel complementar à mitose na manutenção de uma população estável de células nos tecidos e órgãos. Este programa é ativado diariamente, removendo milhões de células danificadas ou envelhecidas. A apoptose é considerada a forma predominante de morte celular programada, garantindo a eliminação silenciosa de células, isto é, sem ativação do sistema imune.

Durante a apoptose, as células sofrem uma grande variedade de modificações morfológicas e bioquímicas. Estas alterações são em grande parte mediadas por uma família de proteases conhecida por caspases. As caspases são normalmente expressas como precursores inativos ou procaspases, que adquirem atividade proteolítica na presença de um determinado estímulo. Depois de ativos, estes enzimas clivam outras procaspases, proteínas essenciais e ADN, sendo assim responsáveis pela amplificação da cascata apoptótica. A clivagem de todos estes substratos resulta na alteração fenotípica das células apoptóticas, as quais passam a apresentar uma redução no seu volume (*shrinkage*), condensação de cromatina e formação de protrusões na membrana plasmática (*blebbing*).

A composição fosfolipídica da membrana plasmática é também afetada durante a apoptose. Numa célula viável, a bicamada lipídica é assimétrica: a fosfatidilserina (PS) e a fosfatidiletanolamina (PE) estão presentes no folheto interno, enquanto a fosfatidilcolina (PC) e a esfingomielina (SM) localizam-se no folheto externo. Esta assimetria é destruída pelo transporte bidirecional de fosfolípidos através da membrana plasmática, mediado por scramblases (*scrambling*). Particularmente, durante a apoptose, a PS é movida do folheto interno para o folheto externo, o que serve de sinal para a fagocitose das células apoptóticas, um processo essencial para a manutenção da integridade do hospedeiro.

A Anoctamina 6 (ANO6) é uma proteína ubíqua e multifuncional pertencente a uma família proteica formada por dez membros homólogos entre si (ANO1-10; TMEM16 A-K). Esta é identificada como um canal de cloreto regulado por volume e ativado por cálcio (do inglês: *Calcium activated Chloride Channel* – CaCC), canal catiónico não seletivo, componente do ORCC (do inglês: *Outwardly Rectifying Chloride Channel*) e scramblase de fosfolípidos ativada por cálcio. A ANO6 participa numa enorme variedade de processos biológicos, tais como a coagulação sanguínea, desenvolvimento do esqueleto, regulação do volume e migração celular, entre outros. A identificação da ANO6 como uma scramblase de fosfolípidos levantou várias questões acerca do seu envolvimento na apoptose. Diferentes estudos indicam que esta proteína contribui para este processo como um canal iónico, participando eventualmente no *shrinkage* das células e na ativação de caspases. No entanto, no que diz respeito à sua função como scramblase, o papel da ANO6 é ainda incerto.

O CFTR (do inglês: *Cystic Fibrosis Transmembrane conductance Regulator*) é um canal de cloreto regulado por cAMP (Adenosina de monofosfato cíclico), expresso na membrana apical de células epiteliais do intestino, pâncreas, vias respiratórias e glândulas sudoríparas. Mutações no gene que codifica para esta proteína são a causa da Fibrose Quística, a doença mortal autossómica recessiva responsável pelo maior número de mortes na população caucasiana. Apesar da enorme diversidade de variantes de mutações identificadas (cerca de 1.500), a deleção de um resíduo de fenilalanina (F) no codão 508 localizado no cromossoma 7 (ΔF508) é encontrada em 90% dos pacientes com Fibrose Quística. Esta mutação resulta num *folding* aberrante do CFTR e consequentemente um defeito no seu tráfego do retículo endoplasmático para a membrana plasmática.

A Fibrose Quística é principalmente caracterizada por uma por uma perturbação da homeostase iónica e fluídica. De entre os variados sintomas encontrados nos pacientes afetados, destaca-se a

produção excessiva de muco espesso, infeções persistentes nas vias respiratórias pela bactéria *Pseudomonas aeruginosa*, infertilidade masculina e insuficiência pancreática e intestinal. Apesar dos esforços contínuos em compreender o CFTR a um nível funcional e molecular, a Fibrose Quística continua a ser considerada uma doença letal. A atenuação dos sintomas permitiu aumentar a esperança média de vida para cerca de 37 anos. No entanto, a doença pulmonar crónica e a resultante perda de função pulmonar continuam a ser os principais problemas por resolver, sendo responsáveis por 80% da mortalidade.

Curiosamente, o CFTR foi previamente descrito como um regulador do estado redox intracelular, da acidificação do citoplasma e organelos e dos níveis de ceramida nas jangadas lipídicas, três processos determinantes para a apoptose e possivelmente responsáveis pela disfunção apoptótica encontrada na Fibrose Quística. Apesar de algumas observações não serem coerentes, a maioria dos estudos defende que mutações no CFTR aumentam a suscetibilidade das células para uma morte necrótica. Contrariamente ao que se sucede na apoptose, durante a necrose os componentes celulares são libertados para os tecidos circundantes e o sistema imune é ativado. Desta forma, especula-se que esta disfunção pode contribuir para as inflamações persistentes que caracterizam a Fibrose Quística.

A interação do CFTR com outros canais e proteínas transportadoras tem sido tópico de investigação ao longo dos anos. De entre as proteínas identificadas, destaca-se o ORCC, um canal inativo em células viáveis e envolvido no *shrinkage* e *scrambling* de fosfolípidos durante a apoptose. Em 2010 Martins *et. al* identificou a ANO6 como componente do ORCC, existindo uma possível interação entre esta proteína e o CFTR.

Tendo em conta todas estas evidências, o objetivo deste projeto foi o estudo da relação entre a ANO6 e o CFTR durante a morte celular programada. Particularmente, o trabalho focou-se na apoptose induzida por ROS (do inglês: *Reactive Oxygen Species*), uma vez que o CFTR é descrito como um regulador do estado redox intracelular.

A primeira fase deste projeto baseou-se no estudo do impacto dos ROS na atividade da ANO6, não só em termos de corrente elétrica, mas também no que diz respeito à sua função de scramblase. Com este objetivo, a expressão endógena da ANO6 foi manipulada em células HEK293 e HeLa e a sua função foi analisada por *patch clamp* ou citometria de fluxo, após tratamento com diferentes indutores de *stress* oxidativo. Os resultados demonstraram que a ANO6 é ativada por ROS, transportando cloreto e catiões para o espaço extracelular no início da apoptose, um evento que contribui para o *shrinkage* das células. À medida que a via apoptótica avança, a ANO6 passa também a funcionar como scramblase, movendo a PS para o folheto externo da membrana plasmática. Como o silenciamento da ANO6 não diminuiu a morte celular, é concluído que esta proteína não é absolutamente essencial para a apoptose mediada por ROS. No entanto, esta observação não é surpreendente, visto que a morte celular programada é um processo essencial em qualquer sistema biológico, dependendo de uma grande variedade de moléculas e componentes. Assim, é muito provável que uma célula que não expresse a ANO6 compense este defeito com outras proteínas.

A segunda parte deste trabalho focou-se na importância do CFTR para apoptose mediada por ROS e a identificação de uma possível interação funcional entre esta proteína e a ANO6. Estudos de co-expressão em células HEK293 revelaram que a presença das duas proteínas aumenta a corrente elétrica induzida por ROS e intensifica o *scrambling* de fosfolípidos durante a apoptose. Curiosamente, a co-expressão da ANO6 e do CFTR revelou ser suficiente para induzir uma apoptose significativa em condições controlo. Adicionalmente, a linha celular CFBE estavelmente transfetada com CFTR *wt* ou ΔF508 foi escolhida como uma ferramenta para o estudo da influência da mutação mais proeminente da

Fibrose Quística na apoptose. A indução de *stress* oxidativo nas duas linhas celulares demonstrou que a expressão do CFTR *wt* intensifica a apoptose, um fenómeno independente da abertura do poro e ativação do canal.

Em suma, este estudo permitiu demonstrar que a ANO6 e o CFTR cooperam durante a apoptose mediada por ROS. Estas duas proteínas revelaram ter uma relação funcional no que diz respeito à ativação de uma corrente iónica e também ao *scrambling* de fosfolípidos. É especulado que a expressão do CFTR na membrana plasmática aumenta a atividade da ANO6, envolvida nestes dois fenómenos apoptóticos. No entanto, é também provável que o contrário seja verdade, visto que a ANO6 foi já identificada como componente das correntes induzidas por cAMP em células que expressam o CFTR. A compreensão do papel da ANO6 e do CFTR durante a morte celular programada pode servir de motor para obter uma nova visão acerca da disfunção apoptótica encontrada na Fibrose Quística e, eventualmente, desenvolver novas terapias como tentativa de atenuar o processo inflamatório.

Palavras-chave: Morte programada celular, Apoptose, Anoctamina 6, CFTR, Fibrose Quística

INDEX

INDEX OF FIGURES AND TABLES

ABBREVIATIONS

$[Ca^{2+}]_i$	Intracellular Ca^{2+} concentration
µg	Microgram (10^{-6} g)
µL	Microliter (10^{-6} L)
µm	Micrometer (10^{-6} m)
µM	Micromolar (10^{-6} M)
7-AAD	7-Aminoactinomycin D
A	Ampere
ABC	ATP - binding cassette
Ac	Acid ceramidase
ACA	N-(p-Amylcinnamoyl)anthranilic Acid
AIF	Apoptosis Inducing Factor
AM	Acetoxymethyl
AMP	Adenosine Monophosphate
Annx V	Annexin V
ANO	Anoctamin
ANOVA	Analysis of variance
APAF 1	Apoptotic Peptidase Activating Factor 1
ArA	Arachidonic acid
Asm	Acid sphingomyelinase
ATP	Adenosine Triphosphate
AVD	Apoptotic Volume Decrease
B Lymph	B Lymphocytes
bp	Base pair
C	Cytosine
C	Celsius
Ca^{2+}	Calcium ion
CaCC	Ca^{2+}-activated Cl^- channels
cAMP	cyclic AMP
CD8	Cluster of Differentiation 8
CF	Cystic Fibrosis
CFBE	Cystic Fibrosis Bronchial Epithelial (cell line)
CFTR	Cystic Fibrosis Transmembrane conductance Regulator
Cl^-	Chloride ion
CO_2	Carbon Dioxide
Con	Control
C-terminal	Carboxyl- terminal
Cyt c	Cytochrome C
D	Aspartic acid
DCF	2',7'-dichlorofluorescein

DIC	Differential Interference Contrast
DMEM	Dulbecco's Modified Eagle Medium
DMSO	Dimethyl sulfoxide
DNA	Deoxyribonucleic acid
EGTA	Ethylene Glycol Tetraacetic Acid
ER	Endoplasmic Reticulum
eYFP	Enhanced Yellow Fluorescent Protein
F	Phenylalanine
FBS	Fetal Bovine Serum
FITC	Fluorescein isothiocyanate
FK	Forskolin
FRET	Förster Resonance Energy Transfer
FSC	Forward Scatter
G	Guanine
G	Glutamic acid
G	Gram
GSH	Glutathione
GSHEE	Glutathione reduced Ethyl Ester
H	Hour(s)
H	Histidine
H_2DCFDA	2',7'-dichlorodihydrofluorescein diacetate
H_2O_2	Hydrogen Peroxide
HEK293	Human Embryonic Kidney 293 (cell line)
HeLa	Henrietta Lacks Cervical Carcinoma (cell line)
HRP	Horseradish Peroxidase
I	Isoleucine
I^-	Iodide
IBMX	3-isobutyl-1-methylxanthine
Ide	Idebenone
Iono	Ionomycin
K^+	Potassium ion
L	Liter
L	Leucine
LPA	Lysophosphatidic Acid
LPL	Lysophospholipids
Lyso-PS	Lyso-Phosphatidylserine
m	Meter
M	Molar
MEM	Minimum Essential Medium
Mg^{2+}	Magnesium ion
min	Minute(s)

mL	Milliliter (10^{-3} L)
mm	Millimeter (10^{-3} m)
mM	Millimolar (10^{-3} M)
MMP	Mitochondrial Membrane Permeabilization
MPTP	Mitochondrial Permeability Transition Pore
MSD	Membrane-spanning domain
mV	Millivolt (10^{-3} V)
N- terminal	Amino- terminal
nA	Nanoampere (10^{-9} A)
NBD	Nucleotide-binding domain
nhTMEM16	*Nectria haematococca* Trasmembrane Protein 16
nM	Nanomolar (10^{-9} A)
nm	Nanometer (10^{-9} m)
ORCC	Outwardly Rectifying Cl^- Channel
PBS	Phosphate Buffered Saline
PC	Phosphatidylcholine
PE	Phosphatidylethanolamine
Pen Strep	Penicillin-Streptomycin
PKA	Protein Kinase A
PLA_2	Phospholipase A2
PS	Phosphatidylserine
PVDF	Polyvinylidene fluoride
Q	Glutamine
R	Regulatory domain
RNA	Ribonucleic acid
ROS	Reactive Oxygen Species
rpm	Rotations per minute
RPMI	Roswell Park Memorial Institute medium
RVD	Regulatory Volume Decrease
s	Second(s)
scrmbld	Scrambled
siRNA	Small interfering RNA
SM	Sphingomyelin
SSC	Side Scatter
STS	Staurosporine
TA	Tannic Acid
tBHP	Tert-butyl hydroperoxide
TMEM16	Transmembrane Protein 16
TNF	Tumor Necrosis Factor
TNF-R	Tumor Necrosis Receptor
V	Volt

V	Valine
WB	*Western Blot*
wt	Wildtype
XkR8	Xk-related protein 8
YFP	Yellow Fluorescent Protein

1. INTRODUCTION

1.1 REGULATED CELL DEATH – APOPTOSIS

Multicellular organisms maintain a stable population of cells during their lifespan, keeping a tight control between cell division and cell death. Every day the activation of an intracellular death mechanism leads to the elimination of billion harmed or aged cells, which are no longer needed. This process is known as regulated or programmed cell death and can be divided into several types, being apoptosis the most predominant and studied form[1–5].

Apoptosis was named in 1972 by Kerr and co-workers[6], after a Greek word used to describe the dropping of leaves from trees, suggesting that cell loss is beneficial for the survival of the host. The authors intended to distinguish this process from a different type of cell death known as necrosis. Unlike apoptosis, where cell removal happens without compromising the whole organism, necrosis is a highly immunogenic mechanism. Furthermore, it is considered as the result of a persistent stimulus which leads to an accidental cell death, whereas apoptosis is genetically determined[1,6–8].

The apoptotic pathway involves several molecules and organelles, which are believed to be conserved in all animals[5]. Inside this group, caspases play a major role. This family of proteases is normally expressed as inactive precursors or procaspases, which acquire proteolytic activity in the presence of a specific stimulus. Once active, these enzymes amplify the apoptotic pathway by cleaving other procaspases and intracellular key prote ins at specific aspartic residues. Regarding apoptosis, caspases can be divided in two classes: initiator (caspase-2, 8, 9 and 10) and executioner (caspase-3, 6 and 7). The first group is responsible to activate the executioner caspases, which will then cleave a wide variety of substrates, leading to the final cell death[1,8,9].

The phenotype of an apoptotic cell is mainly characterized by reduced volume, or shrinkage, chromatin condensation and membrane blebbing[1,7,8,10,11]. After these transformations, the cytoplasm and organelles are tightly condensed into apoptotic bodies, keeping their integrity. Once these structures are formed, they are quickly engulfed by phagocytes (**Fig. 1.1**) and digested in phagolysosomes, without production of anti-inflammatory cytokines. This allows the protection of the surrounding tissue from potential released proteases and oxidizing molecules, avoiding inflammation[1,7].

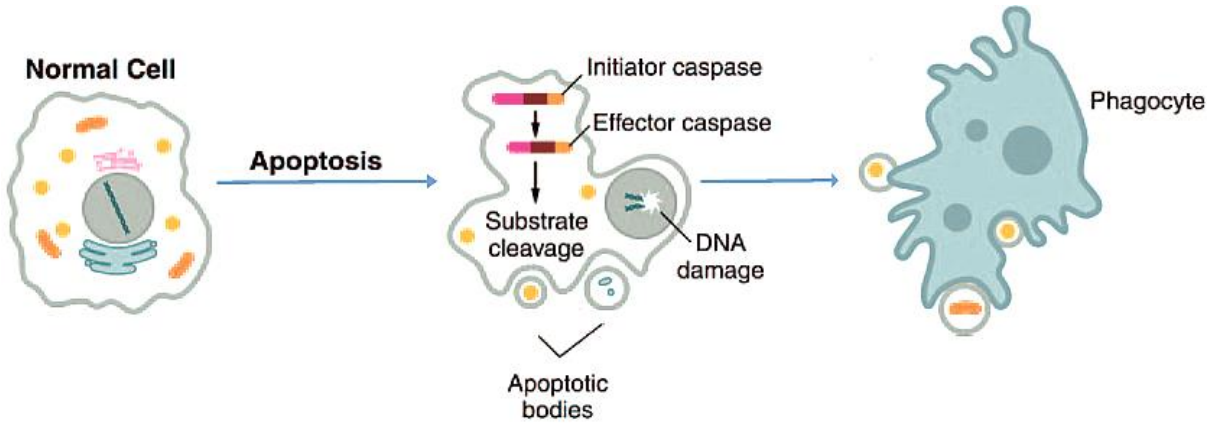

Figure 0.1. Representation of morphological transformations occurring during apoptosis and engulfment of the dying cell by phagocytes. Initiator caspases activate executioner or effector caspases, able to cleave cellular substrates. As a consequence, the apoptotic cell shows reduced volume, DNA damage and fragmentation into apoptotic bodies, which are engulfed by phagocytes. Retrieved and adapted from Fink *et. al*[8].

Apoptosis can be divided in two main signaling pathways: the intrinsic or mitochondrial pathway and the extrinsic or death receptor pathway. The first is activated when cells are exposed to inner stress forms, such as irradiation, heat shock or reactive oxygen species (ROS)[1,2]. During this mechanism, the mitochondrial permeability transition pore (MPTP) is opened, leading to the loss of the mitochondrial transmembrane potential and a stop in the ATP (Adenosine Triphosphate) synthesis[12]. Pro-apoptotic proteins are then released to the cytosol which can either function as activators of caspase-9 (e.g. cyt c – cytochrome c) or as mediators of DNA (Deoxyribonucleic acid) fragmentation (e.g. AIF – Apoptosis Inducing Factor)[1]. On the other hand, the extrinsic pathway is activated once specific ligands bind to their complementary plasma membrane receptors, such as TNF (Tumor Necrosis Factor) to TNF-R (TNF Receptor) or Fas ligand to CD95 (Fas ligand receptor). In this mechanism caspase-8 and 10 are major players[13]. Both signaling pathways end with the activation of executioner caspases, which leads to protein and DNA fragmentation and the consequent morphological transformations seen in apoptotic cells[1]. Caspase-3 is considered a key member of this group, being activated by caspase-8, 9 and 10[1] (**Fig. 1.2**).

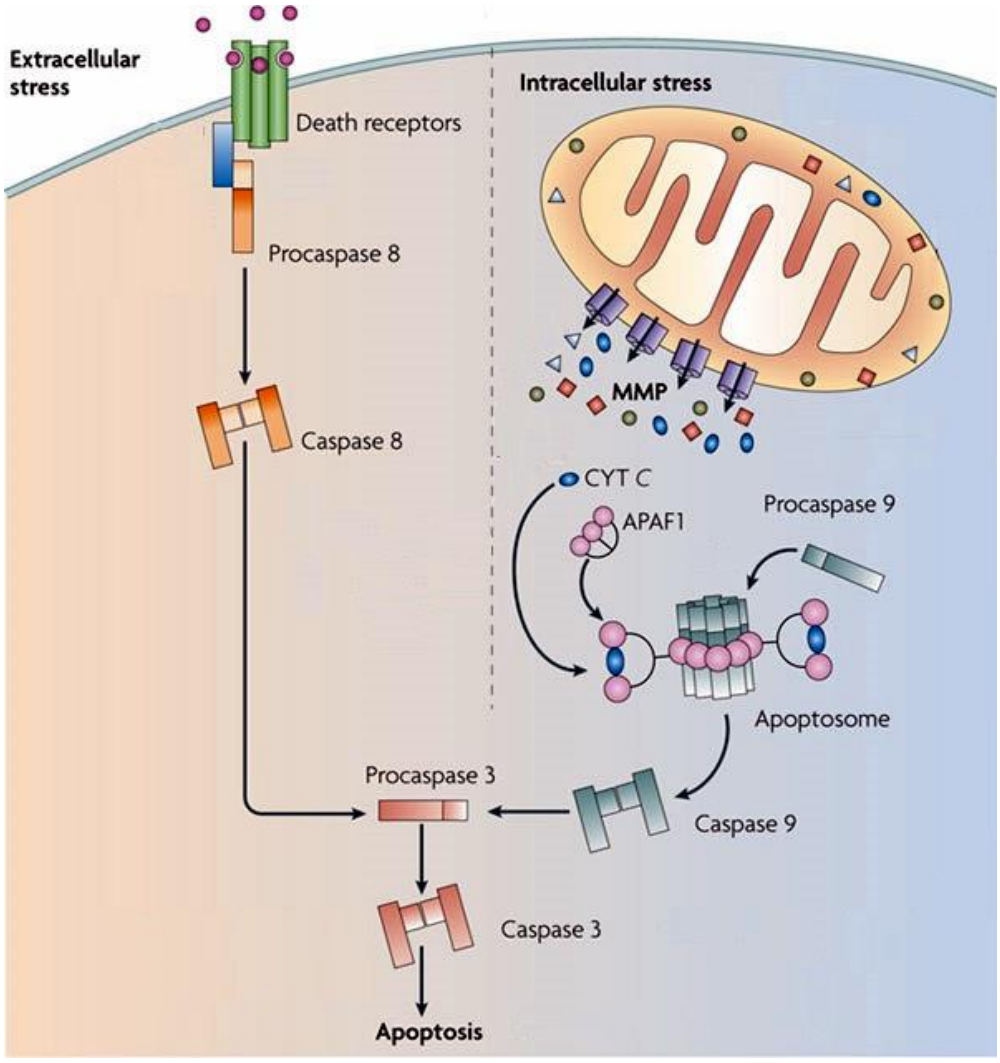

Figure 0.2. Extrinsic and intrinsic apoptotic pathways. Ligand binding to transmembrane death receptors activates the extrinsic pathway, whereas intracellular stress triggers mitochondrial apoptosis. Both biochemical cascades begin with the activation of initiator caspases (caspase-8 and 9, respectively), which catalyze the proteolytic maturation of executioner caspases (caspase-3). The intrinsic pathway is characterized by mitochondrial membrane permeabilization (MMP), resulting in the release of pro-apoptotic proteins into the cytosol, such as cyt c. The innteraction of cyt c with the adaptor protein apoptotic peptidase activating factor 1 (APAF 1) and procaspase 9 form the apoptosome structure, responsible for the activation of caspase-9 and consecutively caspase-3. Retrieved and adapted from Galluzzi *et. al*[14].

The activation of the apoptotic pathway is followed by modifications in the phospholipid composition of the plasma membrane. Normally, the inner leaflet consists of phosphatidylserine (PS) and phosphatidylethanolamine (PE), whereas phosphatidylcholine (PC) and sphingomyelin (SM) are present in the outer leaflet. Phospholipid transport across the plasma membrane is maintained by three different classes of proteins: flippases, floppases and scramblases. Flippases and floppases move phospholipids in a single direction against a concentration gradient, requiring ATP to maintain membrane asymmetry. The first class is responsible for the transport of PS and PE from the outer to the inner leaflet, whereas floppases move PC and SM in the opposite direction. Finally, scramblases are responsible for a bidirectional transport, acting according to the concentration gradient[15,16] (**Fig. 1.3**). The disruption of this asymmetry leads to the activation of immune cells[17], coagulation cascade[15], exocytosis and apoptosis[1,17]. Particularly, during apoptosis, scramblases transport PS across the lipid bilayer to the outer leaflet. This process is known as the "eat me signal", since it serves as a platform for the engulfment of the dying cells by phagocytes[1,15].

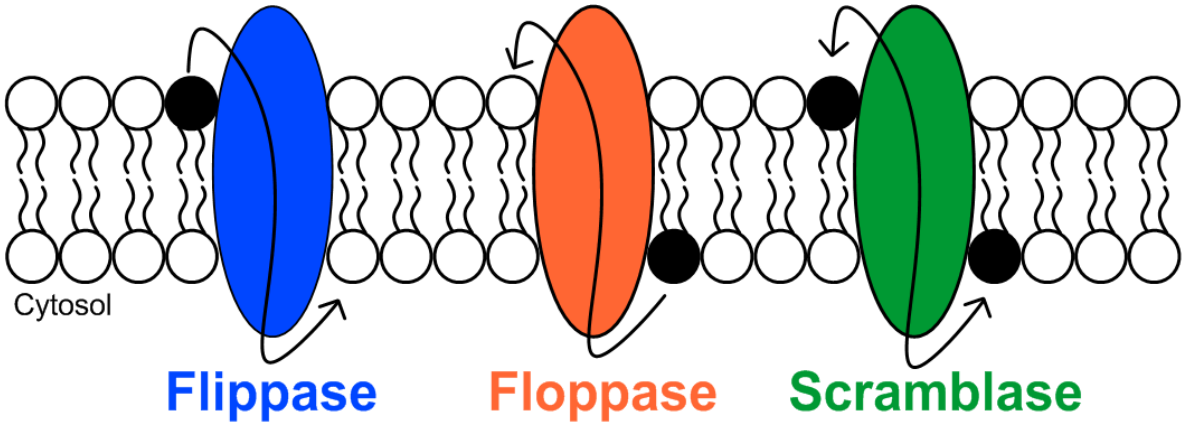

Figure 0.3. Schematic representation of the function of flippases, floppases and scramblases. Flippases move PS and PE from the outer to the inner leaflet, whereas floppases transport PC and SM in the opposite direction, using energy from ATP hydrolysis. Scramblases are ATP-independent and move phospholipids in both directions according to a concentration gradient.

1.2 Anoctamin 6 – A unique member of the Anoctamin family

Anoctamin 6 (ANO6, TMEM16F) is a particular member of the Anoctamins, a family of ten proteins (ANO1-10, TMEM16 A-K). ANO1, ANO2 and ANO6 have been identified as endogenous Ca^{2+}-activated Cl^- channels (CaCC)[18–20]. It is a dimeric plasma membrane protein with ten transmembrane α-helices and a pore loop[21]. ANO6 is homologous to ANO1, sharing a high sequence identity in the putative transmembrane-spanning domains of the pore region[22]. Apart from its function as a CaCC, ANO6 is also described as a volume-regulated[23–25] and outwardly rectifying Cl^- channel (ORCC)[26], a non-selective cation channel[27] and a Ca^{2+}-dependent phospholipid scramblase[28,29]. Because it is a multifunctional protein and has an ubiquitous expression[22], ANO6 became an interesting subject for investigation.

Missense mutations in the TMEM16F gene and production of a defective ANO6 are the cause for the Scott Syndrome, a rare congenital bleeding disorder. Platelets from patients with Scott Syndrome are unable to scramble PS, a process required for the activation of coagulation factors and to keep a regular hemostasis[29–31]. Studies in mice revealed that knockout of the TMEM16F gene results in an increased bleeding time due to a suppression of platelet activation[27]. Moreover, ANO6 is not only involved in blood coagulation, but also in skeletal development[32], apoptosis[23,26,33,34], volume

regulation[23,24], microparticle shedding[22], innate immunity in macrophages[35], breast cancer[36], cell blebbing[35] and migration[37].

Despite all the research, ANO6 mechanism of action is still not completely understood. Although it is clear that high intracellular Ca^{2+} concentrations are required, it is unknown if Ca^{2+} activates ANO6 directly or through another Ca^{2+}-dependent molecule[19]. Another unresolved question is the structure of this protein and how it is able to transport lipids through an ion-conductive pore. Interestingly, Whitlock *et. al* suggests that all anoctamins evolved from phospholipid scramblases and acquired ion channel activity after structural rearrangements. It is possible that the ANO6 pore has a dual molecular composition (lipid and protein) that allows the transport of amphipathic molecules, an idea known as the proteolipidic pore hypothesis. In this regard, the ANO6 ion currents are probably just the result of ions that flow across the plasma membrane together with phospholipids[38]. This model is supported by crystallization of a fungal TMEM16 lipid scramblase homologue, nhTMEM16, a protein formed by ten transmembrane domains and a pore loop. It was found that the pore has a proteolipidic nature, having a hydrophilic region next to the lipid bilayer, surrounded by two transmembrane helices[21,38] (**Fig. 1.4**).

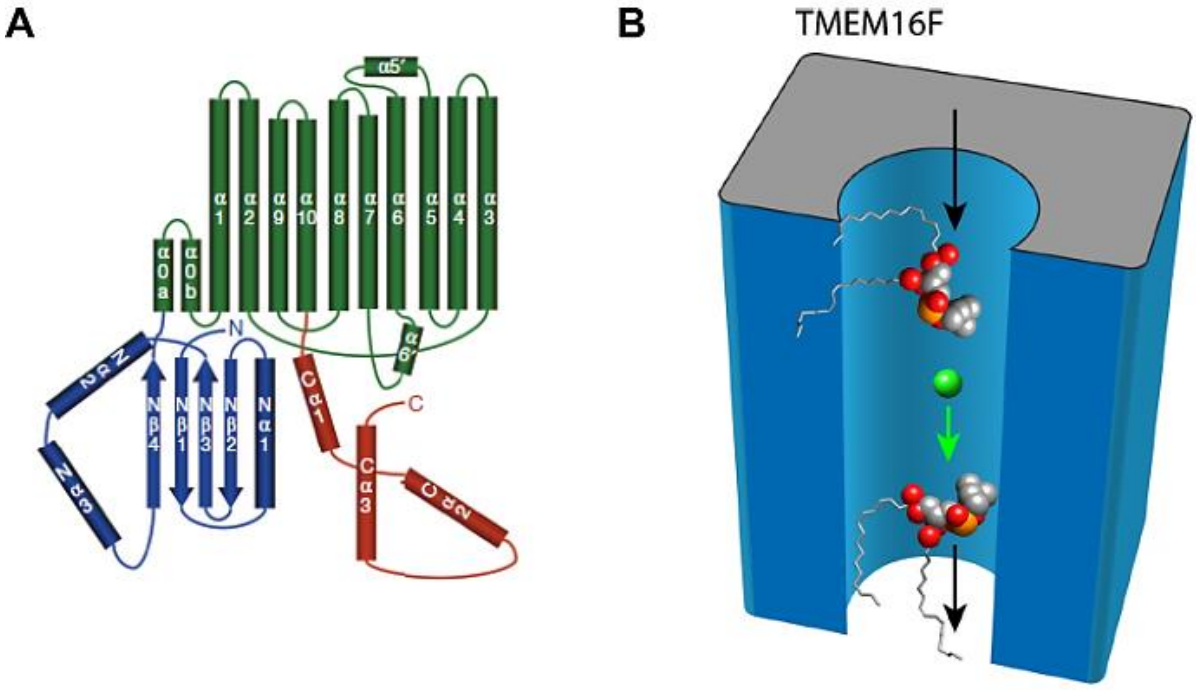

Figure 0.4. Model of Anoctamin structure and ANO6 pore. A) Topology of the Anoctamin homologue in *Nectria haematococca*, nhTMEM16. This structure is formed by ten transmembrane domains with a pore loop (green) and the N- and C-terminal domains in the cytosol (blue and red, respectively). Retrieved from Brunner *et al.*[21]. **B)** Cartoon showing the possible proteoplypidic furrow of ANO6 pore, viewed from the extracellular space. The particular molecular composition of the pore allows the transport of phospholipids and ions across the plasma membrane – along with ions, phospholipid head groups interact with the protein content of the furrow, whereas acyl chains are projected into the hydrophobic bilayer. Retrieved from Whitlock *et.al*.[38]

1.2.1 Role of Anoctamin 6 in Apoptosis

The identification of ANO6 as a Ca^{2+}-dependent phospholipid scramblase[28,29] raised questions about the involvement of this protein in apoptosis. Remarkably, ANO6 has a marked expression in the surface of epithelial cells from mouse colon, which have a high apoptosis rate, compared to colonic crypt cells, known to have a fast proliferation[26].

In this regard, ANO6 was found to be a component of the ORCC, an ubiquitous ion channel known to be inactive in healthy cells and activated during apoptosis, leading to cell shrinkage and phospholipid scrambling[22,26]. As a matter of fact, Martins *et. al* proved that stimulation of both intrinsic and extrinsic apoptotic pathways activate ANO6-dependent currents in T Lymphocytes, human alveolar and airway epithelial cells. These currents were sensitive to the broad anoctamin inhibitors and completely abolished by ANO6 downregulation[26]. The same pattern was found in *Xenopus* Oocytes overexpressing ANO6 after stimulation with Paraquat, a ROS donor[22].

In parallel, Juul *et. al* observed a decrease in cisplatin-induced caspase-3 activity after knockdown of ANO6 in ELA cells[23]. This protein is known to be involved in RVD (Regulatory Volume Decrease)[23–25] and many channels important for this process are also relevant for AVD (Apoptotic Volume Decrease). Therefore, it was speculated that ANO6 facilitates apoptosis by mediating cell shrinkage[23].

Different studies show a clear contribution of ANO6 to apoptosis as an ion channel[26,34]. However, investigations in B Lymphocytes revealed that this protein is not crucial to the PS exposure detected in apoptotic cells[34]. Cell death is a fundamental process in all living systems and it is very likely that other proteins contribute for this process, compensating possible defects. It is now known that ANO3, 4, 7, 9 and 10 are also phospholipid scramblases[22,39] and, aside from the anoctamin family, XkR8 (Xk-related protein 8) is also reported to be responsible for phospholipid scrambling during apoptosis[40].

1.3 CFTR

1.3.1 CFTR and Cystic Fibrosis – An Overview

Cystic Fibrosis (CF) is the most common life-threatening autosomal recessive disease in Caucasians, affecting around 70,000 people worldwide[41]. It is caused by mutations in the CFTR gene (Cystic Fibrosis Transmembrane conductance Regulator) and is mainly characterized by an imbalance of ion and fluid homeostasis[42]. This gene encodes for a cyclic AMP (cAMP)-regulated Cl^- channel expressed in the apical membrane of epithelial cells from the intestine, pancreas, airways and sweat glands[43].

Principal symptoms of CF include: production of thick mucus and subsequent infection by *Pseudomonas aeruginosa* in the airways; pancreatic insufficiency with obstruction of pancreas ducts and damage of the exocrine function; intestine impairment; elevated concentration of electrolytes in sweat and male infertility[41,44].

So far around 1,500 variants of mutations in the CFTR gene have been identified. Despite this diversity, a deletion of phenylalanine (F) at codon 508 (ΔF508) on chromosome 7 is the main cause for CF, affecting 90% of patients. This mutation results in an abnormal folding of CFTR and a trafficking defect from the ER (Endoplasmic Reticulum) to the plasma membrane[45].

The predicted CFTR sequence contains 1,480 amino acids residues[43] arranged in two membrane-spanning domains (MSD), two nucleotide-binding domains (NBD) and one regulatory domain (R)[46] (**Fig. 1.5**). CFTR evolved from the ATP-binding cassette (ABC) transporters, sharing a high sequence and structure similarity with these proteins[42]. Activation of CFTR requires phosphorylation of serine residues in the R domain by the cAMP- dependent Protein Kinase A (PKA). ATP binding to the NBD domains and its subsequent hydrolysis allows the pore opening and provides enough energy to the transport of substances. Once the R domain is dephosphorylated by phosphatases CFTR returns to its closed status. Thus, the balance between kinase and phosphatase activity together with ATP levels are the main regulators of CFTR gating[42,44,47].

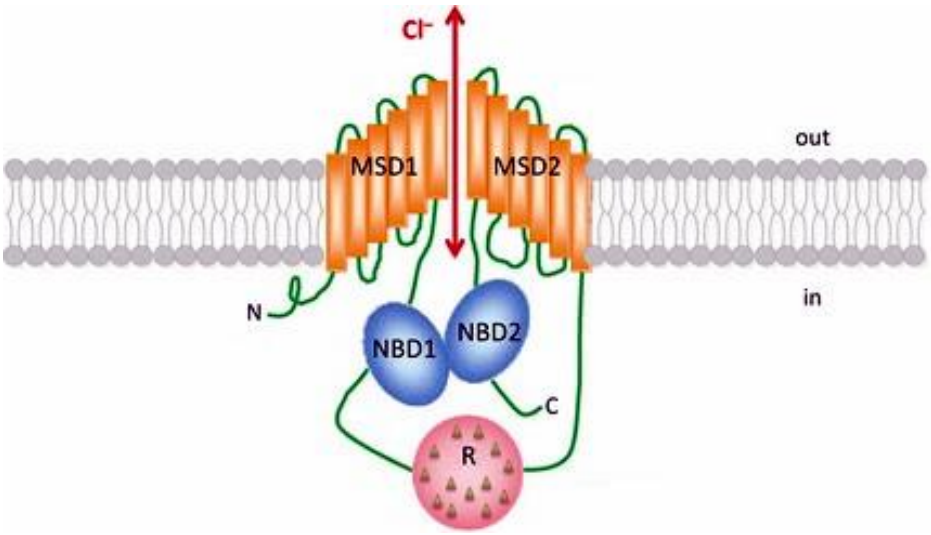

Figure 0.5. Scheme of CFTR structure. CFTR is inserted in the plasma membrane and contains two MSD domains (MSD1, MSD2), two NBD domains (NBD1, NBD2) and one R domain with multiple phosphorylation sites. Retrieved and adapted from Farinha *et.al.*[46].

Regardless the continuous efforts in understanding CFTR at its functional and molecular level, CF remain a lethal disease. By attenuating symptoms, life expectancy has been significantly increased to around 37 years-old. However, chronic lung disease and resulting loss of pulmonary function is still a major uncontrolled problem, being responsible for 80% of mortality[41]. Nowadays, different therapy approaches are under development, either based on the identification of compounds that rescue the CFTR trafficking defect (correctors) or stimulators of channel activity (potentiators)[45].

1.3.2 CFTR, Cystic Fibrosis and Apoptosis

As described before, apoptosis is a non-inflammatory fundamental process essential to the clearance of aged or harmed cells. Notably, CF disease is characterized by a defective apoptosis, a problem that may contribute to the ongoing inflammations. The involvement of CFTR in cell death has been studied over the years and, although some results are controversial, it seems clear that this Cl^- channel is a pro-apoptotic factor[48].

CFTR has been described as a regulator of the redox status in the airways, mediating the transport of GSH (Glutathione) to the extracellular space[49]. GSH is a major antioxidant, responsible for scavenging the ROS produced as a result of cellular metabolism[50]. Indeed, measurements in the lung epithelial lining fluid of CF patients revealed a lower content in GSH compared to healthy individuals[51]. Therefore, mutations in CFTR impair GSH efflux and leads to an increase of the oxidative stress in the airways[52].

On the other hand, as GSH is transported, the intracellular level of this antioxidant decreases. Hence, cells expressing *wt* CFTR are less capable to buffer high concentrations of ROS and have a higher susceptibility to apoptosis. Indeed, a relationship between CFTR, GSH efflux and apoptosis was found in mice proximal tubules where this protein may be responsible for AVD and caspase-3 activation[53]. In a different study HeLa cells were transfected with *wt* or ΔF508 CFTR and it was found an association among CFTR, GSH transport and Bax activation, a pro-apoptotic protein[54].

Intracellular acidification is an essential phenomenon during apoptosis, required for caspase activation and DNA cleavage. Interestingly, CFTR is known to secrete not only Cl^-, but also bicarbonate, regulating the pH from intracellular compartments. Analysis of mucus collected from lungs of CF

patients revealed the presence of high molecular DNA, which contributes to the increased viscosity. One explanation for this observation may be related to the apoptosis dysfunction found in CF epithelial cells[55]. Studies in Chinese hamster lung fibroblasts and mouse mammary epithelial cells proved an association between DNA fragmentation and CFTR. Cells expressing ΔF508 CFTR have a higher intracellular pH, due to the lack of Cl^- and bicarbonate transport. Thus, when these cells are exposed to an apoptotic stimulus, the intracellular pH prevents nuclear condensation and DNA degradation[55,56].

The apoptotic signaling cascade is complex, involving multiple molecules and signals. In this pathway ceramide acts as a messenger mediating the activation of apoptosis[57]. Ceramide intracellular level is regulated by a balance in the activity of two different enzymes: acid sphingomyelinase (Asm) and acid ceramidase (Ac), responsible for ceramide production and degradation, respectively[57,58]. Asm is triggered by *Pseudomonas aeruginosa* infection , leading to the increase of the ceramide content in lipid rafts[59]. Ceramide-enriched lipid rafts are required for pathogen elimination and apoptosis. However, in 2008 a study concluded that ceramide accumulation also facilitates inflammation, cell death and infections in CF[60]. A high level of ceramide in the respiratory tract of uninfected CFTR-deficient mice was found to be responsible for persistent inflammations and death of respiratory epithelial cells. When CFTR is mutated the intracellular vesicles have a higher pH, which leads to an imbalance of Asm and Ac activities and consequently to accumulation of ceramide in membrane lipid rafts. Therefore, by administrating acid sphingomyelinase inhibitors it is possible to stabilize ceramide levels and decrease inflammation[61].

1.4 Interaction between ANO6 and CFTR

The concept that CFTR may interact or regulate other Cl^- channels and transporters has been around for many years. Before the identification of CFTR, ORCC was thought to be the Cl^- channel defective in Cystic Fibrosis[22]. Nowadays, it is known that CFTR and ORCC are independent channels that share functional relationships[62]. Interestingly, Martins *et. al* found that ANO6 is a component of the ORCC channel and may also be regulated by CFTR[26]. However, it is unknown if these ion channels interact directly or through other scaffold proteins[63]. Notably, ANO6 is responsible for ORCC activation during apoptosis, a phenomenon that becomes enhanced in the presence of CFTR. Martins *et. al* also reported a decrease of the cAMP-activated whole-cell conductance in airway epithelial cells expressing CFTR after knockdown of ANO6, which suggests a contribution of ANO6 to CFTR currents[26].

1. OBJECTIVES

The aim of the present work was to study the relationship between ANO6 and CFTR during ROS-mediated apoptosis, using different *in vitro* systems.

The first objective was to understand the impact of ROS in ANO6 activity. To achieve this, HEK293 and HeLa cells were used either to overexpress ANO6 or downregulate the endogenous expression of this protein. In parallel experiments, B Lymphocytes immortalized from a Scott patient and a healthy control[64] were useful to compare the presence and total absence of functional ANO6. The current properties of ANO6 after ROS induction were studied by patch clamp. Moreover, the phospholipid scramblase function of this protein was monitored by flow cytometry using Annexin V labeling.

Because CFTR regulates the intracellular redox status[49], the next question to address would be if CFTR-mediated GSH depletion and consequent intracellular ROS increase explain a possible relationship between these two ion channels. In order to accomplish this, co-expression studies were done in HEK293 cells and the same techniques were applied. Additionally, the CFBE cell line stably transfected with *wt* or ΔF508 CFTR was used as a system to look for the influence in ROS-mediated apoptosis of the most predominant CFTR mutation found in CF patients.

The understanding of the role of ANO6 and CFTR in regulated cell death can be useful to get new insight about the apoptotic dysfunction that characterizes CF and eventually create new therapeutic approaches.

2. MATERIALS AND METHODS

3.1 CELL CULTURE

Cell lines were grown inside an incubator, at 37°C in a 5% CO_2-95% air humidified water-saturated atmosphere. All cell culture was performed according to standard conditions, using sterile equipment. Every 2 to 5 days, cells were trypsinized (70-90% confluency) from 75 or 25 cm^2 flasks (Greiner bio-one - CELLSTAR®, Frickenhausen, Germany) and, if necessary, seeded in plastic plates (M&B Stricker Laborfachhandel GbR, Bernried, Germany) at the required density to preform experiments.

3.1.1 Mammalian Cell Lines and Culture Conditions

HEK293 (Human Embryonic Kidney 293)[65] and HeLa[66] (Henrietta Lacks Cervical Carcinoma) cell lines were cultured in Dulbecco's Modified Eagle Medium (DMEM; Life Technologies - gibco®, Karlsruhe, Germany), supplemented with 10% Fetal Bovine Serum (FBS; Life Technologies - gibco®, Karlsruhe, Germany).

HeLa–Kyoto cells stably transfected with eYFP[67] (Enhanced Yellow Fluorescent Protein) with three point mutations (H148Q, I152L, F46L) were cultured in MEM (Minimum Essential Medium), GlutaMAX™ (Life Technologies - gibco®, Karlsruhe, Germany), supplemented with 10% FBS, 1% Penicillin-Streptomycin (Pen Strep; Life Technologies - gibco®, Karlsruhe, Germany) and 200 µg/mL Hygromycin B (Promocell, Heidelberg, Germany).

B Lymphocytes, isolated from a patient with Scott Syndrome and a control subject[64], were cultured in Roswell Park Memorial Institute medium (RPMI; Life Technologies - gibco®, Karlsruhe, Germany), supplemented with 10% FBS, 1% Pen Strep and 5 mM Hepes Buffer Solution (Life Technologies - gibco®, Karlsruhe, Germany).

CFBE cells[68] (Cystic Fibrosis Bronchial Epithelial cells) stably transfected with *wt* or ΔF508 CFTR were cultured in MEM, supplemented with 10% FBS and 2,5 µg/mL Puromycin (Life Technologies - gibco®, Karlsruhe, Germany).

To trypsinize adherent cells from flasks (HEK293, HeLa, HeLa-Kyoto, CFBE), cultured medium was first removed by aspiration and cells were washed with Dulbecco's Phosphate Buffered Saline (PBS; Life Technologies - gibco®, Karlsruhe, Germany), without Ca^{2+} and Mg^{2+}. Trypsin (Life Technologies - gibco®, Karlsruhe, Germany) was added to culture flasks and incubated at 37°C, 5% CO_2 for 5 min (HEK293, HeLa, HeLa-Kyotto) or 15 min (CFBE). To stop the trypsinization process, medium containing 10% FBS was added to cell suspension, which was then centrifuged at 20 000 rpm for 3 min. For B Lymphocytes, suspension cells were collected and centrifuged at 20 000 rpm for 5 min. In both cases, after the centrifugation step, supernatant was discarded and cells were resuspended in fresh culture medium.

3.1.2 Transient Transfections

All transient transfections were performed using Lipofectamine™3000 reagent (Invitrogen, Germany), according to manufacturer's instructions. Lipofection is a particular method of transfection, where the genetic material is delivered to cells through a cationic lipid that forms liposomes and interacts with nucleic acid molecules (negatively charged). With lipofection it is possible to have a high uptake of the genetic material, allowing an easy overexpression of a protein of interest, using DNA, or a downregulation of a target gene, by siRNA (small interfering RNA)[69,70].

HEK293 and HeLa cells were transfected with a pcDNA3.1 vector encoding for human ANO6. CFTR was transfected only in HEK293 cells, using a pIRES vector with the respective sequence coupled to a CD8 (Cluster of Differentiation 8) receptor, which was proved to be the available plasmid with the best transfection efficiency. In every experiment, an empty pcDNA3.1 vector (mock) served as a control and the same amount of plasmid was used in all transfections. When ANO6 and CFTR were co-expressed in HEK293 cells, a ratio of 1:2 µg was applied. Co-transfection protocol was controlled by co-expressing the mock plasmid either with ANO6 or CFTR (using the same ratio). For patch clamp measurements, all transfections were done using a plasmid containing ANO6 or CFTR sequence linked to a CD8 receptor. Experiments were performed between 48h and 72h after transfections. All the cDNA used is described in the Appendices section (**Appendix I – Table 8.1**).

ANO6 endogenous expression was downregulated in HEK293 and HeLa cells, using different siRNA's (Invitrogen, Paisley, UK) and confirmed by *Western Blot* (WB). A negative control (Ambion®, Darmstadt, Germany) with no sequence similarity for human, mouse or rat gene sequences was used to control the effects of the siRNA delivery. Experiments and collection of protein for WB were done between 24h and 72h after transfection.

3.1.3 Apoptosis Induction

Tert-Butyl Hydroperoxide (tBHP, Sigma, Taufkirchen, Germany) was diluted in deionized filtered water to a final concentration of 100 mM. HEK293 cells were incubated with 100 µM tBHP in OptiMEM (Life Technologies - gibco®, Karlsruhe, Germany), a reduced serum medium (2% serum). CFBE cells were incubated with 100 µM tBHP diluted in MEM. Staurosporine (STS, Merck, Darmstadt, Germany) was dissolved in DMSO (dimethyl sulfoxide) to a final concentration of 1 mM. HEK293, HeLa and B lymphocytes were incubated with 1 µM STS diluted in OptiMEM, DMEM or RPMI, respectively. The appropriate volume of DMSO was added to non-treated controls. Hydrogen peroxide (H_2O_2, Riedel-de Haen, Seelze, Germany) was diluted in MEM to a final concentration of 900 µM and incubated in CFBE cells. Lyso-phosphatidylserine (Lyso-PS, Avanti Lipid, Alabama, U.S.A) was dissolved in chloroform to a final concentration of 10 mM. HEK293 cells were incubated with 10 µM Lyso-PS for 2h diluted in DMEM. The appropriate volume of chloroform was added to non-treated controls. All compounds were incubated for the indicated periods of time at 37°C, 5% CO_2, except Ionomycin (Iono, Biomol, Hamburg, Germany) which was added to cells after cell detachment during experiments to a final concentration of 1, 5 or 10 µM. Inhibitors were purchased from Sigma (Taufkirchen, Germany) and pre-incubated for at least 30 min at 37°C, 5% CO_2.

3.2 PROTEIN ANALYSIS – *WESTERN BLOT*

ANO6 expression was downregulated in HEK293 and HeLa cells (see section 3.1.2 – 3.1.2 Transient Transfections) and confirmed by WB. Additionally, ANO6 endogenous expression was detected in CFBE cells. In order to accomplish this, protein was collected from cells and kept in a lysis buffer (mM: 50 Tris-HCl, 150 NaCl, 50 Tris, 100 DTT, 0.5% NP-40, 1% protease inhibitor cocktail) - Roche, Germany. Then, protein content was separated in an 8,5% SDS-PAGE Polyacrylamide gel and separated proteins were transferred to a PVDF (Polyvinylidene fluoride) membrane (GE Healthcare Europe GmbH, Munich, Germany). To detect ANO6, the membrane was incubated with a primary antibody (rabbit antihuman ANO6 – David Technology, Germany) overnight at 4°C, using a dilution factor of 1:500 – 1:1000. Proteins were visualized using a horseradish peroxidase (HRP) - conjugated goat antirabit secondary antibody (Dilution Factor of 1:10000) and ECL Detection Kit (GE, Healthcare, Munich, Germany). Protein bands were detected using a FujiFilm LAS-3000 (FujiFilm, Tokyo, Japan).

Experiments were kindly performed by Podchanart Wanitchakool.

3.3 FLUORESCENCE MICROSCOPY

3.3.1 ROS Detection

Intracellular ROS detection is possible using fluorescence assays. H_2DCFDA (2',7'-dichlorodihydrofluorescein diacetate, Molecular Probes, Invitrogen, Germany) is a non-fluorescent molecule able to cross plasma membranes. Once in the cytosol, this probe is deacetylated by intracellular esterases and, as a consequence, trapped inside the cell. In the presence of ROS, the deacetylated form is oxidized to a highly fluorescent form, DCF - 2',7'-dichlorofluorescein (**Fig. 3.1)**. Thus, the fluorescence intensity is an index of intracellular ROS level.

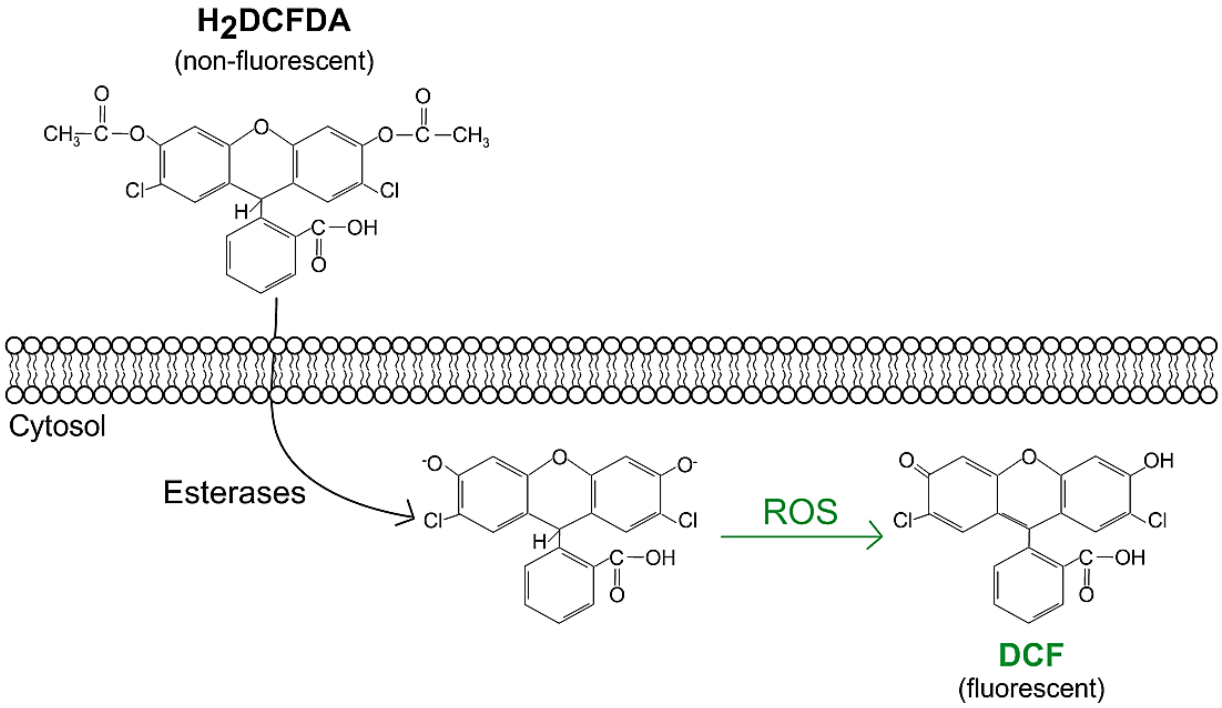

Figure 2.1. Mechanism of ROS detection by H_2DCFDA. H_2DCFDA is able to cross the plasma membrane. Once inside the cell, the probe is deacetylated by esterases, ensuring probe retention in the cytosol. In the presence of ROS, the non-fluorescent molecule is oxidized to DCF, which is highly fluorescent, allowing intracellular ROS detection.

Due to easy oxidation, H_2DCFDA was dissolved shortly before experiments in DMSO to a final concentration of 10 mM. To detect ROS, HEK293 and HeLa cells were seeded in 18 mm collagen/fibronectin-coated glass cover-slips overnight. Cells were loaded with a solution of 10 µM of H_2DCFDA in PBS with Ca^{2+} and Mg^{2+} (Life Technologies - gibco®, Karlsruhe, Germany) for 30 min at 37°C, 5% CO_2. After loading, the probe was washed 2 times with PBS and the ROS inducer was added to cells (tBHP or STS) for the desired period of time. Fluorescence increase was detected with an ApoTome Axiovert 200M fluorescent microscope (Zeiss, Germany), using an excitation wavelength of 493 nm and emission of 520 nm.

Alternatively, ROS was detected using a fluorogenic cytosolic sensor, MAK142 (Taufkirchen, Germany), which becomes fluorescent in the presence of superoxide and hydroxyl radicals. In this case, HEK293 cells were plated in 18 mm collagen/fibronectin-coated glass coverslips overnight and treated with STS. After apoptosis induction, MAK142 was added to cells and fluorescence was monitored. Fluorescence increase was detected with the same microscope, using an excitation wavelength of 646 nm and emission of 654 nm.

3.4 Flow Cytometry – Apoptosis Detection

Flow cytometry is a laser-based technology that allows single cell measurements. It is commonly used to get information about fluorescence of a pre-labeled population of cells. Once samples are injected into the flow cytometer, molecules are excited by a light source and fluorescence of single cells is detected. This is a multifunctional technique, which also allows the analysis of physical properties, such as cell size or granularity, two parameters given by forward (FSC) and side (SSC) scatter, respectively. To study regulated cell death in the present work, a four optical filter BD Accuri™ C6 Cytometer (BD Biosciences, Heidelberg, Germany) was used.

3.4.1 Caspase-3 Activity Measurements

NucView™ 488 Caspase-3 substrate (Biotium, Fremont, USA) is a fluorogenic sensor used for the detection of caspase-3 activity. It is formed by a DNA marker linked to a peptide sequence (DEVD). Once this substrate crosses the cell membrane, the DEVD sequence is cleaved by caspase-3 and the DNA dye is free to stain the nucleus (**Fig. 3.2)**. Therefore, by measuring the fluorescence intensity of the DNA marker it is possible to monitor caspase-3 activity.

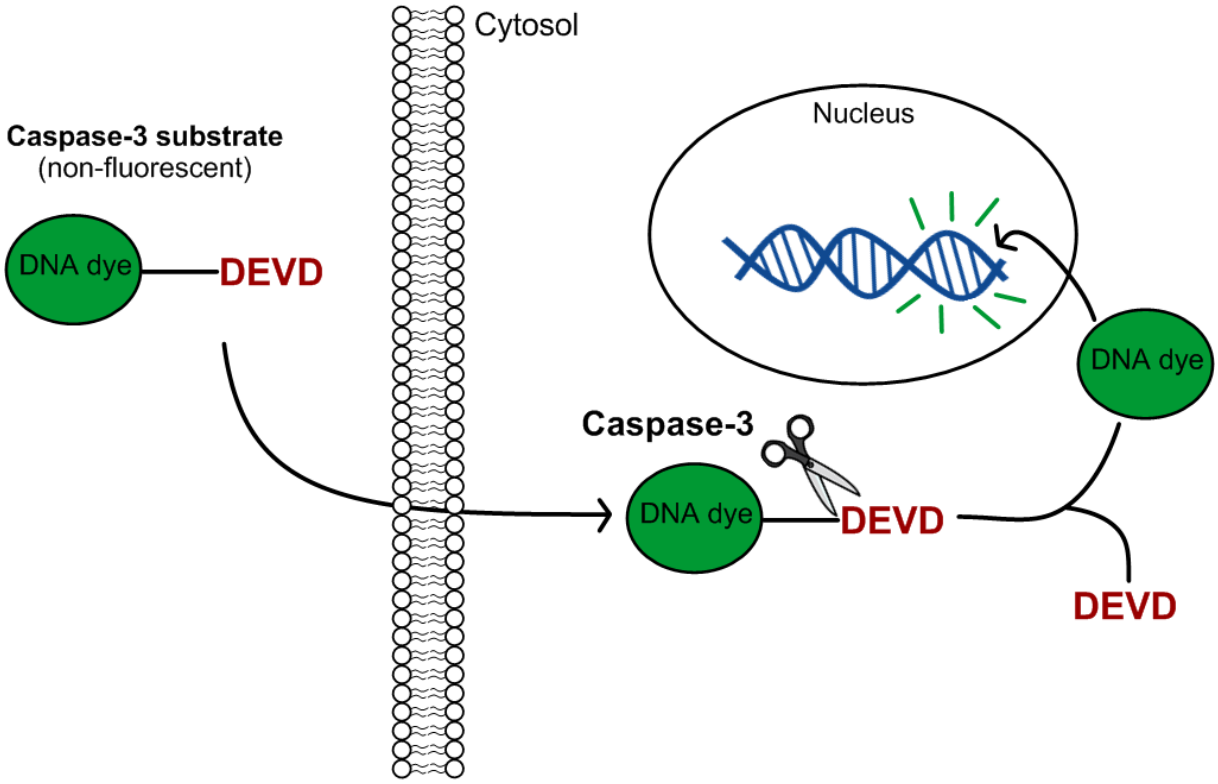

Figure 2.2. Mechanism of Caspase-3 activity detection by NucView™ 488 Caspase-3 substrate. Caspase-3 substrate is formed by a peptide sequence (DEVD) linked to a DNA fluorogenic sensor. Once inside the cell, the substrate is cleaved at the DEVD sequence by caspase-3, releasing the DNA dye, which is then free to stain the nucleus.

In order to detect caspase-3 activation after ROS induction, HEK293 and HeLa cells were seeded overnight and incubated as desired for the indicated periods of time. Following treatment, the media was collected and cells were washed with PBS. After, adherent cells were detached with accutase (Capricorn Scientific GmbH, Ebsdorfergrund, Germany), incubated for 3 to 5 min, at 37°C, 5% CO_2. Then, the reaction was stopped with DMEM, supplemented with 10% FBS and suspension cells were centrifuged 2 times for 10 min (1500 rpm, 4°C). Cells were resuspended in a solution of caspase-3 substrate diluted in PBS (2.5 µL substrate in 100 µL of PBS / sample) and incubated for 30 min at room temperature,

protected from light. Before measurements, DNA labeling was stopped with PBS (300 µL/ sample) and fluorescence was detected by flow cytometry, using filter 1 (excitation - 488nm; emission - 530 nm).

3.4.2 Annexin V and 7-AAD Labeling

As described in the Introduction chapter, exposure of phosphatidylserine is one of the apoptosis hallmarks. Annexin V (Annx V) belongs to the annexin family of proteins, having the particularity of being able to bind specifically to PS in the presence of millimolar concentrations of Ca^{2+} [71]. Thus, by conjugating Annx V with the fluorophore FITC (Fluorescein isothiocyanate) it became possible to monitor PS exposure by flow cytometry.

Annx V labeling is usually coupled to 7-AAD (7-Aminoactinomycin D), a membrane impermeable DNA marker with high affinity for G-C regions[72]. By combining these two dyes it is possible to distinguish between early/late apoptosis and necrosis: PS exposure is an early event in apoptosis, whereas changes in the plasma membrane permeability are characteristic from late apoptotic stages or necrosis. Therefore, fluorescence intensity in an early apoptotic cell will be positive for Annx V and negative for 7-AAD, whereas a late apoptotic or necrotic cell will be positive for both dyes.

By flow cytometry it is possible to measure Annx V and 7-AAD fluorescence intensity and conclude about cell viability. Both parameters can be compared in a 4-quadrants plot, representing either positivity or negativity for Annx V (x axis) and/or 7-AAD (y axis). The quadrants setting is defined with viable cells which maintain the plasma membrane asymmetry and integrity and thus are negative for both dyes (**Fig. 3.3**).

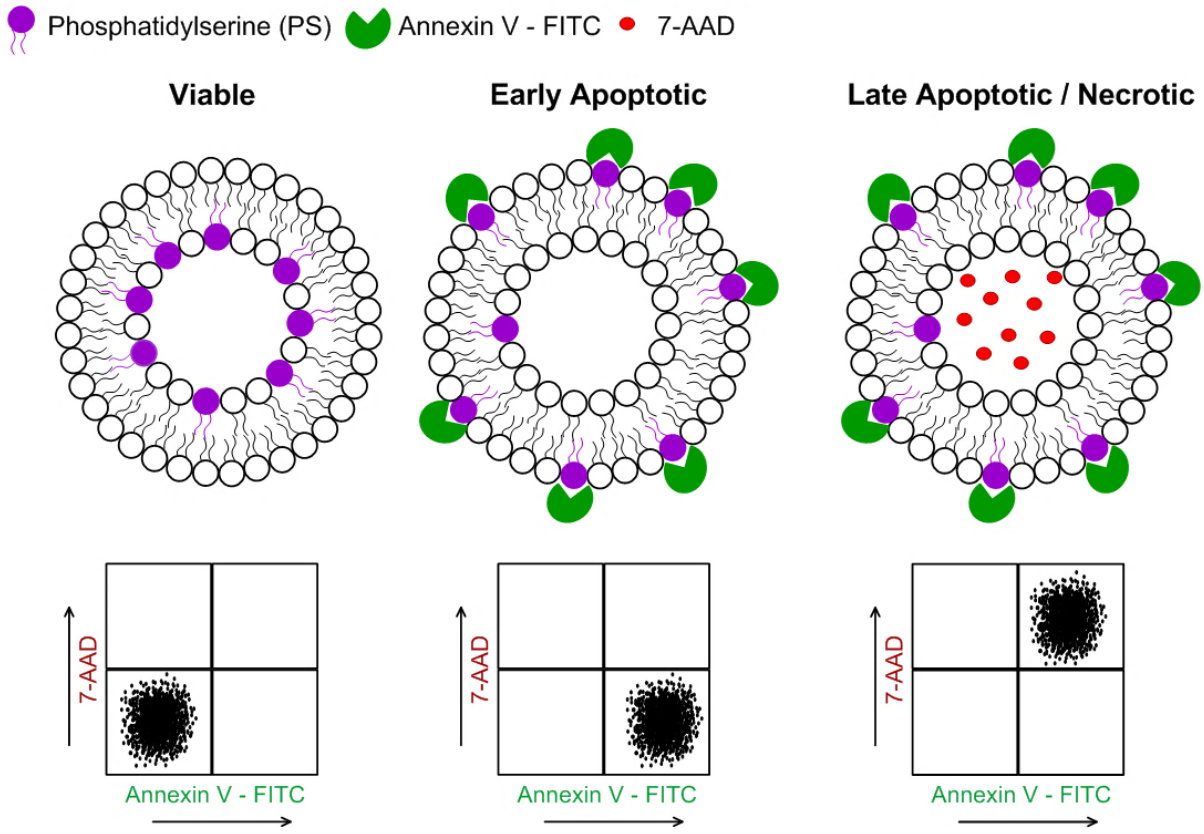

Figure 2.3. Schematic representation of dual staining with Annx V and 7-AAD. In a viable cell the plasma membrane is intact and asymmetric, therefore Annx V and 7-AAD fluorescence intensity is negative (lower-left quadrant). In an early apoptotic cell PS moves from the inner to the outer membrane leaflet, which allows Annx V binding (lower-right quadrant). Once cells enter in late apoptosis/ necrosis, the plasma membrane permeability is compromised and 7-AAD can enter the cell. Thus, cells become positive for both markers (upper-right quadrant).

In order to detect membrane modifications during apoptosis, cells were treated according to the previous section and media was collected after the indicated time points. Adherent cells (HEK293, HeLa and CFBE cells) were then washed with PBS and detached with accutase for 3-15 min at 37°C, 5% CO_2. After cell detachment, accutase reaction was stopped with DMEM/MEM, supplemented with 10% FBS. Suspension cells (B Lymphocytes) were collected after apoptosis induction. In both cases, cells were centrifuged 2 times for 10 min at 1 500 rpm (4°C). Following centrifugations, each sample was incubated in a solution of 5 µL Annx V and 2,5 µL 7-AAD, diluted in 100 µL Annexin V-binding buffer (BioLegend, Fell, Germany) for 10 min at room temperature, protected from light. After labeling, the reaction was stopped with PBS (400 µL/sample). For each experiment, 10 000 events were collected and fluorescence was detected by flow cytometry, using filter 1 for Annx V (excitation – 488 nm; emission - 530 nm) and filter 3 for 7-AAD (excitation – 488 nm; emission – 670 nm). The emission spectra of Annx V and 7-AAD overlap at some extent. Therefore, to avoid a false positive, the signal was always compensated using a pre-determined value.

3.5 HOLOGRAPHIC MICROSCOPY

Holographic microscopy is a non-invasive label-free method used to monitor adherent cells. The HoloMonitor™ M2 (Phase Holographic Imaging AB, Lund, Sweden) is a microscope that uses digital holography to acquire and quantify information about cell shape, volume, area, confluence and thickness[73]. For this purpose, the microscope is placed inside an incubator at 37°C with a humidified atmosphere saturated with 5% CO_2, where cells can be monitored over time.

This method was useful to follow cellular morphology after apoptosis induction in HEK293 cells. In order to accomplish this, cells were seeded one or two days before experiments in collagen/fibronectin-coated petri-dishes and monitored for the desired period of time in the presence or absence of ROS inducer.

3.6 CONDUCTANCE MEASUREMENTS

3.6.1 YFP Fluorescence Quenching Assay

The Yellow Fluorescent Protein (YFP) is particularly interesting due to its sensibility to surrounding halide concentrations. This sensor has a cavity formed by a specific binding site for halide ions, such as iodide (I^-) or chloride (Cl^-)[74]. Binding of anions to this cavity leads to a decrease in the YFP fluorescence intensity over the time (quenching).

HeLa-Kyoto cells stably expressing eYFP were used to measure anion conductance during apoptosis. In this cell line the YFP sequence is modified with three different point mutations (H148Q, I152L and F46L), which enhance the halide affinity[74]. Briefly, cells were seeded in collagen/fibronectin-coated transparent 96 well-plates (Thermo Fisher Scientific, Darmstadt, Germany) and incubated at 37°C, 5% CO_2 with STS diluted in Ringer -40 mM Cl^- solution (mM: 105 NaCl; 0,4 KH_2PO_4; 1,6 $K_2HPO_4 \cdot 3H_2O$; 5 Glucose; 1 $MgCl_2 \cdot 6H_2O$; 1,3 Ca-Gluconate$\cdot 1H_2O$; 40 Na-Gluconate; pH 7.4). After incubation, YFP fluorescence was measured at 37°C by a Microplate Reader (BMG LABTECH, Offenburg, Germany; excitation – 485 nm; emission – 520 nm) each second, during 30 seconds. Following this, a Ringer solution was injected containing NaI to a final concentration of 20 mM (mM: 105 NaCl; 0,4 KH_2PO_4; 1,6 $K_2HPO_4 \cdot 3H_2O$; 5 Glucose; 1 $MgCl_2 \cdot 6H_2O$; 1,3 Ca-Gluconate$\cdot 1H_2O$; 40 NaI; pH 7.4) and fluorescence was measured for 1 minute, every second.

Thus, by using this method it is possible to study channel activity: when ion channels are closed, injection of I^- does not interfere with YFP fluorescent signal; however, once ion channels are opened, I^- is able to cross the plasma membrane and bind to YFP, quenching its fluorescence (**Fig. 3.4**).

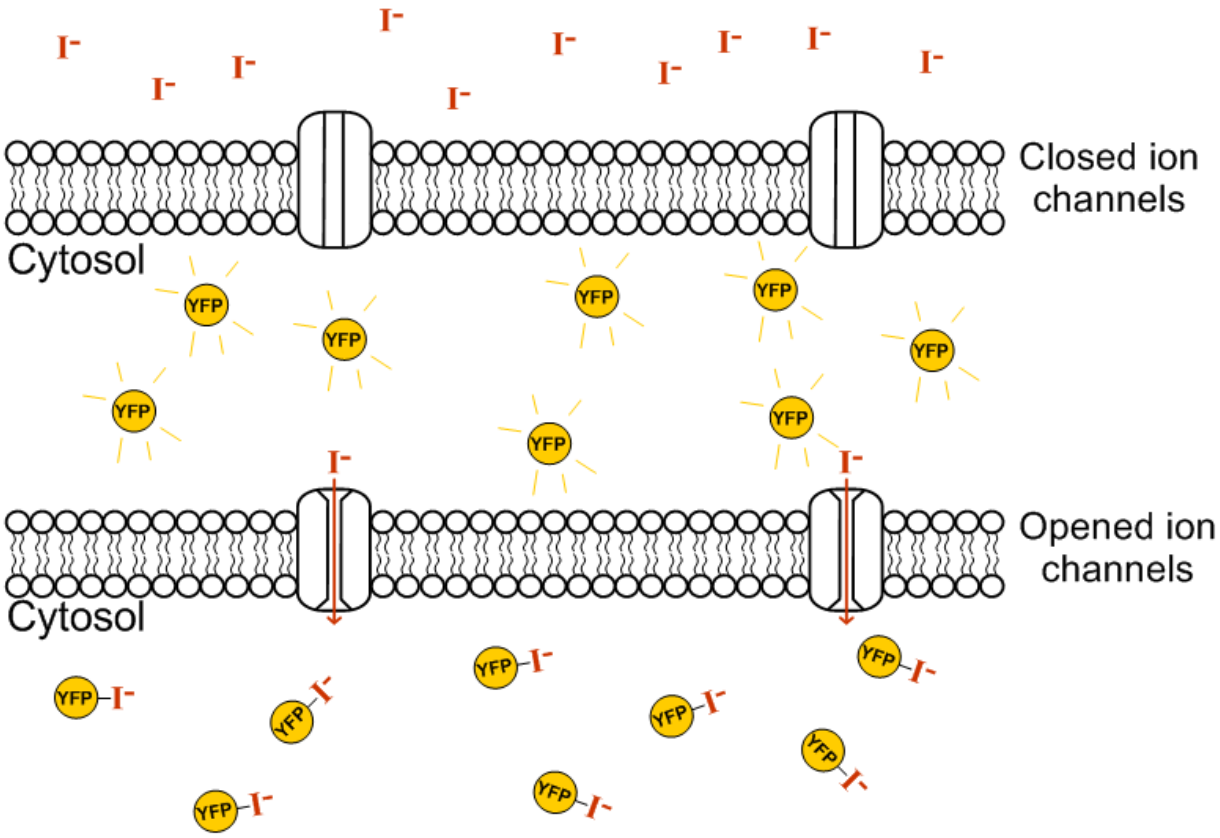

Figure 2.4. YFP Fluorescence Quenching by Iodide (I^-). When ion channels are closed, I^- cannot cross the plasma membrane and YFP remains fluorescent. However, if ion channels are opened, the I^- is able to permeate through the channel pore and bind to YFP cavity, quenching the fluorescent signal.

3.6.2 Patch Clamp

Patch clamp allowed a sensitive measurement of the basal current activated by ROS. In order to accomplish this, HEK293 and HeLa cells were grown in collagen/fibronectin - coated 18 mm glass coverslips and transfected according to section 3.1.2 Transient Transfections, in the presence of the CD8 receptor. After transfection, HEK293 and HeLa cells were treated with tBHP or STS at 37°C, 5% CO_2 for the desired period of time. Following exposure to ROS, cells were incubated 1-2 min with Dynabeads CD8 (Invitrogen, Germany), a step that allowed the identification of the transfected cells.

Coverslips were then mounted in a chamber on the stage of an inverted microscope (IM35, Zeiss, Germany) where whole-cell current was measured. The bath was perfused continuously at 37°C with Ringer solution (mM: 145 NaCl; 0,4 KH_2PO_4; 1,6 $K_2HPO_4 \cdot 3H_2O$; 5 Glucose; 1 $MgCl_2 \cdot 6H_2O$; 1,3 Ca-Gluconate$\cdot 1H_2O$; pH 7.4). In order to prove that the detected current results from Cl^- movement, Ringer was replaced with a 5 mM Cl^- solution (mM: 5 NaCl; 0,4 KH_2PO_4; 1,6 $K_2HPO_4 \cdot 3H_2O$; 5 Glucose; 1 $MgCl_2 \cdot 6H_2O$; 8 Ca-Gluconate$\cdot 1H_2O$, 140 Na-Gluconate; pH 7.4). Regarding tBHP experiments, the ROS inducer was diluted in the bath solution to ensure the presence of the compound during measurements. The patch pipette was filled with a solution containing 95 mM K-Gluconate, 30 mM KCl, 1.2 mM $NaH_2PO_4 \cdot H_2O$, 4.8 mM $Na_2HPO_4 \cdot 2H_2O$, 5 mM Glucose, 2.38 mM $MgCl_2 \cdot 6H_2O$, 1 mM EGTA (Ethylene Glycol Tetraacetic Acid) and 0.726 mM Ca-Gluconate$\cdot 1H_2O$, with freshly added 3 mM ATP and pH adjusted to 7.2.

Membrane voltage was clamped in steps of 20 mV from -100 to +100 mV from a holding voltage of -100 mV. Currents and voltages were recorded using a patch clamp amplifier EPC 9 and PULSE software (HEKA, Lambrecht, Germany), as well as a Chart software (AD-Instruments, Spechbach, Germany).

Experiments were kindly performed by Lalida Sirianant and Jiraporn Ousingsawat.

3.7 Calcium Signaling Measurements – Fura-2 AM

HEK293 and HeLa cells were seeded in collagen/fibronectin 18 mm coated glass coverslips and treated with tBHP and/or STS (see section 3.1.3 – Apoptosis Induction). Following ROS induction, cells were loaded with 2 µM Fura-2 AM (Molecular Probes, Invitrogen, Germany) diluted in ringer solution, in the presence of 0.02% Pluronic, (Molecular Probes, Invitrogen, Germany) for 1h at room temperature. After loading, the coverslips were mounted in a cell chamber and perfused continuously with ringer solution.

Fura-2 AM is a membrane-permeable calcium indicator formed by an ester group (AM-acetoxymethyl). When loaded into cells, the AM group is cleaved by esterases, allowing retention of the sensor in the cytosol.

In order to measure the intracellular concentration of Ca^{2+} ($[Ca^{2+}]_i$), Fura-2AM fluorescence was detected using an inverted microscope Axiovert S100 (Zeiss, Germany) Flua 40x/1.30 oil objective (Zeiss, Germany) and a high speed polychromator system (VisiChrome, Visitron Systems, Germany), at an excitation wavelength of 340/380 nm, and emission 470-550 nm using a CCD-camera (CoolSnap HQ, Visitron Systems, Germany).

The software package Meta-Fluor (Universal imaging, USA) allowed imaging acquisition and data analysis. Intracellular Ca^{2+} was calculated according to the 340/380 nm fluorescence ratio, after background subtraction and calibration[75].

Experiments were kindly performed by Ana Fonseca.

3.8 Statistical Analysis

For Statistical Analysis, student's *t*-test (paired and unpaired samples) and analysis of variance (ANOVA) were used as suitable. Values were accepted as significant if p-value < 0.05.

3. RESULTS

4.1 ANO6 IS ACTIVATED BY ROS

The first goal of this study was to determine if ANO6 is activated by ROS. To accomplish this, overexpression studies were done in HEK293 or HeLa cells and apoptosis was induced either by tBHP or STS. In parallel experiments ANO6 endogenous expression was downregulated by siRNA and confirmed by *Western Blot* in both cell lines.

4.1.2 ANO6 plays a role in tBHP-induced apoptosis of HEK293 cells

Tert-butyl hydroperoxide or tBHP is an oxidative stress inducer commonly used in different biological systems[76], being a good tool to study the influence of ROS in ANO6 activity. In order to identify the time frame required for ROS increase in HEK293 cells, H_2DCFDA fluorescence was monitored after incubation with 100 µM tBHP for 30 min, 1h and 2h. By this assay it was possible to conclude that 30 min of exposure is sufficient to trigger ROS production to a detectable level, compared to negative control. Moreover, this effect persists at least for 2h upon incubation, when a significant difference in cell morphology can be still observed in the correspondent DIC (Differential Interference Contrast) picture (**Fig. 4.1 A**).

As previously outlined, one of the apoptotic hallmarks is cell shrinkage[1,11], which contrasts to swelling observed during necrosis[8]. These two processes can be activated by the same physiological and pathological stimuli, depending on the degree of exposure[1]. Indeed, in rat hepatocytes, tBHP is described to induce both necrosis and apoptosis[76]. Because the present study is focused on regulated cell death, the identification of the mechanism induced by 100 µM tBHP in HEK293 cells was mandatory. To accomplish this, cell volume was monitored by holographic microscopy during 3h of exposure to the ROS inducer. These measurements indicated that cells start to shrink substantially after 1h30min of incubation with tBHP (**Fig. 4.1 B**).

A relationship between caspase activation and shrinkage is well described. In fact, it is believed that these proteins mediate the morphological changes seen in apoptotic cells[1]. Interestingly, in agreement with these statements, a 60% increase in caspase-3 activity was detected after 2h of exposure to tBHP, a simultaneous phenomenon to volume reduction. This increase is expressed as a shift of the fluorescence peak of caspase-3 substrate, compared to control cells (**Fig. 4.1 C, D**).

GSH is the reduced form of glutathione and the most prevalent thiol present in cells, responsible for the protection of DNA, proteins and lipids. When cells are exposed to ROS, GSH is oxidized or transported to the extracellular space, being no longer available to play its role[50]. Therefore, supplementation of GSH is expected to rescue cells form ROS-induced apoptosis. This hypothesis was tested using a membrane permeable synthetic derivative of GSH, Glutathione reduced Ethyl Ester (GSHEE). It was observed that pre-incubation of HEK293 cells with 10 mM GSHEE for 2h resulted in a 3-fold inhibition of tBHP-induced caspase-3 activity (**Fig. 4.1 C, D**).

In conclusion, tBHP increases intracellular ROS which is likely mediating cell shrinkage and caspase-3 activation. For this reason, this compound can be used as a tool to study ANO6 involvement in ROS-mediated apoptosis of HEK293 cells. Additionally, Annx V and 7-AAD flow cytometry measurements revealed that tBHP-induced cell death can be strongly inhibited by Idebenone (Ide), a synthetic analog of the coenzyme Q10/ubiquinone (**Appendix II – Fig. 8.1**). Ubiquinone belongs to the mitochondrial respiratory chain, participating in the ATP synthesis by transporting electrons[77]. As

previously described, during apoptosis this process is stopped due to mitochondrial permeabilization[12]. Therefore, administration of Idebenone restores partially the ATP synthesis and inhibits apoptosis.

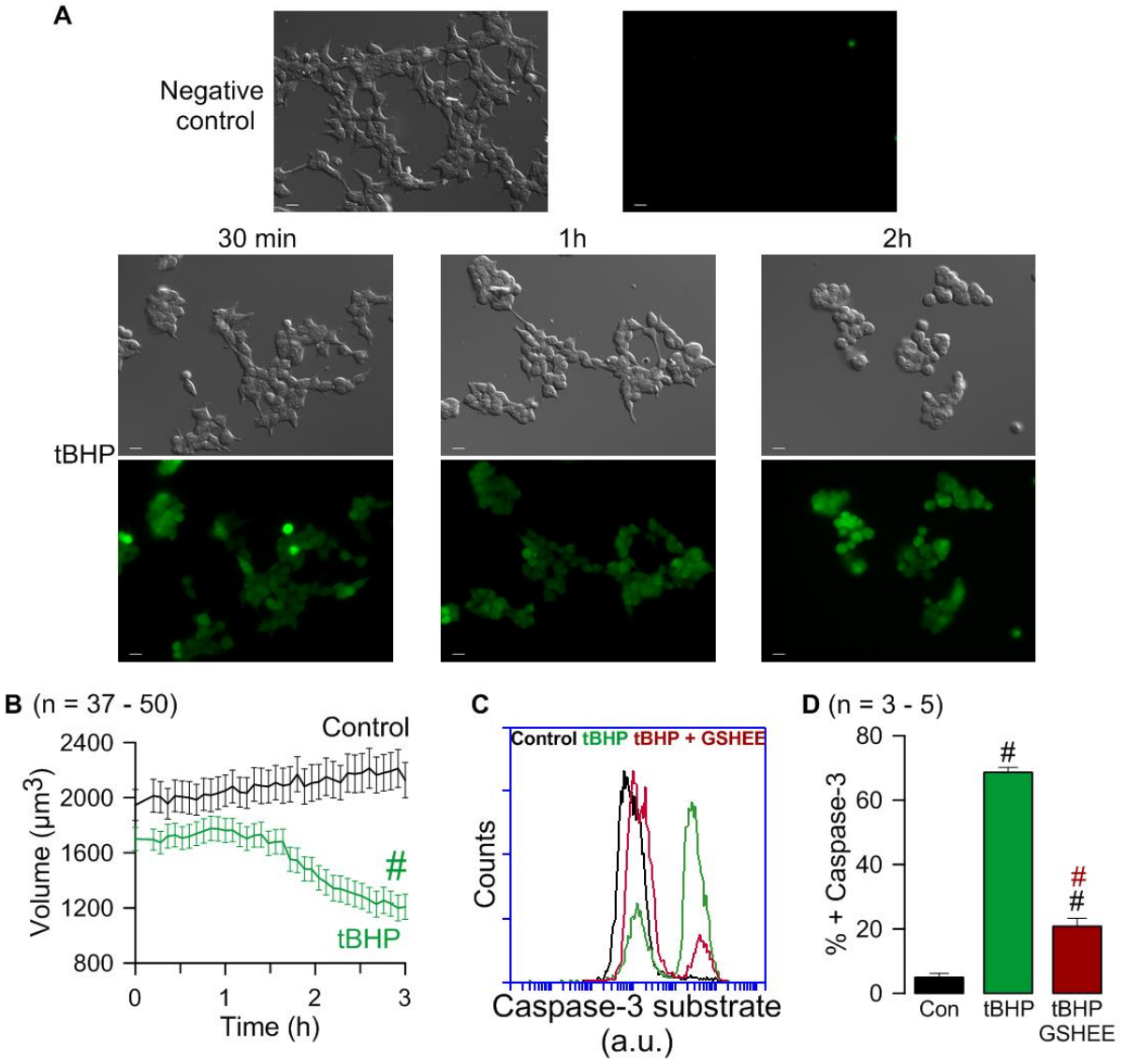

Figure 3.1. ROS production, cell shrinkage and caspase-3 activation by tBHP in HEK293 cells. A) Representative images from three different experiments showing the over-time effect of tBHP (100 µM) in ROS production monitored by H_2DCFDA fluorescence (30 min, 1h and 2h). Bar indicates 20 µm. **B)** Volume (μm^3) measurements of control and tBHP treated cells (100 µM). Cell shrinkage is clear after 1h30min of exposure to tBHP. **C)** Caspase-3 activity induced by treatment with 100 µM tBHP for 2h (green), compared to non-treated cells (black). Inhibition of caspase-3 activation by GSH supplementation (GSHEE 10 mM; pre-incubation for 2h). Each peak corresponds to one representative experiment from a total of 3-5. **D)** Summary of caspase-3 measurements shown in C. (Values are mean ± SEM; #/# unpaired *t*-test to control, # unpaired *t*-test to tBHP treated group, *p*- value < 0.05; n = number of cells, from 3 different experiments for volume measurements, n = number of experiments for caspase-3 activity measurements).

ANO6 is identified as a Ca^{2+}-activated Cl^- channel[19,20] and a non-selective cation channel[18]. Therefore, to understand the ROS effect in ANO6 activity, the function of this protein was firstly studied in terms of current. Whole-cell currents were measured by patch clamp in HEK293 cells transfected with mock or ANO6 after incubation with 100 µM tBHP for 30 min, an exposure time sufficient to increase the intracellular level of ROS (**Fig. 4.1 A**). Cells overexpressing ANO6 had a significant higher current in the presence of tBHP, compared to mock and non-treated cells. The endogenous expression of ANO6 in this cell line is relatively low (**Appendix III – Fig. 8.2**) which may explain why tBHP did not activate a basal conductance in mock cells compared to control (**Fig. 4.2 A, B, C**).

In order to know if the detected current results from Cl^- movement, the Ringer bath solution was replaced with another containing a reduced concentration of Cl^- (5 mM). By applying this protocol, it was expected an inhibition of the Cl^- current, due to a shift in the concentration gradient. As predicted, the tBHP-induced conductance of ANO6 overexpressing cells was reduced in the presence of the 5 mM Cl^-. However, because ANO6 is poor selective for Cl^- ions, being described also as a non-selective cation channel[27], the current was not completely abolished (**Fig. 4.2 A, B, D**).

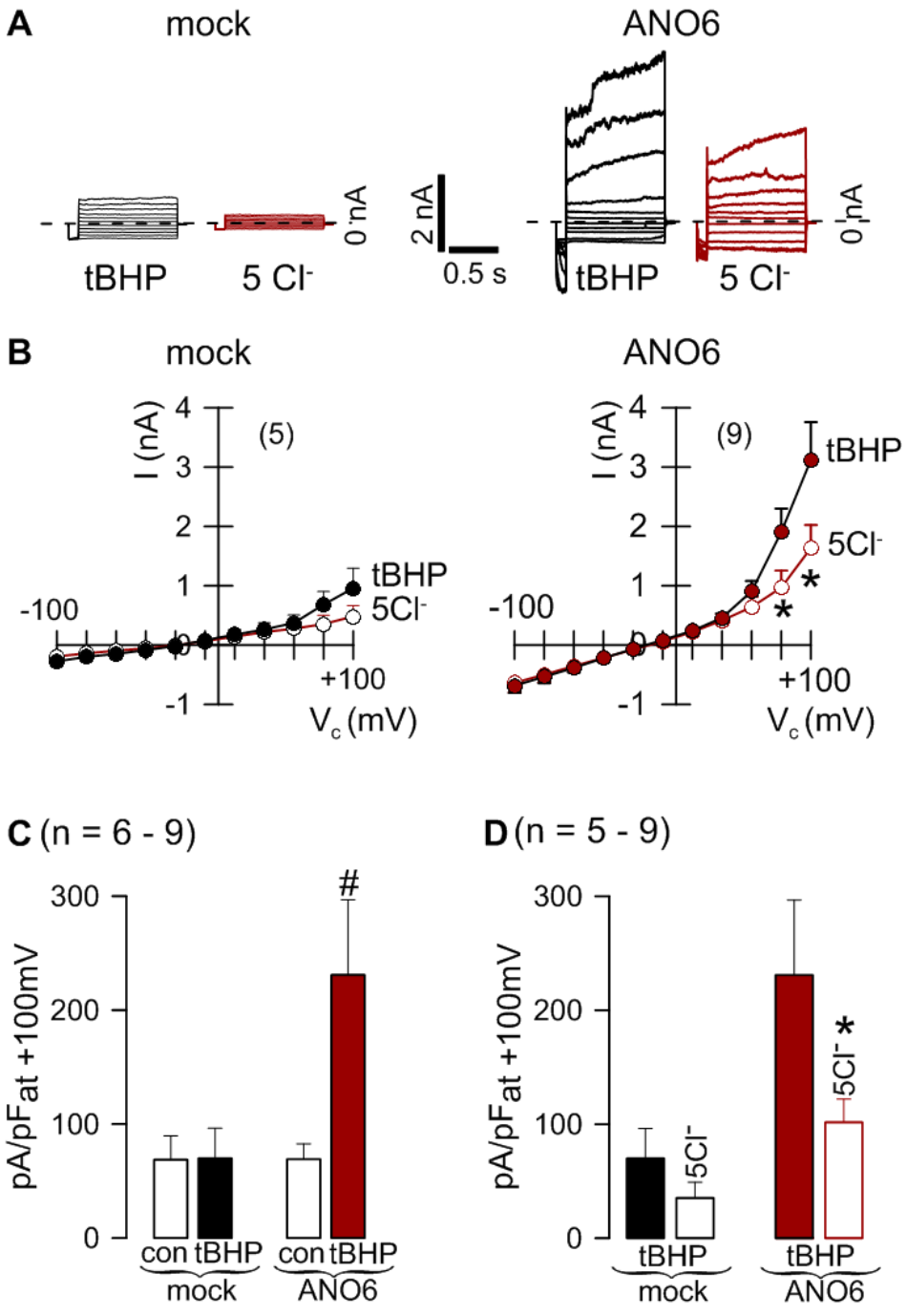

Figure 3.2. tBHP activates an ANO6-dependent Cl^- conductance. A) Current overlays from tBHP treated cells (100 µM; 30 min) and inhibition by $5Cl^-$. Overexpression of ANO6 increases tBHP-induced current compared to mock cells. **B)** Corresponding current-voltage (I/V) relationships from experiments shown in A. **C)** Respective current densities from experiments shown in A. **D)** Summary of inhibition of tBHP- induced current by $5Cl^-$ for mock and ANO6 transfected cells. (Values are mean ± SEM; # unpaired *t*-test to control, * paired *t*-test to tBHP treated cells, *p*-value < 0.05; n = number of cells).

In addition to an ANO6-dependent Cl^- conductance, this protein was also found to contribute to tBHP-induced scrambling. This was observed when HEK293 cells were transfected with mock or ANO6, treated with tBHP and labeled with Annx V and 7-AAD. Flow cytometry measurements revealed a clear difference between mock and ANO6 overexpressing cells in Annx V and Annx V + 7-AAD positive cells, after 3h30 of exposure to tBHP. Remarkably, overexpression of ANO6 by itself and low serum conditions were enough to increase significantly this positivity, compared to mock control group (**Fig. 4.3 A, B**). This observation can be related to a study of Schenk *et. al*, where ANO6 was found to regulate the baseline PS exposure and cell viability of HEK293 cells[78].

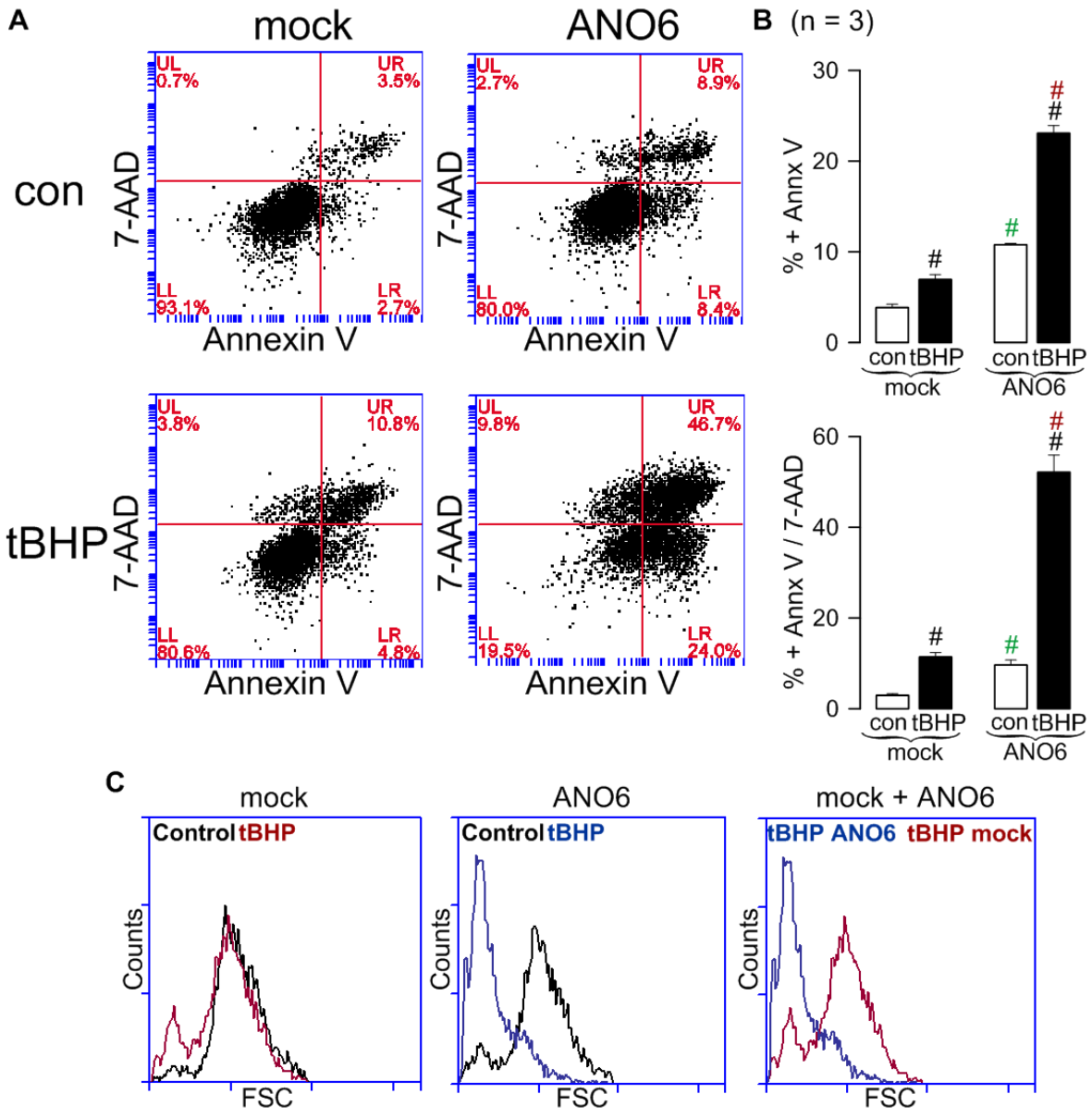

Figure 3.3. ANO6 is activated by tBHP as a phospholipid scramblase. A) Representative original dot-plots of flow cytometry analysis from mock and ANO6 transfected HEK293 cells. **B)** Summary of Annx V and Annx V + 7-AAD positivity after exposure to 100 µM tBHP for 3h30. Treatment with tBHP leads to a significant increase in Annx V / Annx V + 7-AAD positive cells in mock and ANO6 groups, compared to respective controls. Cells overexpressing ANO6 undergo apoptosis faster when exposed to oxidative stress. **C)** Representative FSC histograms of experiments shown in A. ANO6 overexpression results in a strong shrinkage in the presence of tBHP. (Values are mean ± SEM; # unpaired *t*-test to control, # unpaired *t*-test to mock treated cells, # unpaired *t*-test to mock non-treated cells, *p*- value < 0.05; n = number of experiments).

Additionally, by flow cytometry was also possible to conclude about cell size in the presence and absence of tBHP – whereas, mock cells show just a small shift in the FSC histogram compared to control, ANO6 overexpression resulted in a strong cell shrinkage induced by tBHP (**Fig. 4.3 C**).

It is interesting to note the different time points between detection of ANO6 Cl^- conductance and scrambling. While a Cl^- conductance was observed only after 30 min of exposure to tBHP (**Fig. 4.2**), the same conditions were not enough to induce scrambling (data not shown).

In order to know if ANO6 is essential for PS exposure triggered by ROS, the endogenous expression of this protein was silenced in HEK293 cells by siRNA (**Appendix III – Fig. 8.2**) and the same protocol was applied. However, transfection with siRNA likely resulted in off target effects, enhancing cell death induced by tBHP compared to scrambled cells (**Appendix IV – Fig. 8.3**), which can be explained by upregulation of other proteins involved in the apoptotic pathway.

4.1.3 ANO6 contribution to STS-mediated apoptosis of HEK293 and HeLa cells

Staurosporine is a cell permeable alkaloid isolated from the bacterium *Streptomyces staurosporeus*, commonly used to study apoptosis[79]. Aside from functioning as a non-specific protein kinase inhibitor[80], this compound is also described to increase the intracellular level of ROS[81]. Hence, like tBHP, STS can be used as a tool to study the possible effect of ROS in ANO6 activity. Indeed, intracellular ROS production in HEK293 cells was detected after incubation with 1 µM STS for 24h, using the fluorogenic sensor MAK142 (**Fig. 4.4 A**). In agreement with results from the previous section, overexpression of ANO6 and exposure to STS led to an increase of the Annx V and Annx V + 7-AAD positive cells (**Fig. 4.4 B, C**).

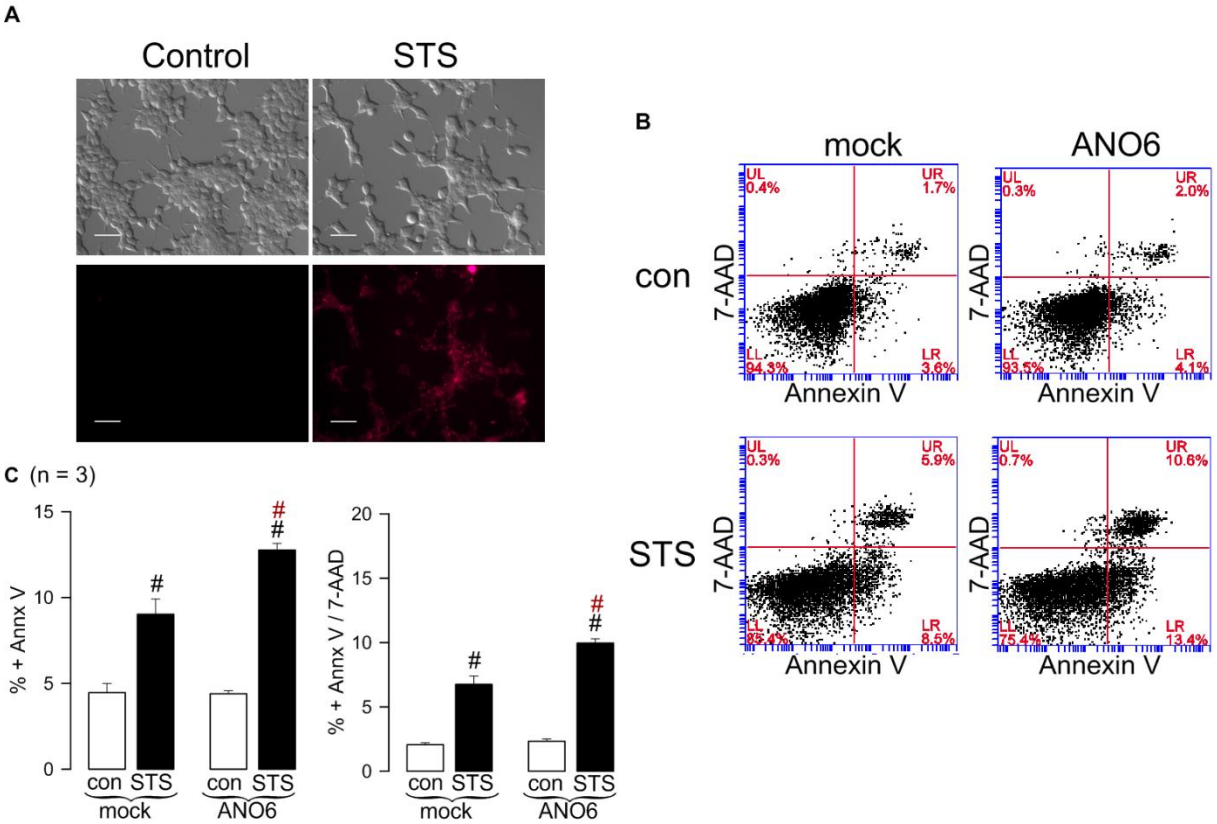

Figure 3.4. ANO6 contribution to PS exposure induced by the ROS-producer STS. A) Representative images from three different experiments showing ROS production after treatment with 1 µM STS for 24h, monitored with MAK142 fluorescence. Bar indicates 20 µm. **B)** Representative original dot-plots of flow cytometry analysis from mock and ANO6 transfected HEK293 cells in the presence and absence of 1 µM STS for 24h. **C)** Summary of Annx V and Annx V + 7-AAD positivity of

experiments shown in B. Treatment with STS and ANO6 overexpression leads to a significant increase in Annx V and Annx V + 7-AAD positive cells, compared to mock. (Values are mean ± SEM; # unpaired *t*-test to control, # unpaired *t*-test to mock treated cells, *p*- value < 0.05; n = number of experiments).

After observing that ANO6 is involved in ROS-mediated apoptosis of HEK293 cells, it was interesting to look if this is also true for another cell line. With this purpose, HeLa cells were incubated with 1 µM STS for 5h. As expected, exposure to STS led to ROS production and caspase-3 activation (**Fig. 4.5 A, B, C**). Also, overexpression of ANO6 enhanced significantly the Annx V positivity after incubation with STS, compared to mock (**Fig. 4.5 D, E**). Surprisingly, downregulation of endogenous expression by siRNA (**Appendix III – Fig. 8.2**) did not reduce cell death (**Fig. 4.6**).

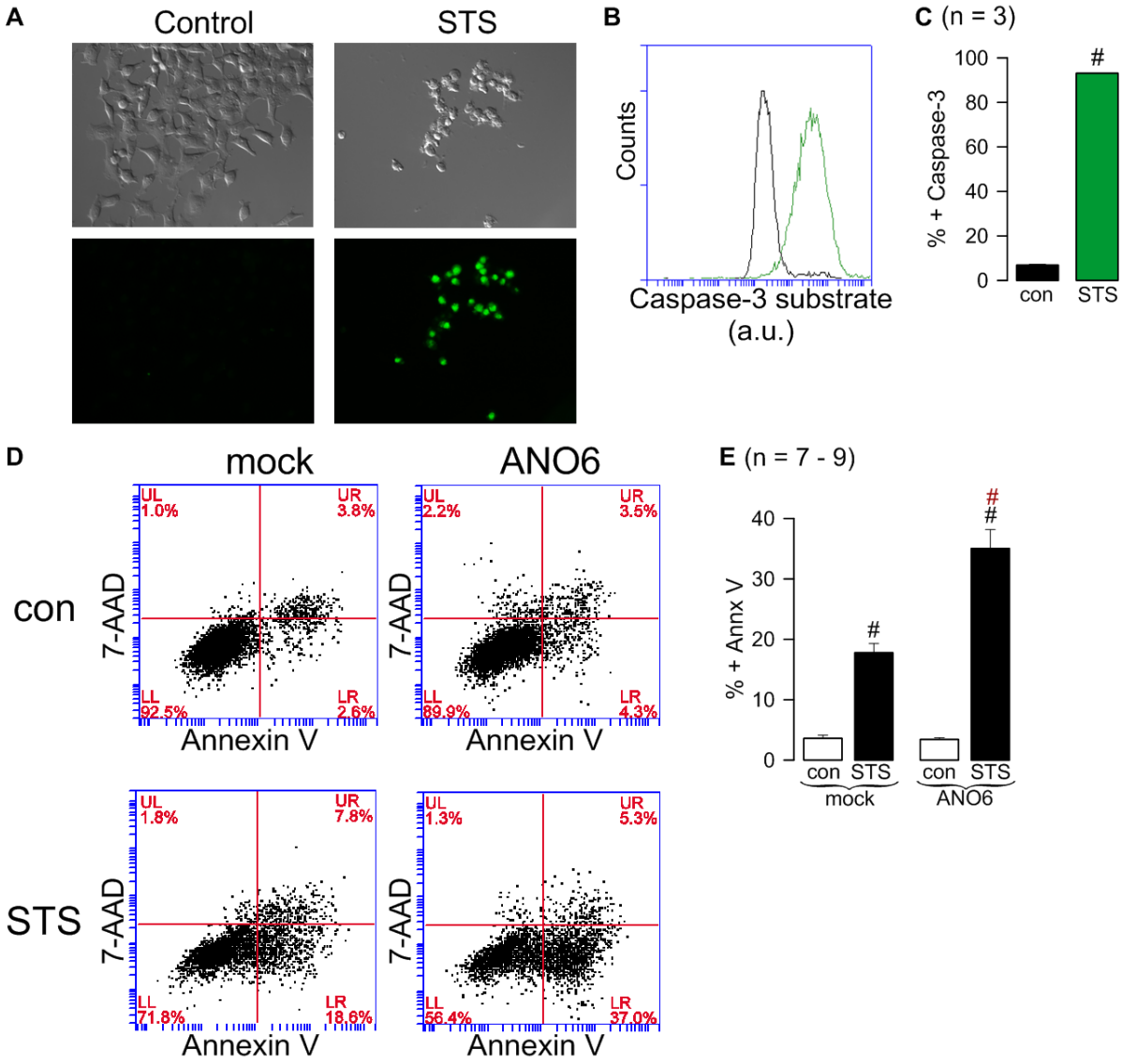

Figure 3.5. STS leads to ROS increase and caspase-3 activation, mediating PS exposure enhanced by overexpressed ANO6 in HeLa cells A) Representative images from three different experiments showing ROS production by 1 µM STS monitored with H_2DCFDA fluorescence (5h incubation). Bar indicates 20 µm. **B)** Representative original dot-plots of flow cytometry analysis from mock and ANO6 transfected HeLa cells in the presence and absence of 1 µM STS for 5h. **C)** Summary of Annx V positivity of experiments shown in B. ANO6 overexpression results in an increase of Annx V positive cells after exposure to STS. (Values are mean ± SEM; # unpaired *t*-test to control, # unpaired *t*-test to mock treated cells, *p*-value < 0.05; n = number of experiments).

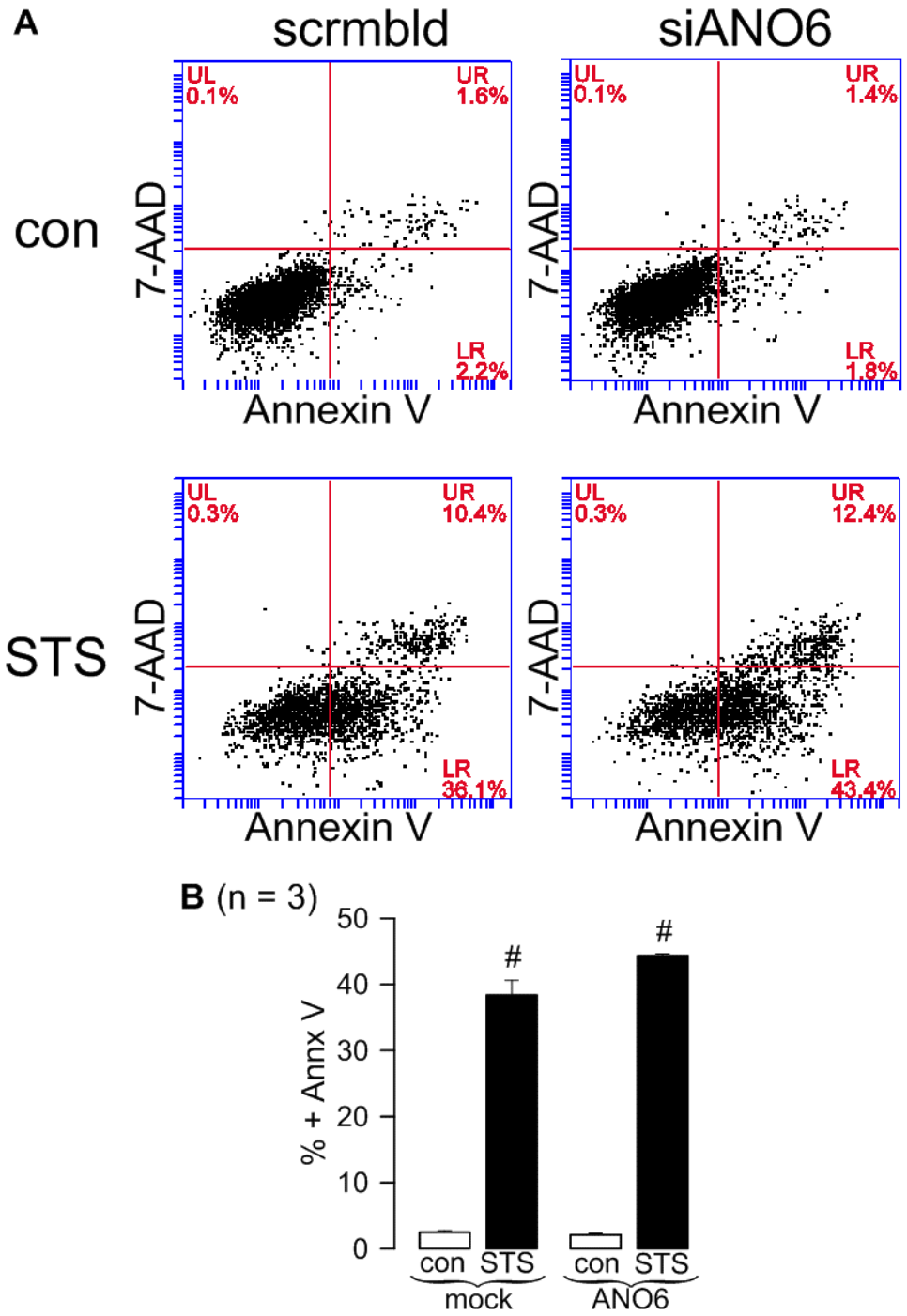

Figure 3.6. Downregulation of ANO6 in HeLa cells does not inhibit Annx V positivity induced by STS. A) Representative original dot-plots of flow cytometry analysis from scrambled and siANO6 transfected HeLa cells in the presence or absence of STS for 5h. **B)** Summary of Annx V positivity of experiments shown in A. STS induces Annx V positivity independently of ANO6 expression level. (Values are mean ± SEM; # unpaired *t*-test to control, *p*-value < 0.05; n = number of experiments).

ANO6 contribution to ROS-mediated apoptosis of HeLa cells was also studied in terms of current. First, by using the YFP-quenching assay, it was possible to detect an anion conductance activated by STS in HeLa-YFP cells (**Fig. 4.7 A, B**). This conductance is also observed by patch clamp and can be inhibited by downregulation of ANO6 and replacement with a 5 mM Cl^- solution (**Fig. 4.7 C, D, E**).

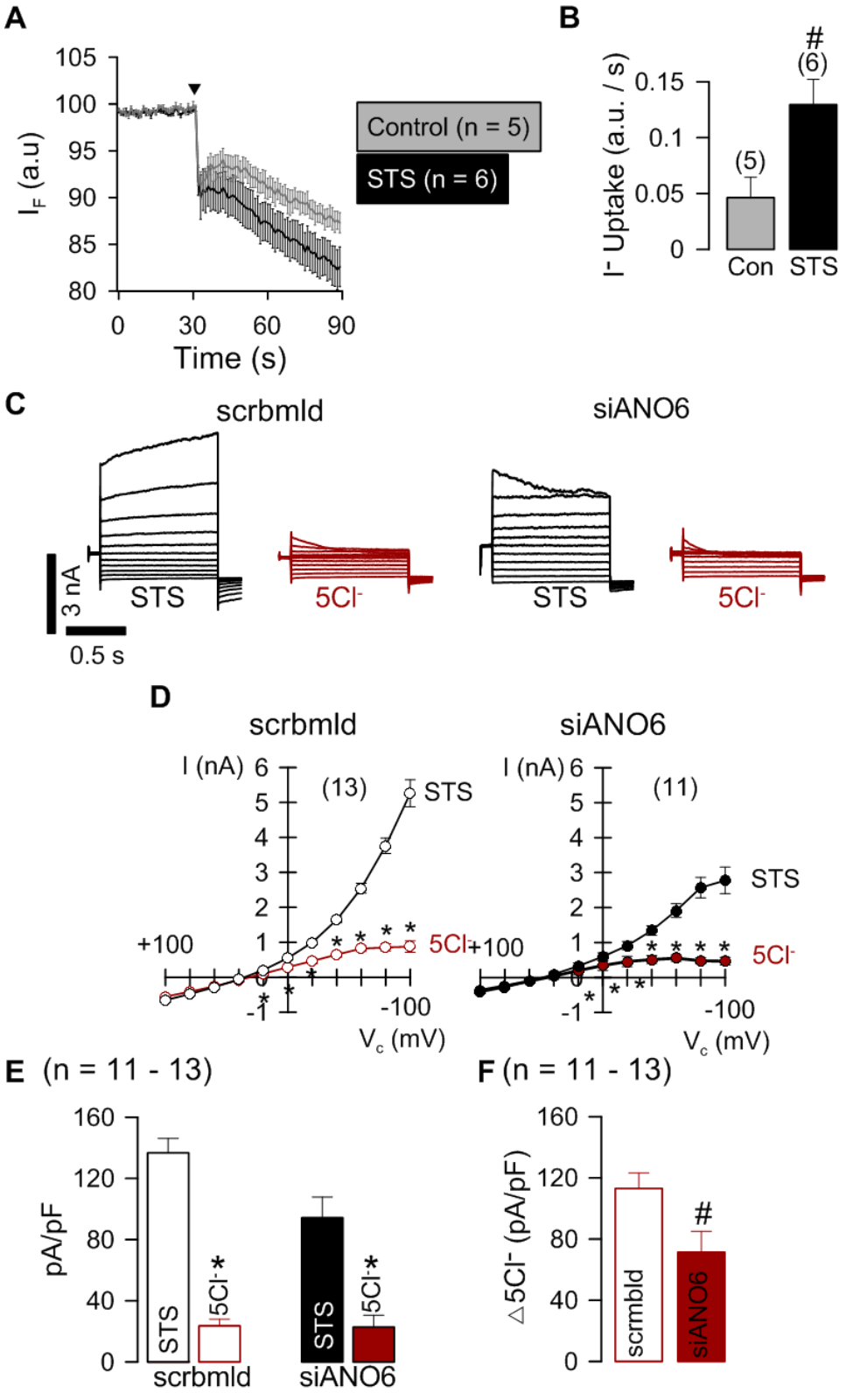

Figure 3.7. STS activates ANO6 currents in HeLa cells. **A)** YFP fluorescence measurements of HeLa-YFP cells in the absence and presence of 20 mM I^- (▼). Activation of an anion conductance after exposure to 1 µM STS for 5h, indicated by I^- efflux. **B)** Summary of I^- uptake experiments shown in A. **C)** Overlay of whole-cell currents in HeLa cells, showing an activation of a STS-induced Cl^- current, reduced by ANO6 silencing. **D)** Current-voltage (I/V) curves of experiments shown in B. Reduction of extracellular Cl^- concentration results in a clear inhibition of baseline current detected after incubation with 1 µM STS for 3h-4h. **E)** Summary of delta current density at + 100 mV after current inhibition by $5Cl^-$ solution. (Values are mean ± SEM; # unpaired *t*-test to control $p < 0.05$, # unpaired *t*-test to mock treated cells, * paired *t*-test to tBHP treated, *p*-value < 0.05; n = number of experiments).

4.2 CFTR ENHANCES ANO6 EFFECT DURING ROS-MEDIATED APOPTOSIS

The next step of this project was focused on CFTR and the possible interaction of this protein with ANO6. As described before, CFTR is a main regulator of the intracellular redox status, transporting GSH to the extracellular space[49]. Moreover, a functional relationship between this channel and ANO6 is also described[26]. Thus, it is hypothesized that CFTR-mediated cytosolic ROS increase may lead to ANO6 activation. If this is true, the presence of both proteins should enhance cell death under oxidative stress conditions.

To address this question, HEK293 cells were co-transfected with ANO6 and CFTR and incubated with 1 µM STS for 24h. As a control, cells were either transfected with mock, ANO6 or CFTR. Like expected, single expression of ANO6 resulted in a significant increase of Annx V positive cells in the presence of STS, compared to control and mock treated cells. Notably, the same was detected for CFTR single transfection, which is in agreement with the function of this protein as a pro-apoptotic factor. Co-expression of both proteins increased by a two-fold factor the Annx V positivity, compared to single expression of ANO6 and CFTR. Surprisingly, the presence of both proteins was sufficient to trigger cell death under control conditions to a significant level, evidenced by Annx V and 7-AAD positivity (**Fig. 4.8**).

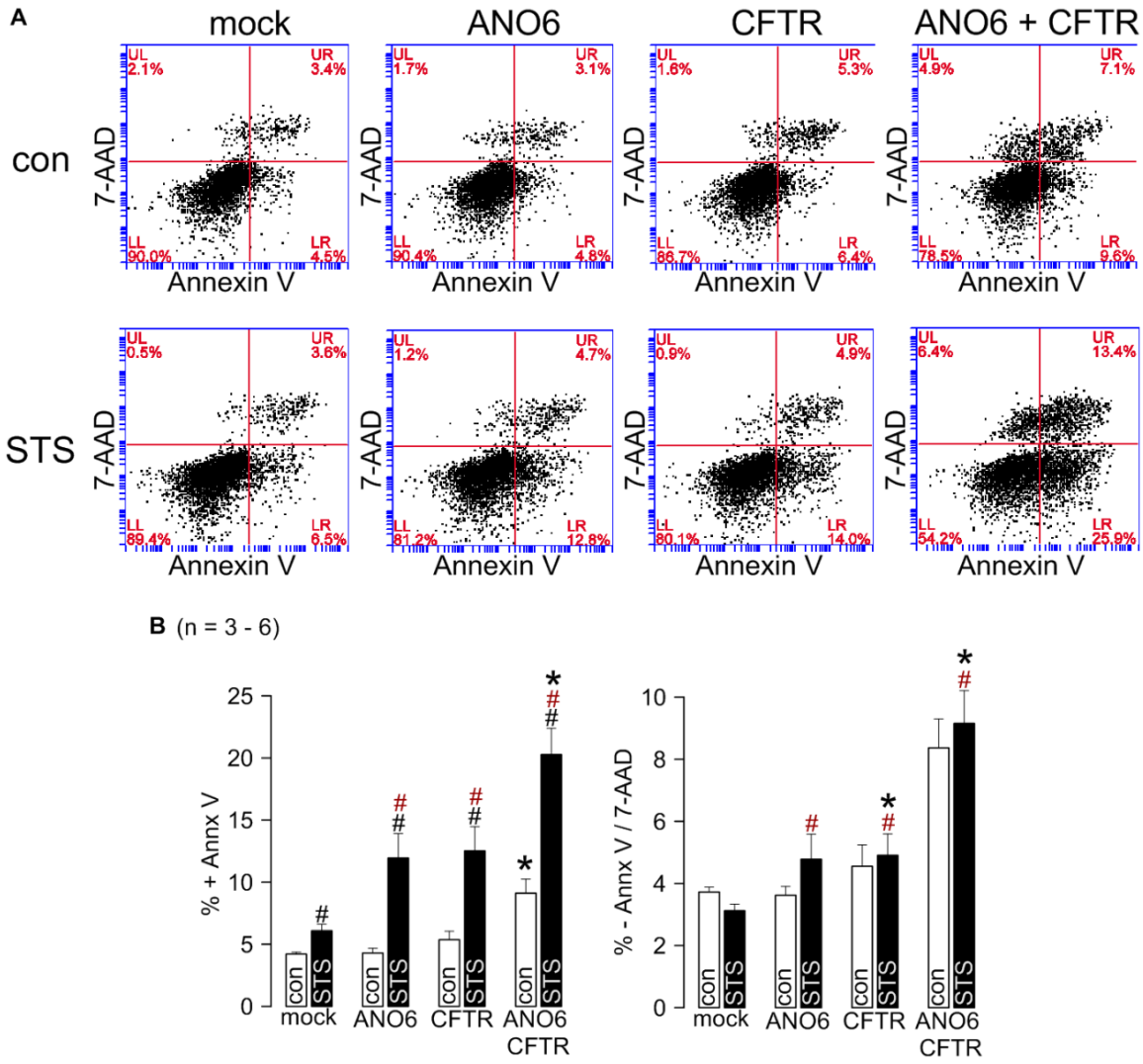

Figure 3.8. CFTR enhances ANO6 contribution to apoptosis induced by STS in HEK293 cells. A) Representative original dot-plots of flow cytometry analysis from cells transfected with mock, ANO6, CFTR or ANO6 and CFTR in the presence or

absence of 1 µM STS for 24h. **B)** Summary of Annx V and Annx V + 7-AAD positivity of experiments shown in A. In each group incubation with STS results in a significant increase of Annx V positive cells. Overexpression of ANO6 or CFTR augments this effect. Co-expression of both proteins enhances ANO6 and CFTR contribution to apoptosis. (Values are mean ± SEM; # unpaired *t*-test to control, # unpaired *t*-test to mock treated group, * One-way ANOVA indicates significant difference compared to single expression, *p*-value < 0.05; n = number of experiments).

The finding that ANO6 and CFTR cooperate in PS exposure during STS-induced cell death led to wonder if the same is true in terms of current activation. Therefore, single and co-expressed cells were measured by patch clamp after incubation with 1 µM STS for 6-8h. In agreement with flow cytometry data, overexpression of ANO6 or CFTR led to a significant increase in the basal current activated by STS, an effect strongly enhanced by the co-expression of both proteins. In the four studied groups (mock, ANO6, CFTR and ANO6 + CFTR), STS-induced current was inhibited by replacement with 5 mM Cl^- solution in the extracellular space, showing that the whole-cell conductance is partially formed by Cl^- ions (**Fig. 4.9**).

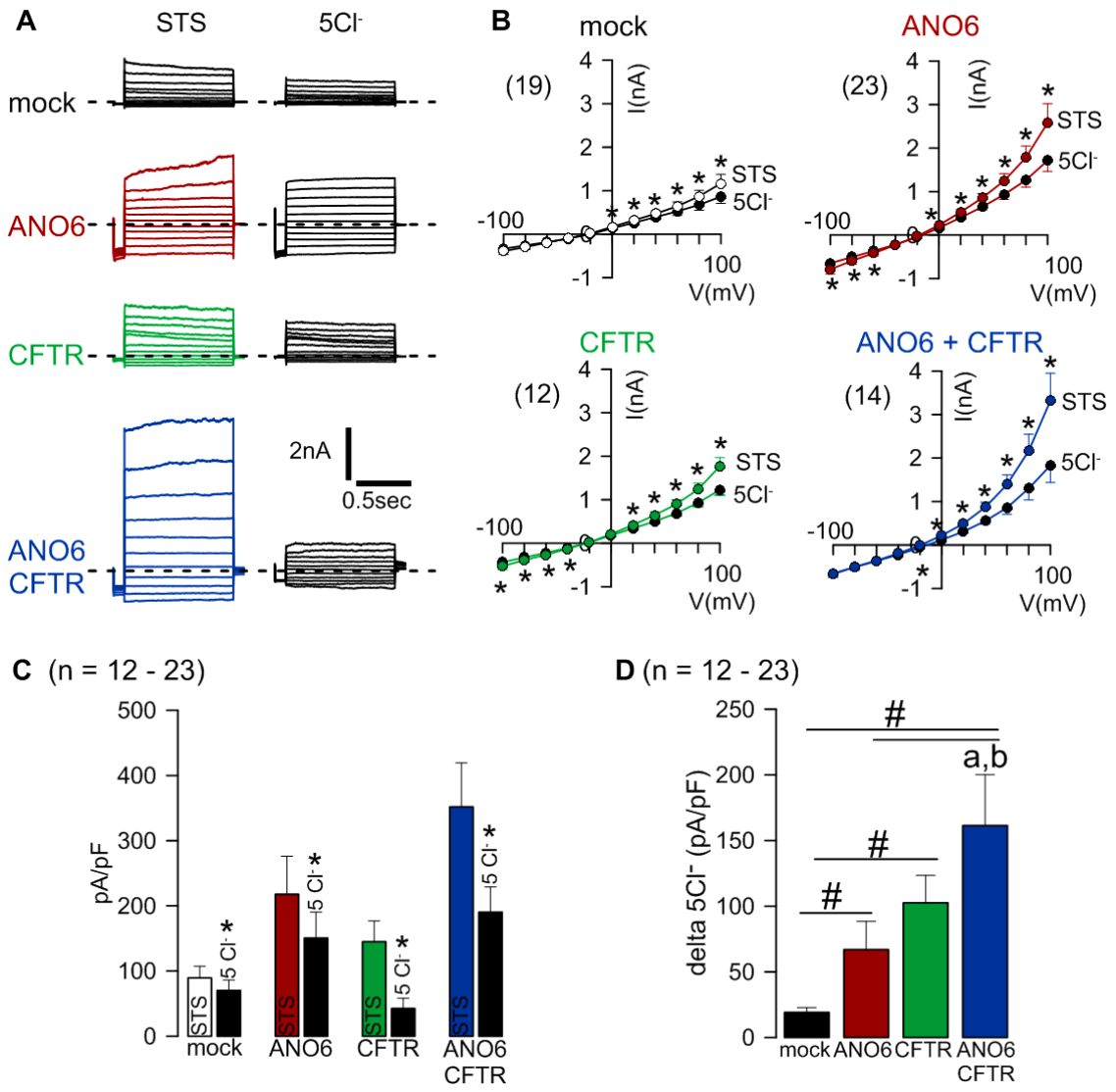

Figure 3.9. Enhanced apoptotic whole-cell Cl^- currents in cells expressing ANO6, CFTR and ANO6 + CFTR. A) Current overlays from STS-treated HEK293 cells (1 µM 6h-8h) and inhibition by $5Cl^-$. Single expression of ANO6 or CFTR increases STS-induced compared to mock cells. Co-expression of both proteins enhances ANO6 and CFTR effect. **B)** Corresponding current-voltage relationships (I/V) from experiments shown in A. **C)** Respective current densities from experiments shown in A. **D)** Delta of corrected current density at +100 mV after Cl^- replacement. (Values are mean ± SEM; * paired *t*-test to STS treated cells, # significant difference to indicated groups by unpaired *t*-test, a,b indicates significant difference calculated by one-way ANOVA to mock and ANO6 respectively, *p*-value < 0.05; n = number of cells).

4.2.1 ΔF508 CFTR mutation partially rescues cells from apoptosis

The earlier experiments preformed in HEK293 cells demonstrated that both ANO6 and CFTR contribute to apoptosis, having a possible functional interaction when co-expressed (**Fig. 4.8, 4.9)**. CFBE cells stably expressing *wt* or ΔF508 CFTR were chosen as an *in vitro* system to study CFTR function and approach the results to a clinical significance.

The first question was related to CFTR role during cell death and the impact of the trafficking mutation (ΔF508) in this process. With this purpose, CFBE cells (*wt* and ΔF508 CFTR) were exposed to oxidative stress and their susceptibility to cell death was evaluated. Simultaneous incubation of both cell lines with 100 µM tBHP for 24h led to a substantially difference in the Annx V and Annx V + 7-AAD positive cells. While at the same time-point CFBE *wt* CFTR cells were in a late apoptotic stage – Annx V + 7-AAD positive – cells expressing the mutant CFTR form were still in the early steps – Annx V positive – (**Fig. 4.10 A, B**). It was also observed a considerable difference in the size of the two cell lines after exposure to tBHP – CFBE *wt* CFTR cells showed a significant shrinkage compared to ΔF508 CFTR cells which had similar dimensions to control (**Fig. 4.10 C**).

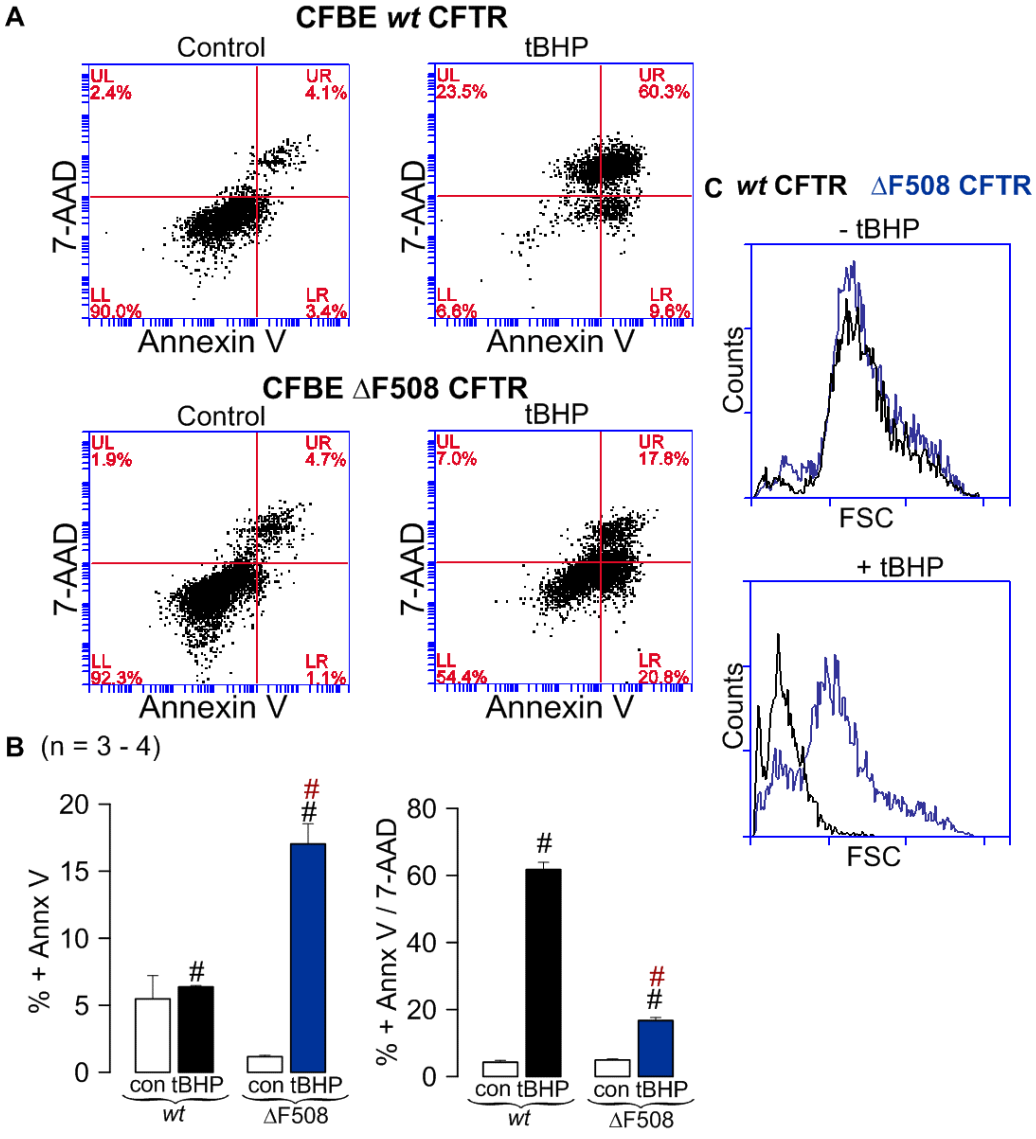

Figure 3.10. Effect of CFTR in tBHP-induced cell death. A) Representative original dot-plots of flow cytometry analysis from CFBE *wt* and ΔF508 CFTR cells in the absence or presence of 100 µM tBHP for 24h. **B)** Summary of Annx V and Annx V + 7-AAD positivity of experiments shown in A. **C)** FSC histograms of experiments shown in A. Expression of *wt* CFTR

significantly enhances tBHP-mediated cell death, compared to ΔF508 CFTR cells. (Values are mean ± SEM; # unpaired *t*-test to control, # unpaired *t*-test to CFBE *wt* CFTR treated group, *p*-value < 0.05; n = number of experiments).

Additional experiments were also performed using another ROS inducer, H_2O_2, and the same observations were taken. However, an over-time flow cytometry study revealed that hydrogen peroxide was likely inducing necrosis in this cell line, given by the fact that cells were never positive only for Annx V (**Appendix V – Fig. 8.4**), which indicates that plasma membrane integrity was compromised.

4.2.2 CFTR contribution to apoptosis is not by GSH transport through the CFTR pore

Previous studies indicate that CFTR contribution to ROS-mediated apoptosis is explained by GSH transport through the pore, which increases cell susceptibility to oxidative stress[53,54]. However, in none of these studies it was shown what happens when CFTR is stimulated and the pore is opened. Following this idea, it is logical to think that if the channel is persistently stimulated, this antioxidant will be continuously transported across it, compromising the GSH cytosolic pool and cell survival. An increase of the intracellular level of ROS would then activate the ANO6 expressed in this cell line (**Fig. 4.11 A**) and lead to apoptosis.

To answer this question CFBE *wt* CFTR cells were stimulated with 100 µM IBMX (3-isobutyl-1-methylxanthine) and 2 µM FK (Forskolin) for 24h and cell death was accessed by Annx V and 7-AAD labeling. IBMX and FK are two different tools used to raise the intracellular level of cAMP and thus activate CFTR. However, the persistent CFTR stimulation was not enough to induce apoptosis to a significant level (**Fig. 4.11 B, C**), meaning that opening of CFTR pore is not sufficient to mediate a decrease in the intracellular GSH pool/increase in the cytosolic ROS enough to trigger apoptosis.

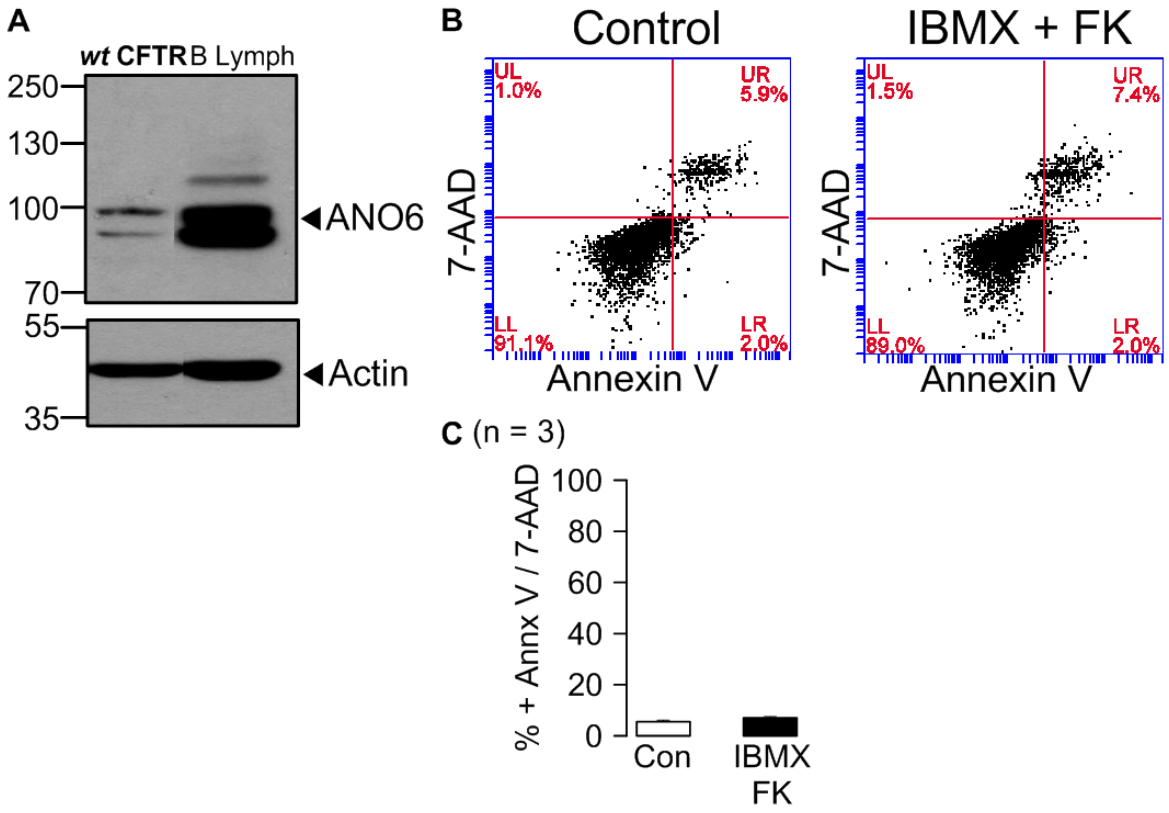

Figure 3.11. Persistent stimulation of CFTR is not sufficient to trigger spontaneous apoptosis. A) *Western Blot* of ANO6 endogenous expression in CFBE *wt* CFTR cells. B Lymphocytes (B Lymph) were used as a positive control. **B)** Representative original dot-plots of flow cytometry analysis from CFBE *wt* CFTR cells in the presence or absence of 100 µM IBMX and 2 µM FK for 24h. **C)** Summary of Annx V and 7-AAD positivity from experiments shown in B. Long-term supply of high

concentrations of cAMP in cells expressing *wt* CFTR does not lead to spontaneous apoptosis (Values are mean ± SEM; n = number of experiments).

This result is also supported by the lack of reduction of tBHP-induced apoptosis in CFBE *wt* CFTR cells by the CFTR-inh 172 (CFTR inhibitor). Indeed, when cells expressing *wt* CFTR were exposed to oxidative stress (100 µM tBHP, 24h) in the presence of the CFTR-inh 172 (5 µM), cell death was not reduced, evidenced by Annx V + 7-AAD positivity (**Fig. 4.12 A, B**). The same was observed in terms of cell size on the FSC histograms, where a strong shrinkage was induced by tBHP but not inhibited by the CFTR-inh 172 (**Fig. 4.12 C**).

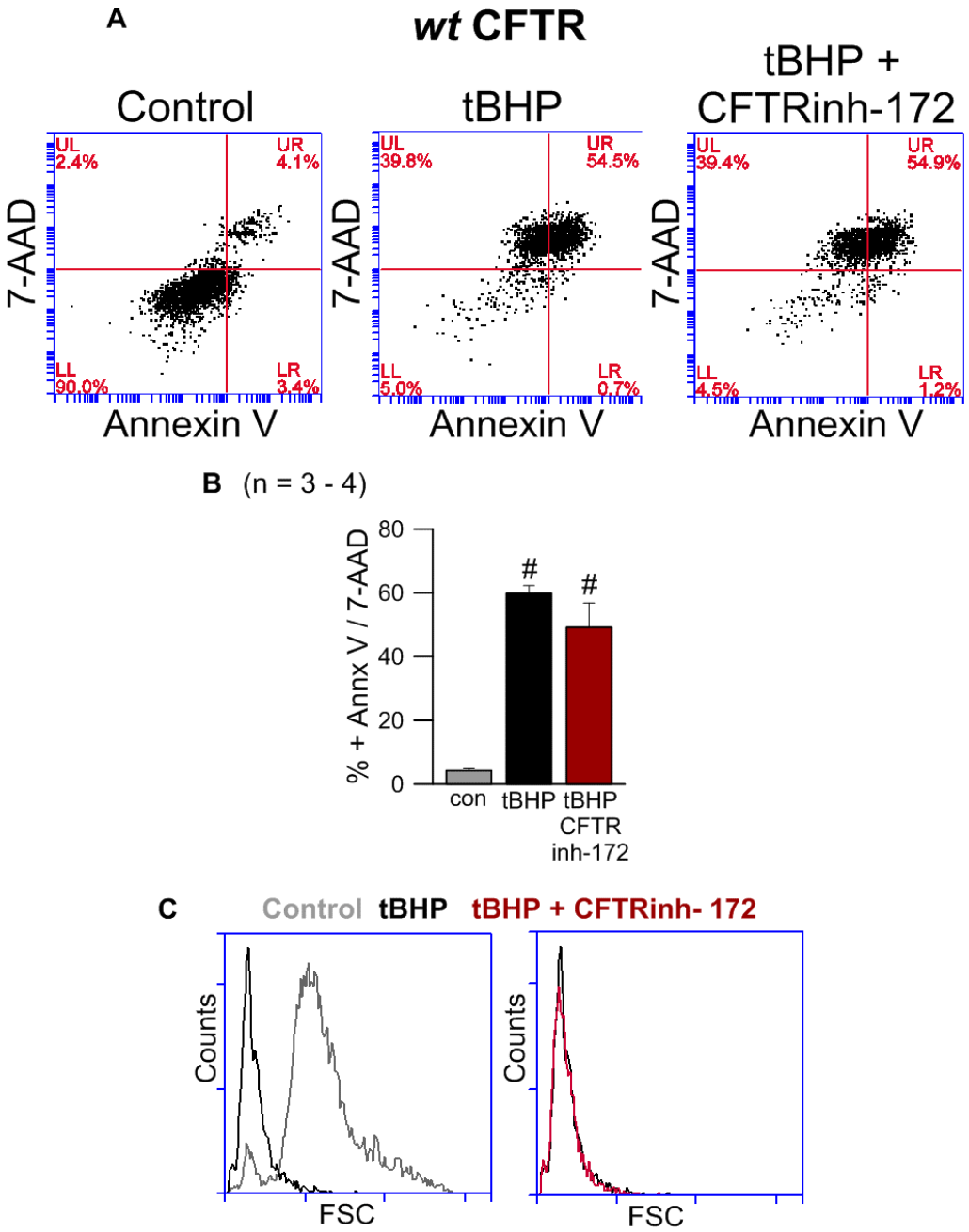

Figure 3.12. CFTR inhibition does not reduce tBHP-induced cell death. **A)** Representative original dot-plots of flow cytometry analysis from CFBE *wt* CFTR cells in the presence and absence of 100 µM tBHP or 5 µM CFTR inh-172 for 24h. **B)** Summary of Annx V and 7-AAD positivity of experiments shown in A. **C)** FSC of experiments shown in A. Inhibition of CFTR does not rescue cells from apoptosis. (Values are mean ± SEM; # unpaired *t*-test to control, *p*-value < 0.05; n = number of experiments).

4. DISCUSSION

5.1 ANO6 PLAYS A ROLE DURING ROS-MEDIATED APOPTOSIS

This work provides evidence that ANO6 is involved in ROS-mediated apoptosis as a Ca^{2+}- activated Cl^- channel, non-selective cation channel and phospholipid scramblase in two different *in vitro* systems (HEK293 and HeLa cell lines) with two ROS inducers (tBHP and STS). It is first activated during the early steps of apoptosis, extruding Cl^- and likely cations to the extracellular space. This event may contribute to cell shrinkage, which is known to result primarily from a loss of K^+ and water[82]. As the intrinsic apoptotic pathway moves forward, the phospholipid scramblase ANO6 function becomes relevant, mediating PS exposure in the outer membrane leaflet.

Although overexpression of this protein augments apoptosis in the presence of ROS, downregulation does not rescue cell death, indicating that ANO6 role in this process is not crucial. Additional experiments in B lymphocytes support this conclusion, where it was observed that the absence of functional ANO6 in Scott cells did not reduce apoptosis induced by STS compared to *wt* B lymphocytes. Nonetheless, *wt* exhibited a higher % of cells in the early apoptotic stage - Annx V single positive (**Appendix VI – Fig. 8.5**). This result may either imply that Scott cells are more sensitive to STS-induced apoptosis, undergoing to later stages faster than *wt*; or that the absence of functional ANO6 leads to the activation of a different cell death pathway. Indeed, when cells die through the necrotic pathway, the membrane integrity is compromised, allowing binding of Annx V and 7-AAD[1].

The fact that ANO6 is not essential to ROS-mediated apoptosis is not surprising since regulated cell death is a fundamental process in all living systems, depending on many molecules and cellular components[5]. It is very likely that a cell with no ANO6 compensates this defect with other proteins. In addition, Juu *et. al* defends that the ion channels activated during apoptosis considerably differ between cell lines, a phenomenon that may be also true for ANO6[23].

5.1.1 ANO6 currents are prior to phospholipid scrambling

The different timeline between ANO6 activation as an ion channel and phospholipid scramblase was already described in a study by Kmit *et. al*, where elevation of intracellular Ca^{2+} by ionomycin resulted in immediate ANO6 currents but a delayed scrambling[34]. Here it is shown that the same is true when ANO6 is activated by ROS. In particular, tBHP incubation for only 30 min in HEK293 cells resulted in an ANO6-dependent Cl^- conductance, whereas a differential scrambling was only detected after 3h30min.

It is possible that PS exposure is a consequence of a persistent stimulation of the channel. Indeed, patch clamp measurements revealed that activation of ANO6 with high concentrations of Ca^{2+} or for a long period of time results in a current impossible to inhibit (data not shown). It is very likely that only on these conditions the channel starts to scramble phospholipids and this may as well be the reason why CaCC-AO1, a broad anoctamin inhibitor, was unable to decrease tBHP- induced scrambling in HEK293 cells (**Appendix VII – Fig. 8.6**).

5.1.2 Mechanism of ANO6 activation by ROS

Phospholipid scrambling can be activated through two distinct pathways: the caspase-dependent pathway or by Ca^{2+} mobilizing agonists[15]. ANO6 contribution to both processes seems uneven – it is very clear that this protein is essential to the Ca^{2+}-mediated PS exposure, however when it comes to ANO6 role in the apoptotic induced scrambling, controversial observations emerge.

ANO6 is known to be activated by high intracellular Ca^{2+} concentrations, between 10 and 100 µM[22]. In this regard, ANO6 contribution to Ca^{2+}-mediated PS exposure was also found in this study, when overexpression of this protein in HEK293 and HeLa cells resulted in a differential scrambling induced by ionomycin (**Appendix VIII – Fig. 8.7, 8.8**). Here, downregulation of ANO6 by siRNA in HEK293 cells (**Appendix III – Fig. 8.2**) significantly reduced the detected scrambling (**Appendix VIII – Fig. 8.7**). This is supported by the correspondent experiment in B Lymphocytes (*wt* vs. Scott), where the same observation was done, even though Scott cells still showed a residual scrambling that may be explained by the expression of ANO9 known to also act as phospholipid scramblase (**Appendix VIII – Fig. 8.9**).

During apoptosis, Ca^{2+} is released as a consequence of intracellular stress by the mitochondria and the ER store[12]. Therefore, the most predictable mechanism of ANO6 activation would be through this Ca^{2+} release detected in apoptotic cells. In fact, Fura-2AM measurements revealed a significant increase in the cytosolic Ca^{2+}, after incubation with tBHP in HEK293 cells and STS in HeLa cells (**Appendix IX – Fig. 8.10**). However, the detected concentration of Ca^{2+} (80 nM and 300 nM, respectively) is not sufficient to explain ANO6 activation. Interestingly, incubation with STS in HEK293 cells did not even raise the intracellular Ca^{2+} to a significant level compared to control (**Appendix IX – Fig. 8.10**).

Another possible mechanism is related to cell shrinkage and supported by previous findings from Martins *et. al*, where ANO6 was identified as component of the ORCC, a channel known to cause cell shrinkage and phospholipid scrambling during apoptosis[26]. Moreover, Juul *et. al* found a relationship between this protein and caspase-3 activation and thus cell shrinkage[23]. Hence, it is very likely that the same relationship between ANO6, caspase-3 activation and cell shrinkage is applied to ROS-mediated apoptosis. This is supported by the finding that HEK293 cells overexpressing ANO6 in the presence of tBHP show a considerable difference in the cell size compared to mock cells.

Interestingly, this year Lalida *et. al* found an alternative mechanism for ANO6 activation, independent of global Ca^{2+} rising, that relies on plasma membrane conformation. It was proved that the cleavage of phospholipids in the plasma membrane, by phospholipase A2 (PLA_2), leads to the opening of ANO6 pore. This is explained by the release of fatty acids in the cytosol, such as arachidonic acid (ArA), and the consequent accumulation of lysophospholipids (LPL) in the membrane. It was established that the membrane tension, caused by the presence of LPL, and a local increase of Ca^{2+} in specific domains are the two major players responsible for the activation of ANO6 as an ion channel[25].

ROS are known to induce lipid peroxidation and damage of the plasma membrane[83]. Therefore, another possibility to explain the findings in this work may be associated to membrane tension. This hypothesis was also addressed to study tBHP-induced apoptosis in HEK293 cells. In this regard, ACA (N-p-Amylcinnamoyl anthranilic Acid), a PLA_2 inhibitor, was used as a tool to see if by inhibiting this enzyme in the presence of ROS, membrane conformation would be reestablished and scrambling reduced. However, this compound revealed to be toxic once applied for a long-term period (data not shown). To overcome this problem, ArA was used and expected to compensate the phospholipid oxidation during ANO6 activation. This hypothesis was supported by the fact that ArA has been shown to inhibit PLA_2-induced ANO6 currents[25]. Here it was found that incubation of ArA in the presence of tBHP enhances cell death (**Appendix X – Fig. 8.11**). Nonetheless, this result does not necessarily indicate that this hypothesis is not true, since ArA is also known to be an apoptotic inducer[84], responsible for the activation of the cyclooxygenase, lipoxygenase and epoxygenase pathways, three major mechanisms involved in inflammation.

Finally, because LPL was found to activate an anoctamin-dependent conductance in HEK293 cells[25], it was also interesting to look for the effect in scrambling. Incubation of HEK293 with 10 µM Lyso-PS (a kind of LPL) for 2h resulted in an increase of Annx V positive cells. However, the detected scrambling was not inhibited by downregulation of ANO6 (**Appendix III – Fig. 8.2, Appendix X – Fig. 8.12**). Thus, it is very likely that this effect is due to lysophosphatidic acid (LPA), a downstream product of LPL known to induce apoptosis and irrelevant for ANO6 activation[25,85].

As referred before, ROS-mediated cell death is not reduced by CaCC-AO1, however this is not true when it comes to tannic acid (TA). Tannic acid is a polyphenolic biomolecule known to bind to proteins, such as ANO6, and stabilize biological membranes. Remarkably, when applied to HEK293 cells in the presence of tBHP, TA reduced the % of Annx V + 7-AAD positive cells, by a 3-fold factor (**Appendix X – Fig. 8.13**). This strong inhibition is likely through membrane stabilization and protection of lipid oxidation, which is in agreement with the alternative mechanism found by Lalida *et. al*[25].

5.2 CFTR PLAYS A ROLE DURING ROS-MEDIATED APOPTOSIS

As outlined in the Introduction chapter, CFTR is described by many as a pro-apoptotic factor involved in the regulation of the intracellular redox status, acidification and ceramide content in lipid rafts[49,52–54,56,59–61]. The apoptotic process in CF has been studied over the years and, although some conclusions are controversial, it seems that a defect on the clearance of apoptotic cells contribute to the ongoing inflammations and tissue injury[48]. Also, oxidative stress and infections are two major mediators of pulmonary damage which results in necrosis of lung epithelial cells[54].

In the present project CFTR function was studied in HEK293 and CFBE cells. In the first cell line, this protein was shown to enhance STS-mediated phospholipid scrambling and to have a Cl^- conductance during ROS-mediated apoptosis. Likewise, studies in the CFBE cell line provided evidence that CFTR helps cells to undergo apoptosis once exposed to oxidative stress. Because the mutant CFTR form (ΔF508) rescues partially cells from tBHP-induced apoptosis it is concluded that the presence of this protein in the plasma membrane is essential.

However, unlike what it is reported in previous studies[53], here it was found that CFTR contribution to ROS-mediated apoptosis is independent of channel activation and pore opening. Indeed, persistent stimulation of CFTR by supply of cAMP with IBMX and FK did not result in spontaneous apoptosis of CFBE cells. Also, tBHP-induced cell death was not reduced by the CFTR-inh 172. A high concentration of cytosolic ROS is known, not only to decrease GSH levels, but also to induce GSH transport to the extracellular space[50]. Therefore, it is possible that GSH permeation across CFTR only happens in the presence of intracellular oxidative stress. This might explain why it was detected a substantial difference in tBHP-induced apoptosis between the *wt* and ΔF508 CFTR forms, but persistent stimulation of the channel did not lead to cell death to a detectable level. It is also possible that the differential susceptibility of the two CFBE variants to ROS is related to intracellular acidification. In fact, measurements done in a study from Jungas *et.al* led to the conclusion that cells expressing *wt* CFTR have a lower intracellular pH in the presence of H_2O_2 compared to ΔF508 CFTR[54].

Remarkably, here CFTR was also found to contribute to cell shrinkage induced by tBHP. This result resembles ANO6 role in tBHP-induced apoptosis of HEK293 cells and is in agreement with previous studies where CFTR is reported to contribute to cell shrinkage[53] and to act as volume-regulated Cl^- channel[82].

The apoptotic dysfunction in CF is hard to establish because CF epithelial cells are characterized by an accentuated ER stress[48]. Understanding this particularity of the disease may help to control the

inflammatory process in CF, a symptom that remains one of the major unresolved problems. It is believed that in the presence of a specific stimulus, cells expressing a mutant CFTR form have a higher tendency to undergo necrosis[54]. One of the characteristics of the necrotic cell death is the release of DNA debris that initiate inflammatory responses. On the contrary, if cells die through the apoptotic pathway, fragmented DNA is tightly packed in apoptotic bodies which are then phagocytosed, protecting the surrounding tissue from inflammations[54].

Indeed, large DNA fragments are found in the lung epithelia from CF patients[55], supporting this concept. Remarkably, additional experiments in this study can be also taken as a hint that this is true. Particularly, the over-time response of CFBE cells to H_2O_2 revealed that cells expressing the mutant CFTR had a significantly higher population of cells positive for 7-AAD in the presence of the ROS inducer, compared to *wt* CFTR (**Appendix V – Fig. 8.4**). Single binding of 7-AAD to the nucleus is not a common event, happening once cell morphology is completely damaged and degraded. This may indicate that stimulation of cells with ROS without CFTR in the membrane results in a burst of the dying cell.

5.3 ANO6 AND CFTR ARE CO-WORKERS DURING REGULATED CELL DEATH

The hypothesis that ANO6 and CFTR cooperate during apoptosis emerged from previous reports where ROS was suspected to have an influence in ANO6 activity[22,26] and CFTR was described to mediate GSH efflux[49]. Moreover, a functional relationship between these two channels was also described[26].

In this study it is proved that ANO6 and CFTR interact during ROS-mediated apoptosis. This is supported by experiments in HEK293 cells where co-expression of these proteins resulted in a two-fold increase of Annx V positive cells after exposure to STS, compared to single transfection groups. Furthermore, it was demonstrated that ANO6 and CFTR co-expression results in a significant spontaneous apoptosis, that is in the absence of any oxidative stress inducer.

Additionally, separate experiments of ANO6 and CFTR function during apoptosis point out for a contribution of these two proteins to cell shrinkage, a process dependent on the activation of ion channels. Also, overexpression of ANO6 or CFTR and exposure to STS in HEK293 cells significantly augmented the basal current, compared to mock-transfected cells. Because this effect is stronger for ANO6, it is speculated that CFTR expression enhances this current. Nonetheless, Martins *et. al* found that cAMP- induced CFTR currents can be inhibited by downregulation of ANO6, suggesting that the two mechanisms can occur[26].

In conclusion, exposure of cells to oxidative stress and consequent ROS production leads to mitochondrial permeabilization, release of Ca^{2+} and pro-apoptotic proteins, responsible for caspase cleavage. These events terminate with ANO6 activation, which may support cell shrinkage and phospholipid scrambling, two apoptotic hallmarks enhanced in the presence of CFTR (**Fig. 5.1**).

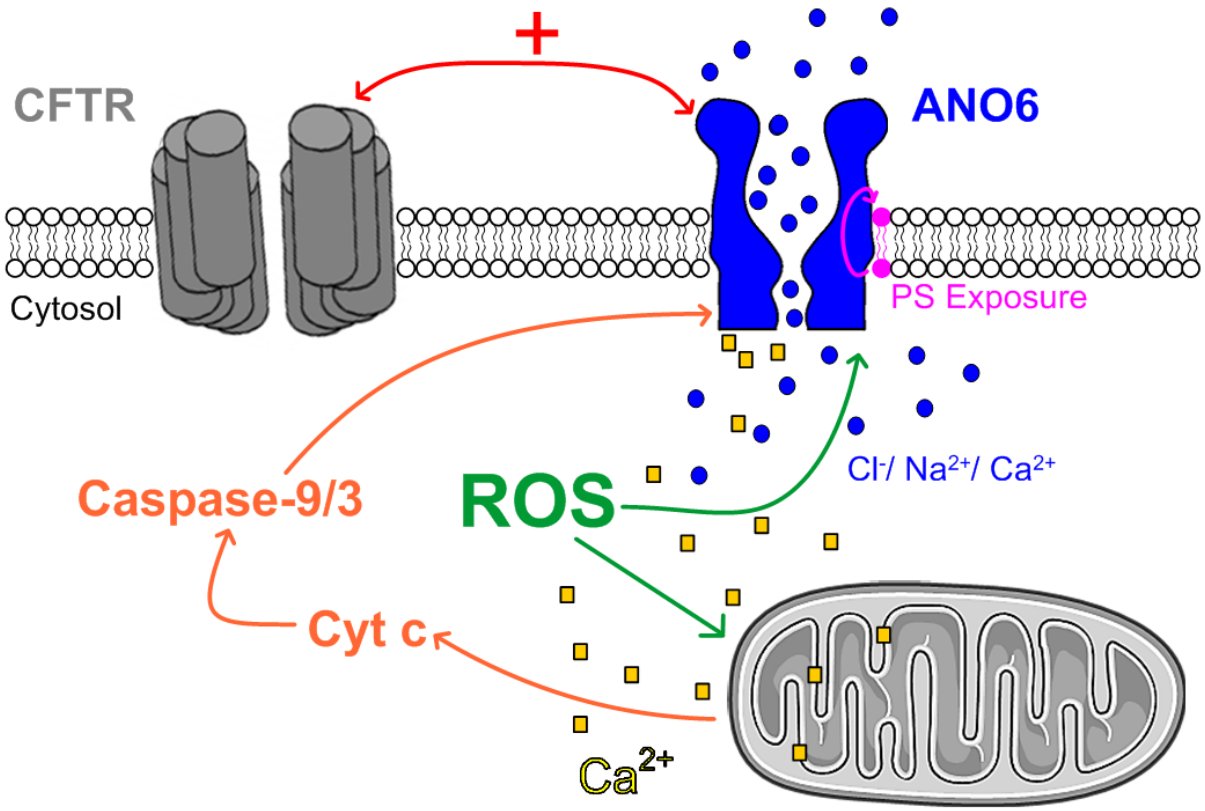

Figure 4.1. Proposed role of ANO6 and CFTR in apoptotic cell death. CFTR and ANO6 are two independent channels with a functional relationship during regulated cell death. Oxidative stress leads to mitochondrial permeabilization, release of Ca^{2+} and cytochrome c, which will lead to caspase-9 and 3 activation. ANO6 may support cell shrinkage and phospholipid scrambling, two activities enhanced in the presence of CFTR.

5. FUTURE PERSPECTIVES

Understanding the interaction of ANO6 and CFTR during regulated cell death may help to control CF apoptotic dysfunction and inflammations. For this reason, it is strongly encouraged that these investigations are pursued in an attempt to gain knowledge about the molecular mechanism behind this functional interaction.

Regarding ANO6 role in ROS-mediated apoptosis, further studies in B Lymphocytes are required. One possibility is the analysis of the parallel response of *wt* and Scott cells to STS by flow cytometry measurements of Annx V and 7-AAD labeling. This experiment may help to test the hypothesis that the absence of functional ANO6 leads to the activation of a different cell death pathway. PLA_2 inhibitors and ArA can also be tested by path clamp experiments in order to understand if the ROS-induced basal apoptotic current can be inhibited by a reduction of the plasma membrane tension.

Concerning CFTR involvement in apoptosis, it would be interesting to mimic inflammatory CF conditions in the CFBE *in vitro* system and look if the susceptibility to cell death is still dependent on the CFTR expression on the membrane. Similar experiments could be also done in primary cultured cells isolated from airways of an animal model (*wt* or knocked-out for CFTR), where spontaneous apoptosis could be evaluated by a simple caspase-3 assay.

Because it was concluded that CFTR involvement in tBHP-induced cell death cannot be explained by cAMP-channel activation, thorough studies of the effect of ROS in CFTR activity could unravel why CFBE *wt* CFTR cells are more susceptible to ROS-mediated apoptosis. Firstly, it would be interesting to patch this cell line in the presence of tBHP and look for a CFTR current, which may or may not be inhibited by the CFTR-inh 172. Additionally, measurements of the intracellular pH could prove if CFTR contribution to intracellular acidification is a factor during tBHP-induced apoptosis. Although persistent channel stimulation did not result in cell death, one can look for glutathione or ROS levels of CFBE cells in the presence or absence of IBMX and FK.

The major breakthrough of this project was the evidence that ANO6 and CFTR cooperate during regulated cell death. In this regard a co-immunoprecipitation or a FRET (Förster resonance energy transfer) analysis can be performed to prove an interaction between these two proteins. Additionally, because it is suggested that CFTR may enhance ANO6 function, a biotinylation of ANO6 endogenous membrane expression in CFBE cells would be also interesting. By this experiment it would be possible to compare if CFTR trafficking defects also affect ANO6 expression in the plasma membrane.

6. REFERENCES

1. Melorose, J., Perroy, R. & Careas, S. Apoptosis: A Review of Programmed Cell Death. *Statew. Agric. L. Use Baseline 2015* **1,** 495–516 (2015).

2. Ouyang, L. *et al.* Programmed cell death pathways in cancer: a review of apoptosis, autophagy and programmed necrosis. *Cell Prolif.* **45,** 487–98 (2012).

3. Williams, G. Programmed Cell Death : Apoptosis and Oncogenesis Mini review. *Cell* **65,** 1097–1098 (1991).

4. Ashkenazi, A. & Salvesen, G. Regulated cell death: signaling and mechanisms. *Annu. Rev. Cell Dev. Biol.* **30,** 337–356 (2014).

5. Ameisen, J. C. On the origin, evolution, and nature of programmed cell death: a timeline of four billion years. *Cell Death Differ.* **9,** 367–93 (2002).

6. KERR & J. F. R. KERR, A. H. W. A. A. R. C. Apoptosis: A basic biological phenomenon with wide-ranging implications in human disease. *J. Intern. Med.* **258,** 479–517 (2005).

7. Cohen, J. J. *et al.* APOPTOSIS AND PROGRAMMED CELL DEATH IN IMMUNITY.

8. Fink, S. L. & Cookson, B. T. MINIREVIEW Apoptosis , Pyroptosis , and Necrosis : Mechanistic Description of Dead and Dying Eukaryotic Cells. (1907). doi:10.1128/IAI.73.4.1907

9. Li, J. & Yuan, J. Caspases in apoptosis and beyond. 6194–6206 (1993). doi:10.1038/onc.2008.297

10. E.Gulbins, A.Jekle, K.Ferlinz, H.Grassmé, A. F. L. Physiology of apoptosis. *J Physiol Ren. Physiol* **1542,** 33–36 (2000).

11. Maeno, E., Ishizaki, Y., Kanaseki, T., Hazama, A. & Okada, Y. Normotonic cell shrinkage because of disordered volume regulation is an early prerequisite to apoptosis. *Proc. Natl. Acad. Sci. U. S. A.* **97,** 9487–9492 (2000).

12. Kroemer, G., Galluzzi, L. & Brenner, C. Mitochondrial Membrane Permeabilization in Cell Death. *Physiol. Reveiw* 99–163 (2007). doi:10.1152/physrev.00013.2006.

13. Nagata, S. Apoptosis by death factor. *Cell* **88,** 355–365 (1997).

14. Galluzzi, L., Blomgren, K. & Kroemer, G. Mitochondrial membrane permeabilization in neuronal injury. *Nat. Rev. Neurosci.* **10,** 481–494 (2009).

15. Bevers, E. M. & Williamson, P. L. Phospholipid scramblase: An update. *FEBS Lett.* **584,** 2724–2730 (2010).

16. Devaux, P. F., Herrmann, A., Ohlwein, N. & Kozlov, M. M. How lipid flippases can modulate membrane structure. *Biochim. Biophys. Acta - Biomembr.* **1778,** 1591–1600 (2008).

17. Rysavy, N. M. *et al.* Beyond apoptosis : The mechanism and function of phosphatidylserine asymmetry in the membrane of activating mast cells. *Bioarchitecture* **4,** 127–137 (2014).

18. Shimizu, T. *et al.* TMEM16F is a component of a Ca2+-activated Cl- channel but not a volume-sensitive outwardly rectifying Cl- channel. *Am. J. Physiol. Cell Physiol.* **304,** C748–59 (2013).

19. Pedemonte, N. & Galietta, L. J. V. Structure and function of TMEM16 proteins (anoctamins). *Physiol. Rev.* **94,** 419–59 (2014).

20. Kunzelmann, K. *et al.* Anoctamins. *Pflugers Arch. Eur. J. Physiol.* **462,** 195–208 (2011).

21. Brunner, J. D., Lim, N. K., Schenck, S., Duerst, A. & Dutzler, R. X-ray structure of a calcium-activated TMEM16 lipid scramblase. *Nature* **516,** 207–212 (2014).

22. Kunzelmann, K. *et al.* Molecular functions of anoctamin 6 (TMEM16F): A chloride channel, cation channel, or phospholipid scramblase? *Pflugers Arch. Eur. J. Physiol.* **466,** 407–414 (2014).

23. Juul, C. A. *et al.* Anoctamin 6 differs from VRAC and VSOAC but is involved in apoptosis and supports volume regulation in the presence of Ca2+. *Pfl??gers Arch. Eur. J. Physiol.* **466,** 1899–1910 (2014).

24. Almaça, J. *et al.* TMEM16 proteins produce volume-regulated chloride currents that are reduced in mice lacking TMEM16A. *J. Biol. Chem.* **284,** 28571–28578 (2009).

25. Sirianant, L., Ousingsawat, J., Wanitchakool, P., Schreiber, R. & Kunzelmann, K. Cellular volume regulation by anoctamin 6: Ca2+, phospholipase A2 and osmosensing. *Pflugers Arch. Eur. J. Physiol.* **468,** 335–349 (2016).

26. Martins, J. R. *et al.* Anoctamin 6 is an essential component of the outwardly rectifying chloride channel. *Proc. Natl. Acad. Sci. U. S. A.* **108,** 18168–72 (2011).

27. Yang, H. *et al.* TMEM16F forms a Ca2+-activated cation channel required for lipid scrambling in platelets during blood coagulation. *Cell* **151,** 111–22 (2012).

28. Yu, K. *et al.* Identification of a lipid scrambling domain in ANO6 / TMEM16F. 1–23 (2015). doi:10.7554/eLife.06901

29. Suzuki, J. & Nagata, S. Phospholipid scrambling by TMEM16F. *Seikagaku* **83,** 1050–1054 (2011).

30. Bevers, E. M. Compound heterozygosity for 2 novel TMEM16F mutations in a patient with Scott syndrome To the editor : Chimerism levels after stem cell transplantation are primarily determined by the ratio of donor. **117,** 4399–4400 (2011).

31. Heemskerk, J. W. M., Bevers, E. M. & Lindhout, T. Platelet activation and blood coagulation. *Thromb. Haemost.* **88,** 186–193 (2002).

32. Ehlen, H. W. A. *et al.* Inactivation of anoctamin-6/Tmem16f, a regulator of phosphatidylserine scrambling in osteoblasts, leads to decreased mineral deposition in skeletal tissues. *J. Bone Miner. Res.* **28,** 246–259 (2013).

33. Forschbach, V. *et al.* Anoctamin 6 is localized in the primary cilium of renal tubular cells and is involved in apoptosis-dependent cyst lumen formation. *Cell Death Dis.* **6,** e1899 (2015).

34. Kmit, A. *et al.* Calcium-activated and apoptotic phospholipid scrambling induced by Ano6 can occur independently of Ano6 ion currents. *Cell Death Dis.* **4,** e611 (2013).

35. Ousingsawat, J. *et al.* Anoctamin 6 mediates effects essential for innate immunity downstream of P2X7 receptors in macrophages. *Nat. Commun.* **6,** 6245 (2015).

36. Dutertre, M. *et al.* Exon-based clustering of murine breast tumor transcriptomes reveals alternative exons whose expression is associated with metastasis. *Cancer Res.* **70,** 896–905 (2010).

37. Jacobsen, K. S. *et al.* The role of TMEM16A (ANO1) and TMEM16F (ANO6) in cell migration. *Pflugers Arch. Eur. J. Physiol.* **465,** 1753–1762 (2013).

38. Whitlock, J. M. & Hartzell, H. C. A Pore Idea: the ion conduction pathway of TMEM16/ANO proteins is composed partly of lipid. *Pflugers Arch. Eur. J. Physiol.* **468,** 455–473 (2016).

39. Suzuki, J. *et al.* Calcium-dependent phospholipid scramblase activity of TMEM16 protein family members. *J. Biol. Chem.* **288,** 13305–16 (2013).

40. Suzuki, J., Imanishi, E. & Nagata, S. Exposure of phosphatidylserine by Xkrelated protein family members during apoptosis. *J. Biol. Chem.* **289,** 30257–30267 (2014).

41. Cutting, G. R. Cystic fibrosis genetics: from molecular understanding to clinical application. *Nat. Rev. Genet.* **16,** 45–56 (2015).

42. Riordan, J. R. CFTR function and prospects for therapy. *Annu. Rev. Biochem.* **77,** 701–726 (2008).

43. Riordan, J. R. *et al.* Identification the Cystic Fibrosis Gene : Cloning and Characterization of Complementary DNA. *Science (80-.).* **245,** 1066–1073 (1989).

44. Collins, F. S. Cystic fibrosis: molecular biology and therapeutic implications. *Science (80-.).* **256,** 774–779 (1992).

45. Amaral, M. D. & Kunzelmann, K. Molecular targeting of CFTR as a therapeutic approach to cystic fibrosis. *Trends Pharmacol. Sci.* **28,** 334–341 (2007).

46. Farinha, C. M., Matos, P. & Amaral, M. D. Control of cystic fibrosis transmembrane conductance regulator membrane trafficking: Not just from the endoplasmic reticulum to the Golgi. *FEBS J.* **280,** 4396–4406 (2013).

47. Sheppard, D. N. & Welsh, M. J. Structure and Function of the CFTR Chloride Channel. 23–45 (1999).

48. Soleti, R., Porro, C. & Martı, M. C. Apoptotic process in cystic fibrosis cells. 1029–1038 doi:10.1007/s10495-013-0874-y

49. Kogan, I. *et al.* CFTR directly mediates nucleotide-regulated glutathione flux. *EMBO J.* **22,** 1981–1989 (2003).

50. Circu, M. L. & Aw, T. Y. Glutathione and modulation of cell apoptosis. *Biochim Biophys Acta.* **1,** 1767–1777 (2012).

51. Tobergte, D. R. & Curtis, S. Glutathione: a radical treatment for Cystic Fibrosis lung disease? *J. Chem. Inf. Model.* **53,** 1689–1699 (2013).

52. Gao, L., Kim, K. J., Yankaskas, J. R. & Forman, H. J. Abnormal glutathione transport in cystic fibrosis airway epithelia. *Am. J. Physiol. - Lung Cell. Mol. Physiol.* **277,** L113–L118 (1999).

53. l'Hoste, S. *et al.* CFTR mediates apoptotic volume decrease and cell death by controlling glutathione efflux and ROS production in cultured mice proximal tubules. *Am J Physiol Ren. Physiol* **298,** F435–53 (2010).

54. Jungas, T., Motta, I., Duffieux, F., Fanen, P. & Ojcius, D. M. Glutathione Levels and BAX Activation during Apoptosis Due to Oxidative Stress in Cells Expressing Wild-type and Mutant Cystic Fibrosis Transmembrane Conductance Regulator *. *Biochemistry* **277,** 27912–27918 (2002).

55. Gottlieb, R. A. & Dosanjht, A. Mutant cystic fibrosis transmembrane conductance regulator inhibits acidification and apoptosis in C127 cells : Possible relevance to cystic fibrosis.

56. Poujeol, C. *et al.* CFTR modulates programmed cell death by decreasing intracellular pH in

Chinese hamster lung fibroblasts. 810–824 (2001).

57. Tepper, A. D. *et al.* Sphingomyelin Hydrolysis to Ceramide during the Execution Phase of Apoptosis Results from Phospholipid Scrambling and Alters Cell-surface Morphology. 155–164 (2000).

58. Smith, E. L., Schuchman, E. H. & Asm, A. The unexpected role of acid sphingomyelinase in cell death and the pathophysiology of common diseases. 3419–3431 doi:10.1096/fj.08-108043

59. Rassmé, H. G. *et al.* Host defense against Pseudomonas aeruginosa requires ceramide-rich membrane rafts. (2003). doi:10.1038/nm

60. Ulrich, M. *et al.* Ceramide accumulation mediates inflammation , cell death and infection susceptibility in cystic fibrosis. 1–10 (2008). doi:10.1038/nm1748

61. Kleuser, B. & Gulbins, E. Acid Sphingomyelinase Inhibitors Normalize Pulmonary Ceramide and Inflammation in Cystic Fibrosis. doi:10.1165/rcmb.2009-0174OC

62. Tobergte, D. R. & Curtis, S. CFTR and outward rectifying chloride channels are distinct proteins with a regulatory relationship. *J. Chem. Inf. Model.* **53,** 1689–1699 (2013).

63. Kunzelmann, K. & Mehta, A. CFTR: A hub for kinases and crosstalk of cAMP and Ca2+. *FEBS J.* **280,** 4417–4429 (2013).

64. Munnix, I. C. A. *et al.* Store-mediated calcium entry in the regulation of phosphatidylserine exposure in blood cells from Scott patients. *Thromb. Haemost.* **89,** 687–695 (2003).

65. Gerry Shaw, Silas Morse, Miguel Ararat, F. L. G. Potential transformation of human neuronal cells by human adenoviruses and the origin of HTobergte, David R.EK293 cells. *J. Chem. Inf. Model.* **53,** 1689–1699 (2002).

66. Hsu, S. H. *et al.* Genetic characteristics of the HeLa cell. *Science* **191,** 392–4 (1976).

67. Galietta, L. J. V, Haggie, P. M. & Verkman, A. S. Green fluorescent protein-based halide indicators with improved chloride and iodide affinities. *FEBS Lett.* **499,** 220–224 (2001).

68. Bebok, Z. *et al.* Failure of cAMP agonists to activate rescued ΔF508 CFTR in CFBE41o - airway epithelial monolayers. *J. Physiol.* **569,** 601–615 (2005).

69. Felgner, P. L. *et al.* Lipofection: a highly efficient, lipid-mediated DNA-transfection procedure. *Proc. Natl. Acad. Sci. U. S. A.* **84,** 7413–7 (1987).

70. Felgner, J. H. *et al.* Enhanced gene delivery and mechanism studies with a novel series of cationic lipid formulations. *J. Biol. Chem.* **269,** 2550–2561 (1994).

71. Engeland, M. Van *et al.* A review on an apoptosis detection system based on phosphatidyserine exposure. *Proc. Natl. Ac. Sci. USA* **93,** 1–9 (1996).

72. Zembruski, N. C. L., Stache, V., Haefeli, W. E. & Weiss, J. 7-Aminoactinomycin D for apoptosis staining in flow cytometry. *Anal. Biochem.* **429,** 79–81 (2012).

73. Mölder, A. *et al.* Non-invasive, label-free cell counting and quantitative analysis of adherent cells using digital holography. *J. Microsc.* **232,** 240–247 (2008).

74. Zhong, S., Navaratnam, D. & Santos-Sacchi, J. A genetically-encoded YFP sensor with enhanced chloride sensitivity, photostability and reduced pH interference demonstrates augmented transmembrane chloride movement by gerbil prestin (SLC26a5). *PLoS One* **9,** (2014).

75. Grynkiewicz, G., Poenie, M. & Tsien, R. Y. A new generation of Ca2+ indicators with greatly improved fluorescence properties. *J. Biol. Chem.* **260,** 3440–3450 (1985).

76. Martín, C. *et al.* tert-Butyl hydroperoxide-induced lipid signaling in hepatocytes: Involvement of glutathione and free radicals. *Biochem. Pharmacol.* **62,** 705–712 (2001).

77. Papucci, L. *et al.* Coenzyme Q10 prevents apoptosis by inhibiting mitochondrial depolarization independently of its free radical scavenging property. *J. Biol. Chem.* **278,** 28220–28228 (2003).

78. Schenk, L. K., Schulze, U., Henke, S., Weide, T. & Pavenstädt, H. TMEM16F Regulates Baseline Phosphatidylserine Exposure and Cell Viability in Human Embryonic Kidney Cells. *Cell Physiol Biochem* **38,** 2452–2463 (2016).

79. Feng, G. & Kaplowitz, N. Mechanism of staurosporine-induced apoptosis in murine hepatocytes. *AJ-Gastrointest. Liver Physiol.* **282,** G825–G834 (2002).

80. Ward, N. E. & O'Brian, C. a. Kinetic analysis of protein kinase C inhibition by staurosporine: evidence that inhibition entails inhibitor binding at a conserved region of the catalytic domain but not competition with substrates. *Mol. Pharmacol.* **41,** 387–92 (1992).

81. Shimizu, T., Numata, T. & Okada, Y. A role of reactive oxygen species in apoptotic activation of volume-sensitive Cl(-) channel. *Proc. Natl. Acad. Sci. U. S. A.* **101,** 6770–6773 (2004).

82. Kunzelmann, K. Ion channels in regulated cell death. *Cell. Mol. Life Sci.* **73,** 1–17 (2016).

83. Circu, M. L. & Aw, T. Y. Reactive Oxygen Species, cellular redox systems and apoptosis. *Free Radic Biol Med* **48,** 749–762 (2010).

84. Pompeia, C., Lima, T. & Curi, R. Arachidonic acid cytotoxicity: Can arachidonic acid be a physiological mediator of cell death? *Cell Biochem. Funct.* **21,** 97–104 (2003).

85. Ye, X., Ishii, I., Kingsbury, M. A. & Chun, J. Lysophosphatidic acid as a novel cell survival/apoptotic factor. *Biochim. Biophys. Acta - Mol. Cell Biol. Lipids* **1585,** 108–113 (2002).

7. APPENDICES

APPENDIX I – CDNA

Table 7.1 Plasmids accession number and base pairs (bp).

Target	Accession number	bp
ANO6	NM_001025356	27306
CFTR	NM_000492	4440

APPENDIX II - INHIBITION OF TBHP-INDUCED APOPTOSIS BY IDEBENONE

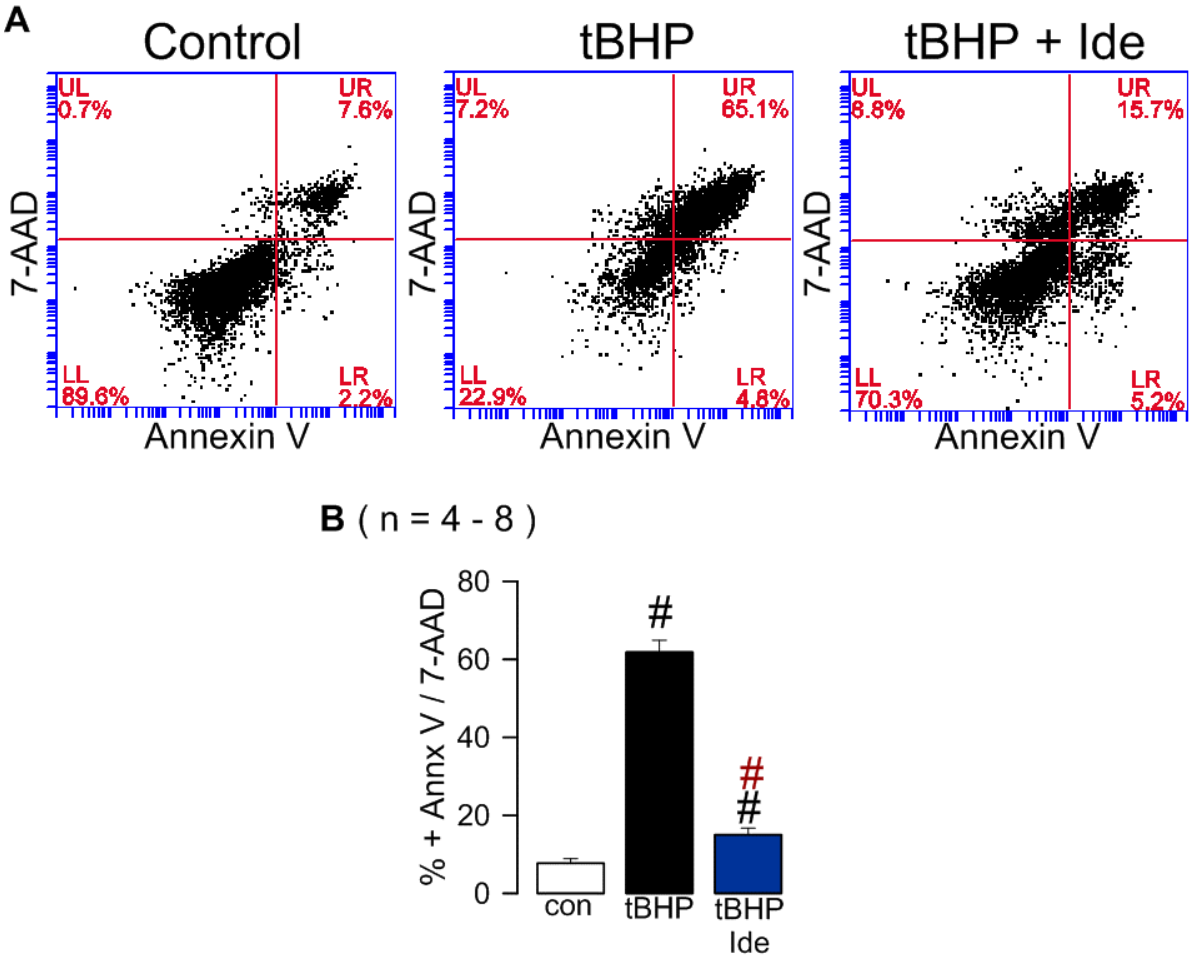

Figure 7.1. Inhibition of tBHP-induced apoptosis by Idebenone. A) Representative original dot-plots of flow cytometry analysis of HEK293 cells in the presence or absence of tBHP (100 µM) and/or Idebenone (20 µM) for 2h. **B)** Summary of Annx V and 7-AAD positivity of experiments shown in A. Idebenone significantly reduced Annx V and 7-AAD positive cells in the presence of tBHP, rescuing ROS-mediated cell death. (Values are mean ± SEM; # unpaired *t*-test to control, # unpaired *t*-test to tBHP treated cells, *p*-value < 0.05; n = number of experiments).

APPENDIX III – DOWNREGULATION OF ANO6 IN HEK293 AND HELA CELLS

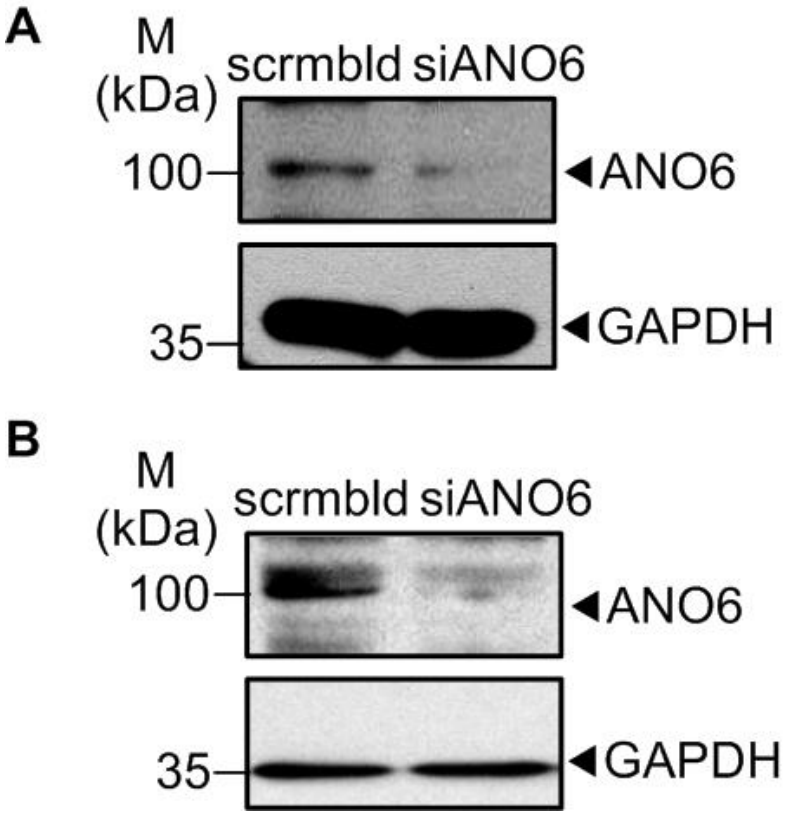

Figure 7.2. ***Western Blot*** **analysis of ANO6 expression** in HEK293 (A) and HeLa (B) cells, after 48h and 24h of transfection with siRNA, respectively.

APPENDIX IV – EFFECT OF ANO6 SILENCING ON TBHP-INDUCED APOPTOSIS OF HEK293 CELLS

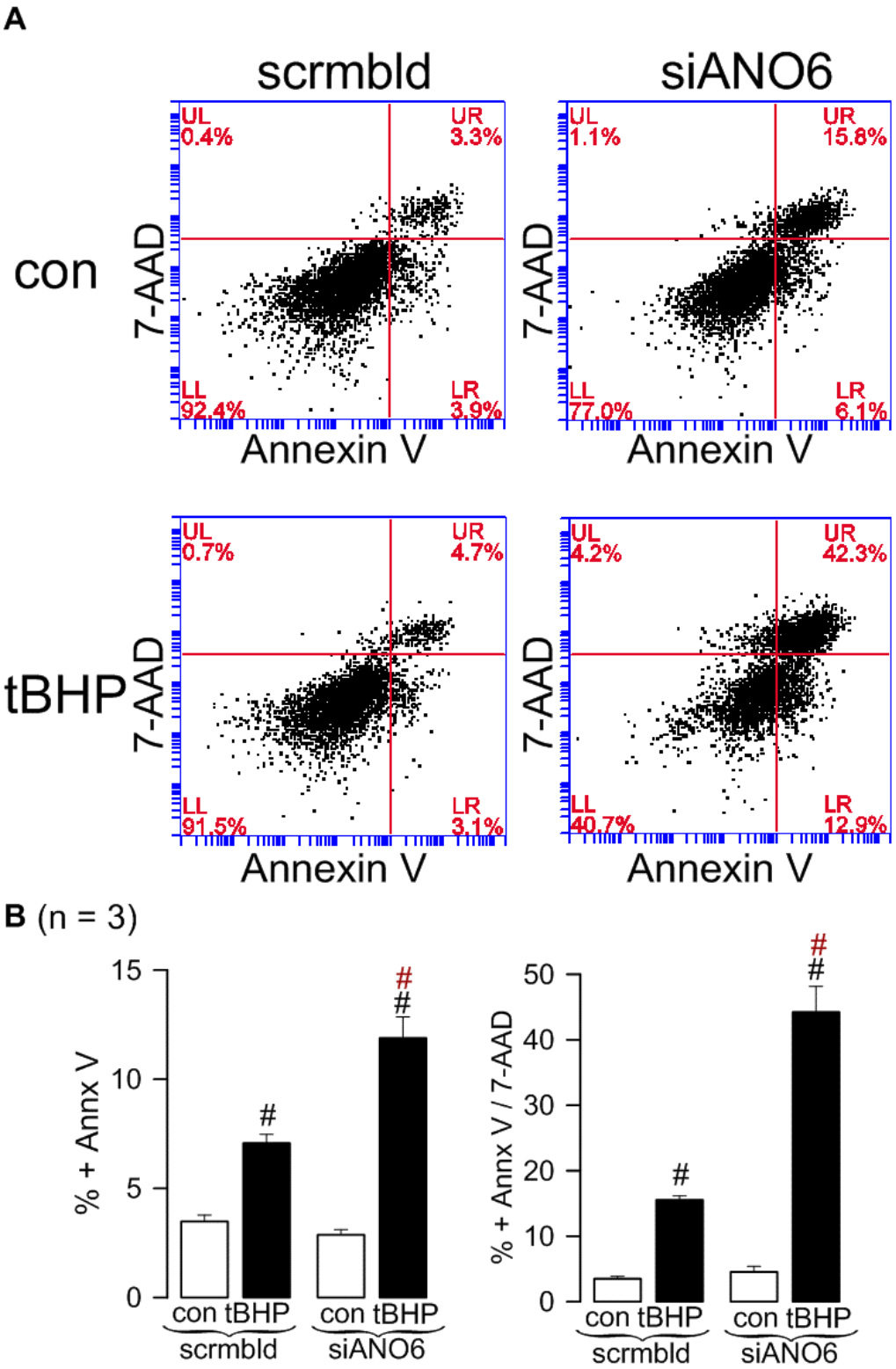

Figure 7.3. ANO6 silencing increases the tBHP-induced apoptosis in HEK293 cells. A) Representative original dot-plots of cells transfected with siANO6 or scrambled in the presence or absence of 100 µM tBHP for 3h30. **B)** Summary of Annx V and Annx V + 7-AAD positivity of experiments shown in A. Downregulation of ANO6 likely resulted in off target effects, enhancing cell death induced by tBHP. (Values are mean ± SEM; # unpaired *t*-test to control, # unpaired *t*-test to scrambled treated cells, *p*- value < 0.05; n = number of experiments).

APPENDIX V - EFFECT OF CFTR IN H_2O_2-INDUCED CELL DEATH OF CFBE CELLS

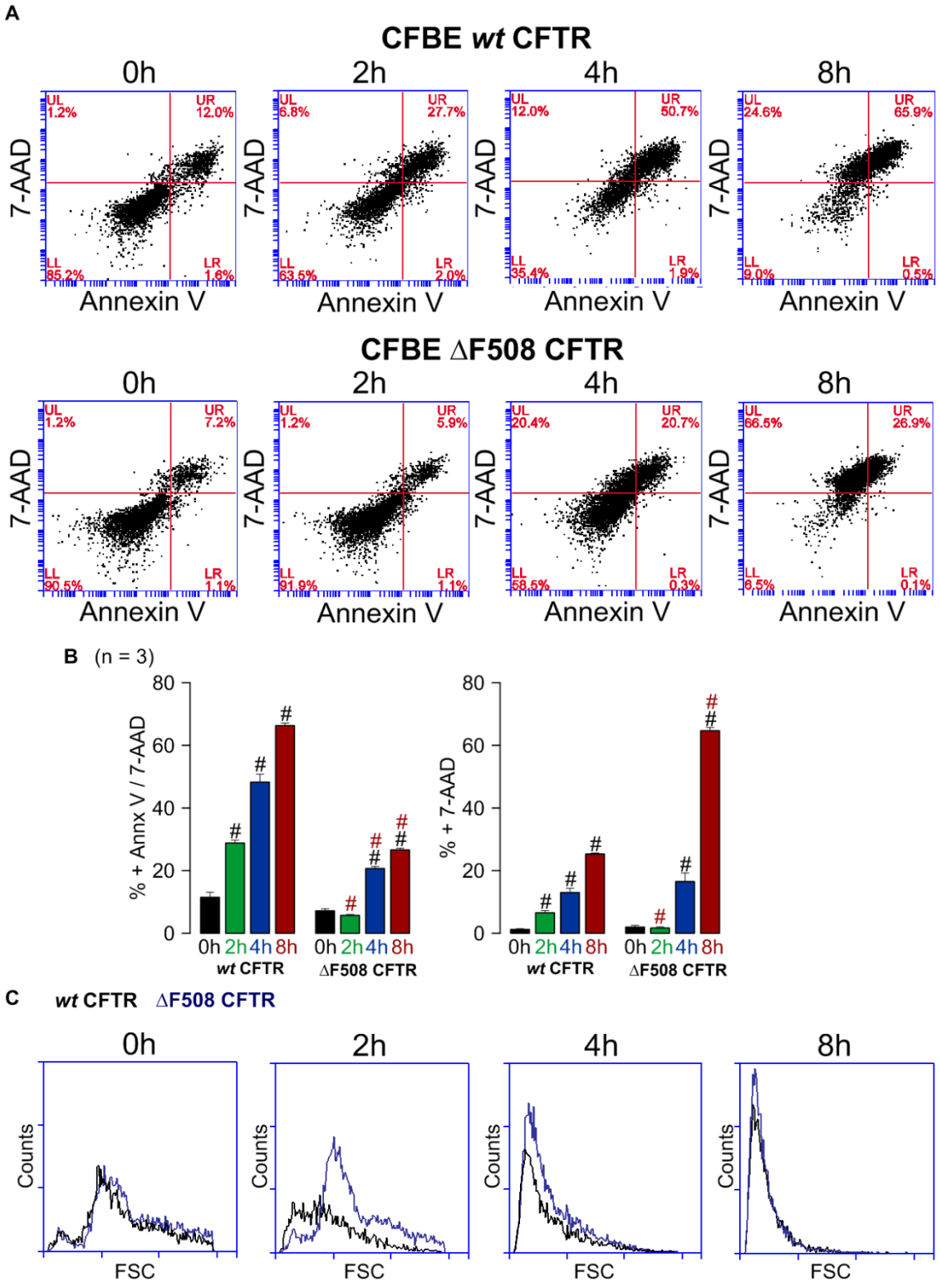

Figure 7.4. CFBE cells expressing *wt* CFTR have a higher susceptibility to H_2O_2-induced cell death. A) Representative original dot-plots from over-time response to 900 µM H_2O_2 (0h, 2h, 4h, 8h) of CFBE *wt* and ΔF508 CFTR cells. **B)** Summary of 7-AAD and Annx V + 7-AAD positivity of experiments shown in A. **C)** FSC histograms of experiments shown in A. (Values are mean ± SEM; # unpaired *t*-test to control, # unpaired *t*-test to H_2O_2 to CFBE *wt* CFTR treated cells, *p*-value < 0.05; n = number of experiments).

APPENDIX VI – EFFECT OF STS IN WT AND SCOTT B LYMPHOCYTES

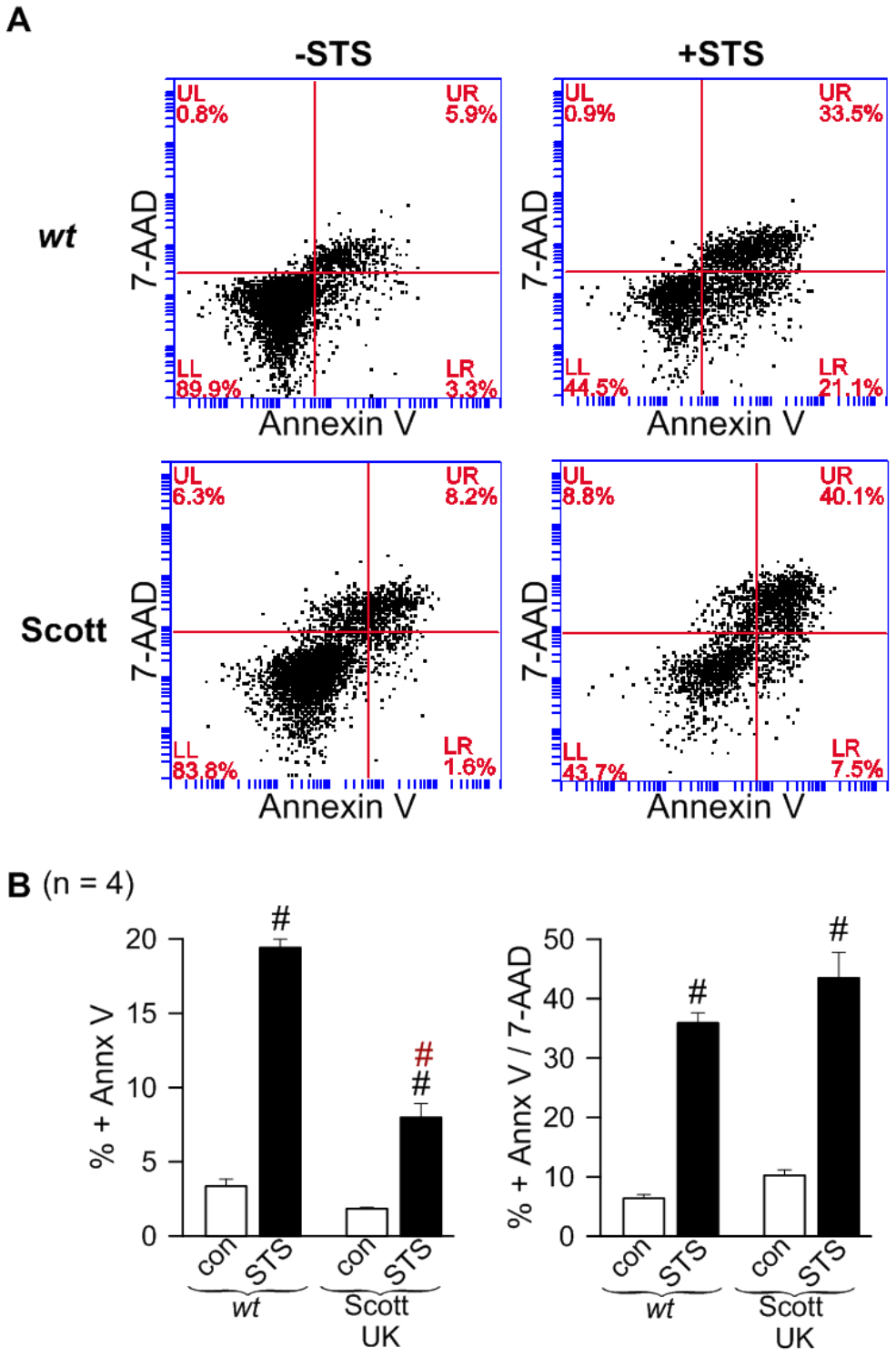

Figure 7.5. STS induces a differential Annx V positivity in *wt* and Scott lymphocytes. A) Representative original dot-plots of flow cytometry analysis of *wt* and Scott lymphocytes non-treated and treated with 1 µM STS for 16h, **B)** Summary of Annx V and Annx V + 7-AAD positivity of experiments shown in A. (Values are mean ± SEM; # unpaired *t*-test to control, # unpaired *t*-test to *wt* B lymphocytes incubated with STS, *p*-value < 0.05; n = number of experiments).

APPENDIX VII - CACC-AO1 DOES NOT INHIBIT TBHP-INDUCED APOPTOSIS OF HEK293 CELLS

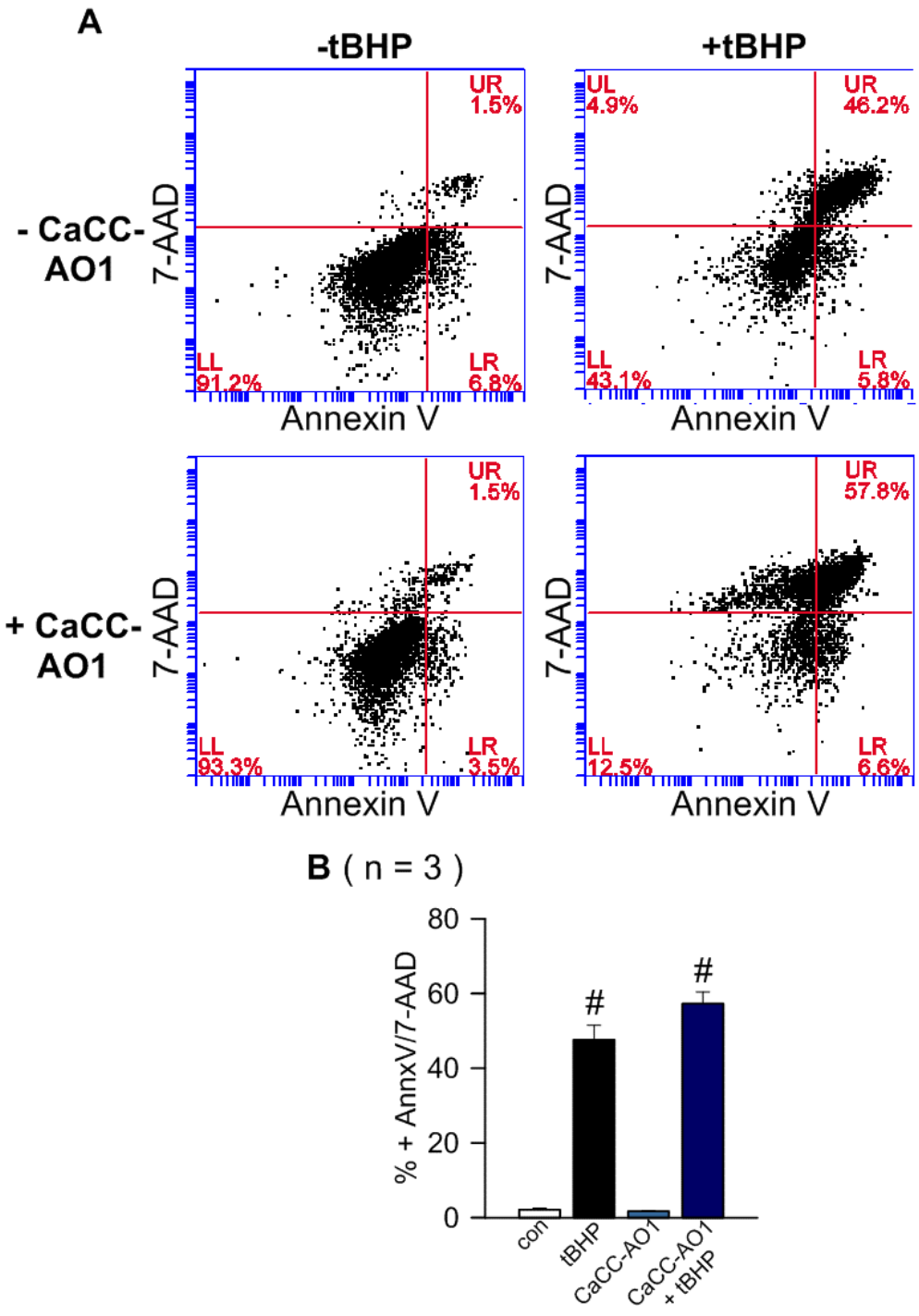

Figure 7.6. Effect of CaCC-AO1 in tBHP-induced apoptosis of HEK293 cells. A) Representative original dot-plots of flow cytometry analysis from HEK293 cells in the presence or absence of 100 µM tBHP and 20 µM CaCC-AO1 for 2h. **B)** Summary of Annx V and 7-AAD positivity of experiments shown in A. Inhibition of ANO6 by CaCC-AO1 does not rescue cells from tBHP induced apoptosis. (Values are mean ± SEM; # unpaired *t*-test to control, *p*-value < 0.05; n = number of experiments).

APPENDIX VIII - ANO6 IS ESSENTIAL FOR CA2+-INDUCED SCRAMBLING

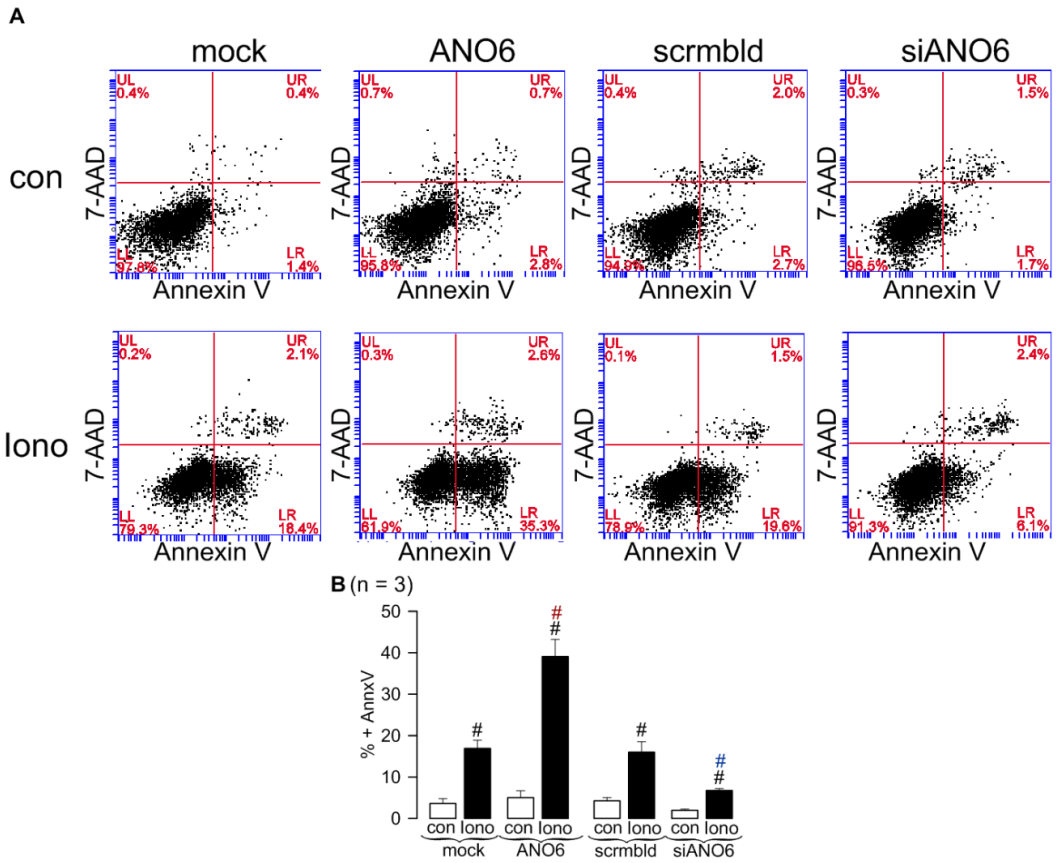

Figure 7.7. Ionomycin induces an ANO6-dependent phospholipid scrambling in HEK293 cells. A) Representative original dot-plots from flow cytometry analysis of HEK293 cells transfected with mock, ANO6, scrambled or siANO6 and stimulated for 20 min with 1 µM Iono. **B)** Summary of Annx V positivity from experiments shown in A. (Values are mean ± SEM; # unpaired *t*-test to control, # unpaired *t*-test to mock-transfected cells in the presence of Iono, # unpaired *t*-test to scrambled-transfected cells in the presence of Iono, *p*-value < 0.05; n = number of experiments).

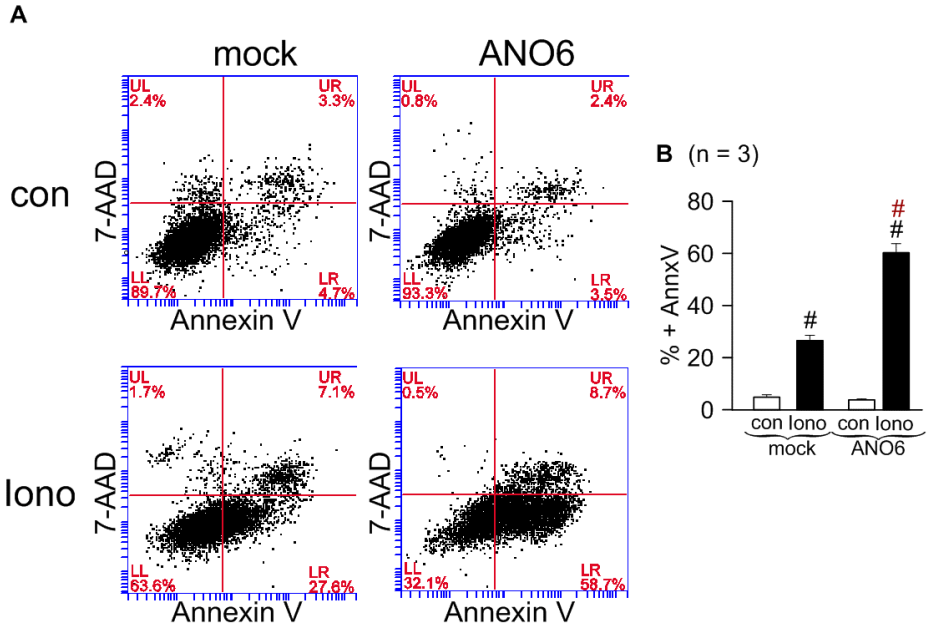

Figure 7.8. Ionomycin induces an ANO6-dependent phospholipid scrambling in HeLa cells. A) Representative original dot-plots from flow cytometry analysis of HeLa cells transfected with mock or ANO6 and stimulated for 30 min with 10 µM

Iono. **B)** Summary of Annx V positivity from experiments shown in A. (Values are mean ± SEM; # unpaired *t*-test to control, # unpaired *t*-test to mock-transfected cells in the presence of Iono, *p*-value < 0.05; n = number of experiments).

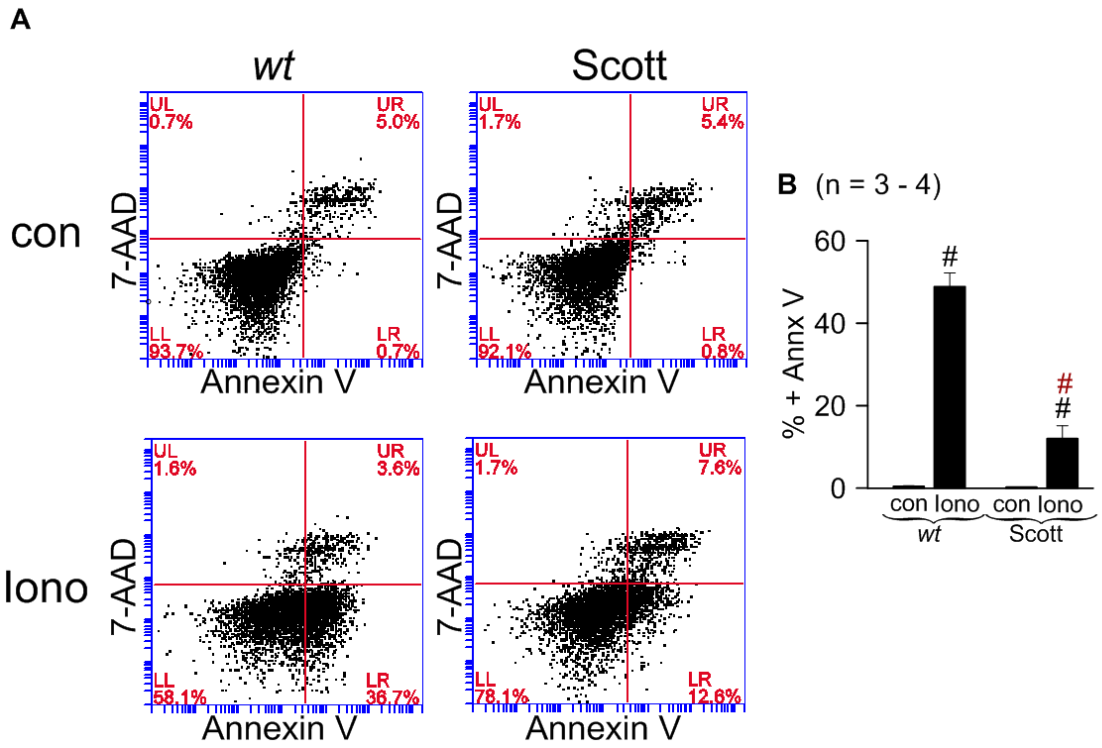

Figure 7.9. Ionomycin induces an ANO6-dependent phospholipid scrambling in B lymphocytes. A) Representative original dot-plots from flow cytometry analysis of *wt* and Scott Lymphocytes stimulated for 10 min with 5 µM Iono. **B)** Summary of Annx V positivity from experiments shown in A. (Values are mean ± SEM; # unpaired *t*-test to control, # unpaired *t*-test to *wt* B lymphocytes in the presence of Iono, *p*-value < 0.05; n = number of experiments).

APPENDIX IX – INTRACELLULAR CA^{2+} CONCENTRATION DURING ROS-MEDIATED APOPTOSIS

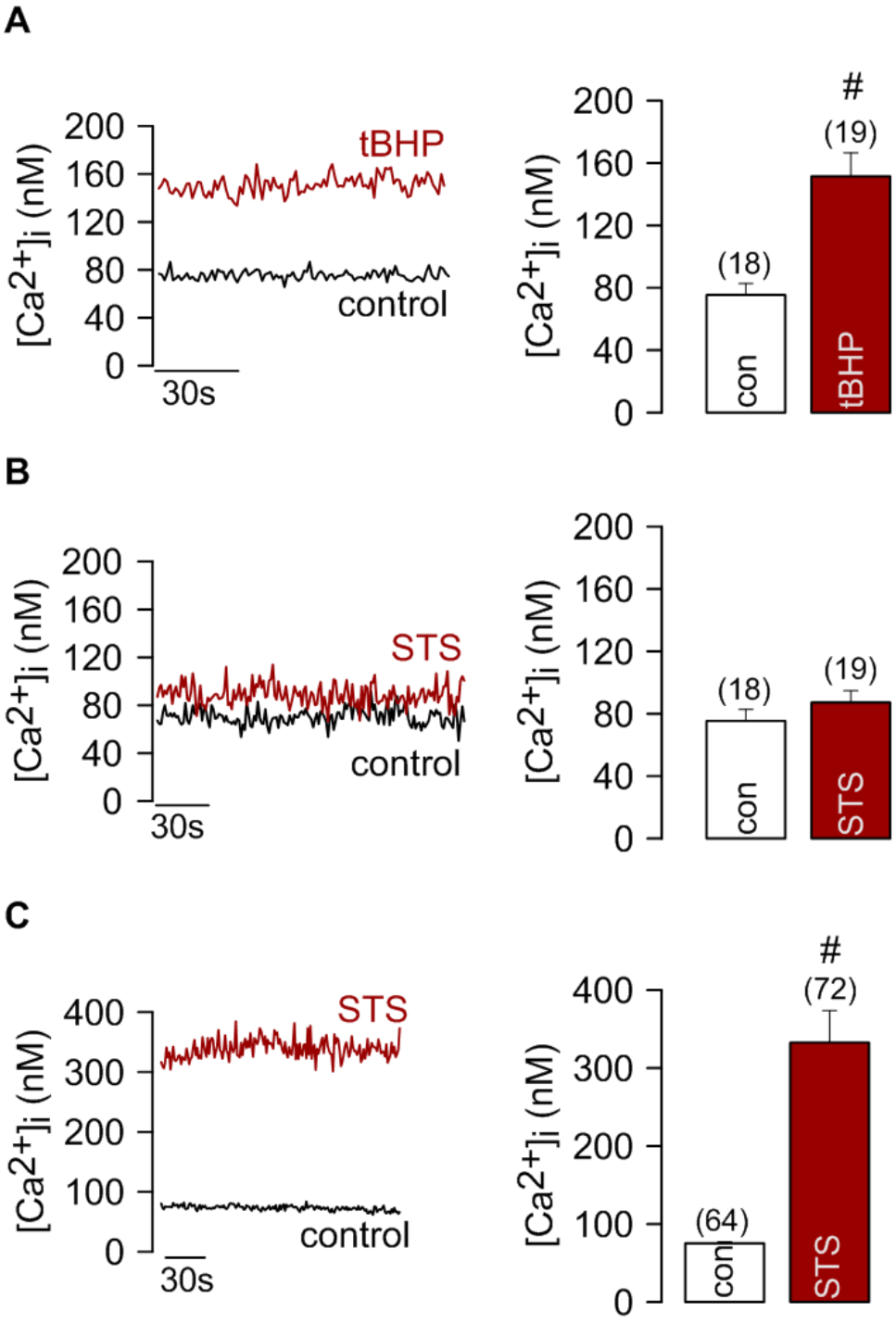

Figure 7.10. ROS effect in intracellular Ca^{2+} concentration. A) Fura-2 AM measurements of HEK293 cells in the presence or absence of 100 µM tBHP for 1h30. **B)** Fura-2 AM measurements of HEK293 cells in the presence or absence of 1 µM STS for 24h. **C)** Fura-2 AM measurements of HeLa cells in the presence or absence of 1 µM STS for 5h. Intracellular Ca^{2+} is significantly increased by tBHP in HEK293 cells and STS in HeLa cells. Incubation with STS in HEK293 cells did not affect $[Ca^{2+}]_i$. (Values are mean ± SEM; # unpaired *t*-test to control, *p*-value < 0.05; n = number of experiments).

APPENDIX X – PLASMA MEMBRANE TENSION IN ROS-MEDIATED APOPTOSIS

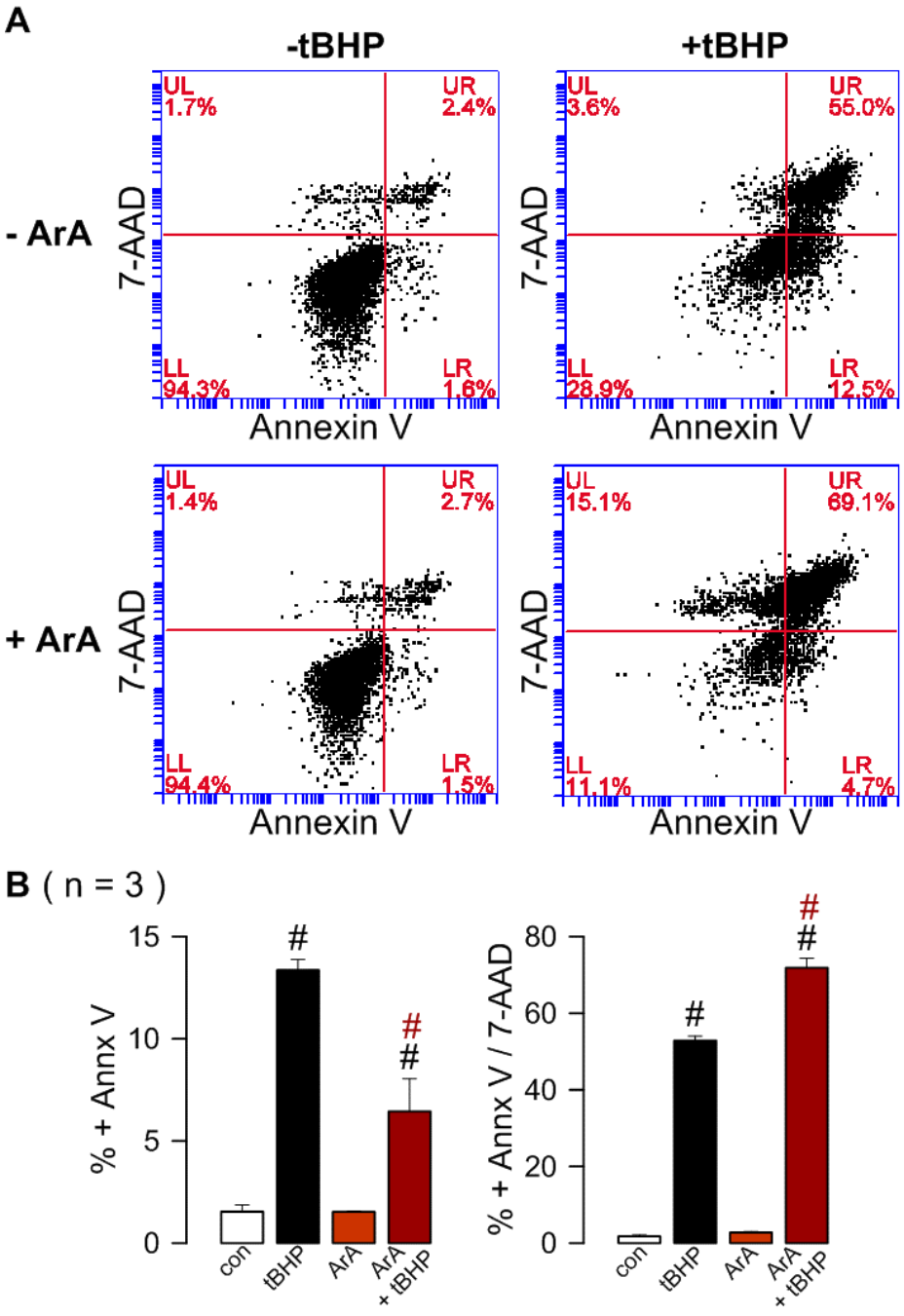

Figure 7.11. Arachidonic acid enhances tBHP-induced apoptosis. A) Representative original dot-plots of HEK293 cells in the presence or absence of 100 µM tBHP and 20 µM ArA for 2h. **B)** Summary of Annx V and Annx V + 7-AAD positivity of experiments shown in A. (Values are mean ± SEM; # unpaired *t*-test to control, # unpaired *t*-test to tBHP-treated cells, *p*-value < 0.05; n = number of experiments).

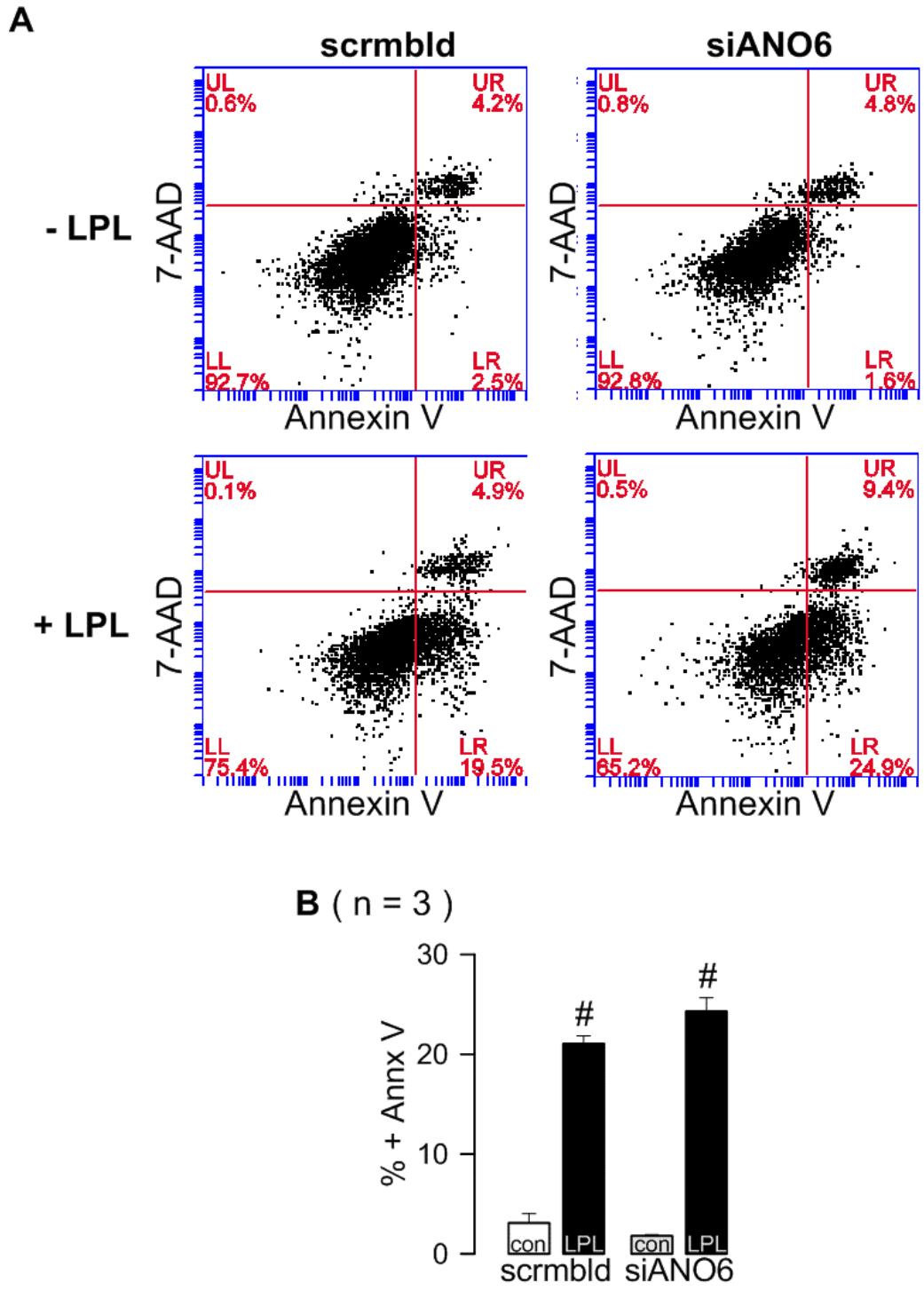

Figure 7.12. LPL induces an ANO6-independent PS exposure in HEK293 cells. A) Representative original dot-plots of HEK293 cells transfected with scrambled or siANO6, in the presence/absence of 10 µM Lyso-phosphatidylserine (Lyso-PS) for 2h. **B)** Summary of Annx V positivity of experiments shown in A. (Values are mean ± SEM; # unpaired *t*-test to control, *p*-value < 0.05; n = number of experiments).

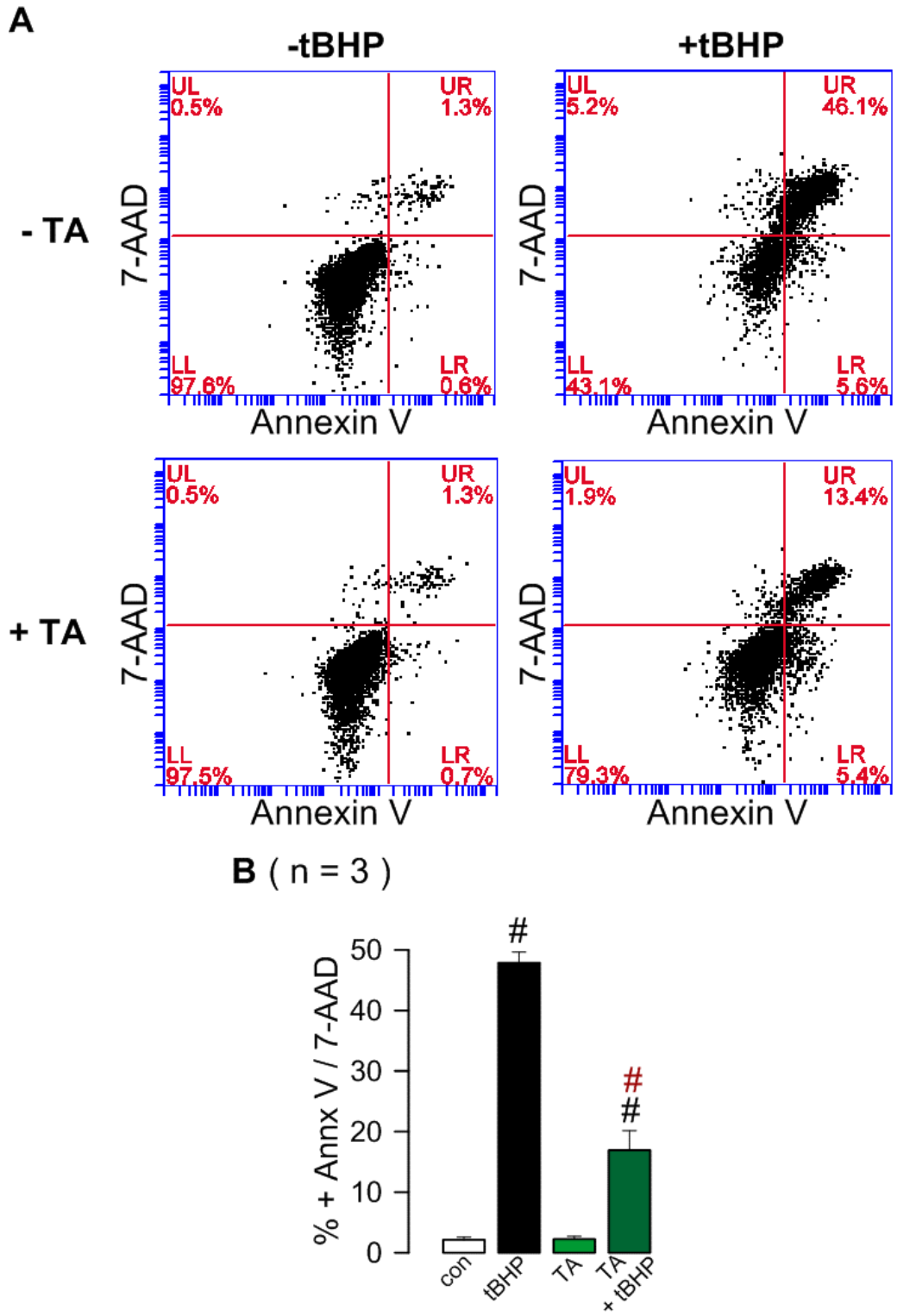

Figure 7.13. Tannic acid inhibits tBHP-induced apoptosis. A) Representative original dot-plots of HEK293 cells in the presence or absence of 100 µM tBHP and 1 µM TA for 2h. **B)** Summary of Annx V and Annx V + 7-AAD positivity of experiments shown in A. (Values are mean ± SEM; # unpaired *t*-test to control, # unpaired *t*-test to tBHP-treated cells, *p*-value < 0.05; n = number of experiments).